Preface

This report acts as a final report related to a master thesis at the Delft University of Technology, Section River Hydraulics. The study is part of a prolonged research from the Dutch universities of Utrecht, Nijmegen, and Delft at the river Allier, a medium sized rain-fed river in Central France. The goal of this study was to derive local flow velocities from the characteristics of local scour holes at a stretch of the river.
Readers who are interested in the characteristics of local scour holes and its relationship to the flow velocity, are referred to chapter 3 and appendix A. A field-work was part of this study and is described in chapter 4, where also the results from this field-work can be found. The shapes of scour holes at the river Allier are described more extensively in appendix B. The local flow directions are presented in paragraph 4.3.
I would like to thank the Section River Hydraulics of the Delft University of Technology for their support during this study. Henk Verheij of the WL Delft Hydraulics institute showed me into the world of scour. Special thanks go out to my daily supervisor Martin Baptist, who had always a listening ear to my problems. It was also very pleasant to work with Lara van den Bosch, a fellow-student who also studies the river Allier. Her opinions broadened my view. My gratitude goes to Rien Kremer of the department of Mathematical Geodesy and Positioning for providing us the DGPS system and for his helpful advice. The successful completion of the field-work was not possible without the help and experience from Jan Rik van den Berg, Jurgen de Kramer, and Antoine Wilbers from the university of Utrecht, and Gertjan Geerling from the University of Nijmegen. Marja, thank you for keeping the spirits high at the campground. The helping hands of Sander Vos and Jasper Dijkstra were of a great merit during the field-work. Last, I would like to thank my family and all my friends, who helped me by all means through this period.

Sander Kapinga
Delft, March 2nd, 2003

Table of contents

Summary

The subject of this study is the river Allier, a medium-sized rain-fed river in Central France and a main tributary of the river Loire. The river has a strongly varying discharge and riverbanks are generally unprotected. Hence, the river has a natural character and can migrate freely. Morphological processes proceed relatively fast. In order to get a better understanding of these processes it is of importance to have knowledge about the local flow velocities that occur during floods. The goal of this thesis is to reconstruct the local flow velocities during the flood of 2001, which could possibly be derived from the characteristics of local scour holes around large wooden debris lying on the riverbed.
Due to the interaction with the water flow and the wooden obstacle, a scour hole with a characteristic scour depth develops around the obstacle. The scour process is assumed to be similar to that around bridge piers because the shape of the scour hole around the large wooden debris resembles to the shape of the hole around a bridge pier, which is an indication that both flow patterns are equal. Empirical scour formulae predict the scour depth on the basis of local flow conditions such as water depth and approach flow velocity. These formulae are used oppositely to derive a local flow velocity from a measured scour depth. The use of different scour formulae may give insight into the correctness of the resulted local flow velocities.
This study concentrates on the last major flood event that occurred in May 2001. The calculations with scour formulae require knowledge about local water levels during the flood, the dimensions of the large wooden debris together with the scour hole, and the characteristics of the riverbed sediment. A field-work was executed to obtain most of the data. Water level measurements are unavailable at the study site implying that the estimated water levels are subjected to uncertainty.
Scour can occur in two conditions: as clear-water scour and as live bed scour. Clear-water scour occurs when there is no sediment supply from upstream. A so-called critical velocity marks the transition between both conditions. The definition of the critical velocity is among others dependent on the water depth and the sediment characteristics of the riverbed. The sediment at the river Allier consists of a mixture of sand and gravel. As a result, armouring of the riverbed occurs. The water flow erodes the smaller particles but leaves the coarser particles behind, which leads to an increase of the critical velocity. The effect of an armoured layer on the transition to live bed scour has not yet been fully understood.
The local flow velocities during a flood could not be extracted from the depth of the scour hole because of the following reasons. The main reason is the lack of knowledge about the development of the scour hole over time. Only the final situation can be regarded after the occurrence of a flood. Also it is uncertain what the local conditions at the wooden obstacles were during the flood, because the river transports considerable amount of small debris at high discharges, which could affect the shape of the object. The shape of the large wooden debris could sometimes not be schematised as a bridge pier and the maximum estimated water levels appeared to be higher than the height of most obstacles. As a consequence, the flow pattern changes and the scour formulae can not be applied. Furthermore, the scour process extends to a longer period of time than the period of the peak of the flood. Hence, these calculations are not able to predict the flow velocities that occurred at the peak of the flood, because the flow conditions before and after the peak also influenced the scour depth.
The existence of scour holes around large wooden debris indicates that the occurred flow velocities during the flood of 2001 should exceed half the local critical velocity. The highest local flow velocities are likely to occur at the upstream part of the point-bar, because the coarsest sediment and the deepest scour holes can be found here. The results of the calculations at the obstacles show the same trend. The spatial variations of the sediment characteristics are an indication that the armoured layer is in motion, which implies that the local flow velocities exceeded the critical velocity during a part of the flood. This is contrary to the results of the calculations at the wooden obstacles, which are generally lower than the critical velocity.
Experiments should be carried out to investigate the effects of changing water levels and the small debris drifting to the obstacle. These experiments could lead to a decrease in the uncertainty of the occurred conditions at the obstacle. Observations of the movement of large wooden debris during a flood also clarify the conditions under which the scour process occurs.

Notation

The following symbols are used in this document:

Δ	relative density: $(\rho_s-\rho_w)/\rho_w$ (-)
α	emperical shape coefficient for calculating the time effect of scour (-)
β	emperical shape coefficient for calculating the time effect of scour (-)
ϕ	the Wentworth scale of particle sizes: $\phi=\log_2(d)$
κ	Von Kármán constant: 0.4 m
θ	angle between the ground level and the upstream slope of the scour hole (degrees)
θ	temperature (°C.)
ρ_s	sediment density, =2650 kg/m^3
ρ_w	fluid density, = 1000 kg/m^3
σ_g	geometric standard deviation of the sediment particle size distribution: $\sigma_g= d_{84}/d_{50}$ (-)
τ	bed shear streas (N/m^2)
τ_c	critical bed shear streas (N/m^2)
υ	kinematic viscosity (m^2/s)
ψ_c	Shields critical mobility parameter (-)
A	width of the scour hole at the obstacle (m)
a	constant for the Q-h relation (-)
B	grid cell width (m)
b	constant for the Q-h relation (-)
b	width of a bridge pier or obstacle (m)
C	Chézy roughness (m$^{1/2}$/s)
D_*	sedimentological diameter of Van Rijn (-)
d_{50a}	median particle size of the armour layer (m)
d_s	depth of a scour hole compared to the ground level (m)
d_{se}	equilibrium scour depth (m)
d_w	water depth at which a wooden obstacle starts to float (m)
d_x	grain size for which x percent of the bed material is finer (m)
$e_{\pm\phi m}$	absolute error around the mean in ϕ-units
Fr	Froude number: $Fr=U/(gh)^{1/2}$
H	height of the obstacle from the ground level (m)
h	water depth (m)
h_0	representative water depth (m)
h_1	water depth at which the schematisation of a cross-section changes (m)
h_{max}	maximum occurred water depth at a scour hole (m)
i	bottom slope (-)
K_{h0b}	flow depth - foundation size (depth - size) factor (-)
K_I	flow intensity factor (-)
K_d	sediment size factor (-)
K_s	pier shape factor (-)
K_θ	foundation alignment factor (-)
K_G	apporach channel geometery (-)
K_t	time factor (-)
K_3	bed correction factor (-)
K_4	correction factor for armouring by bed material size (-)
K_w	correction factor for very wide piers (-)
K_g	factor for the influence of the gradation of the bed material (-)
k_s	equivalent roughness of Nikuradse (m)
L	length of the pier or wooden obstacle (m)
N	total number of cells (-)
R	hydraulic radius (m)

T_{50}	characteristic time scale at which the scour depth is 50% of the equilibrium scour depth (seconds, s)
t	time at which scour was active (hours, seconds)
t_e	time needed for scour hole to reach its equilibrium depth (hours)
$t_{1-\alpha/2,n-1}$	student's t statistical numerical value
U	depth averaged approach flow velocity (m/s)
U_a	depth averaged critical flow velocity of the armoured bed (m/s)
U_c	depth averaged critical flow velocity (m/s)
U_{ca}	depth averaged flow velocity for armoured bed sediment (m/s)
U_{icdx}	the depth averaged approach velocity required to initiate scour at the pier for grain size d_x (m/s)
U_{cdx}	depth averaged critical velocity for incipient motion of particle size d_x (m/s)
u_*	bed shear stress velocity (m/s)
u_{*c}	critical bed shear stress velocity (m/s)
Q	discharge (m^3/s)
Q_i	discharge in cell i (m^3/s)
Q_{tot}	total discharge (m^3/s)
Z	absolute elevation in relation to the averaged sea level at Marseille (IGN 69, m)

1 Introduction

The river Allier in central France is a main tributary of the well-known river Loire. Research at this river started in 1995, mainly in reaches upstream and downstream of the city of Moulins. Here the river has a natural character, which means that riverbanks are generally unprotected and the river is able to migrate freely. The river shows some resemblance with the river Grensmaas a hundred years ago. Therefore the river Allier was thought to be an example for the river Grensmaas after the execution of the "Maaswerken". Although both rivers appeared to be quite incomparable, research continued at the river Allier in order to gain more knowledge about natural river systems.
The river Allier is a medium-sized rain-fed river. Hence it has a strongly varying discharge with high discharge peaks, giving it a dynamic character. The morphological processes proceed relatively fast, implying the river's suitability for study purposes. In order to get a better understanding of the morphological changes of the river Allier, it is important to have a good perception of the overall flow pattern and the occurring flow velocities during floods. The morphological processes are usually described using computational models such as Delft3D. The calibration of these models is difficult because local flow velocities and flow directions are unknown during the occurrence of a flood. The goal of this study is to reconstruct local flow velocities during the flood of 2001, which could possibly be derived from characteristics of local scour holes around obstacles in the riverbed. The results of this study could possibly be used for calibration purposes of computational models.
Local scour holes originate from the interaction between the water flow and an obstacle subjected to this flow. The depth of a scour hole is one of the characteristics that may say something about the occurred flow velocities during a flood. The depth of a scour hole can be predicted using empirical scour formulae from bridge piers. These formulae calculate the scour depth that occurs at a certain flow condition (water depth and flow velocity) and time period. This study inverts the scour formulae in such way that they calculate a flow velocity belonging to a measured scour depth.
This reports acts as a final report related to a master thesis at the Delft University of Technology, Section River Hydraulics. The outline of this report is as follows: chapter 2 starts with a description of the river Allier and a problem definition. The process of local scour around obstacles is described in chapter 3. Next, the necessary data, which are obtained from a field-work executed in the summer of 2002, will be discussed in chapter 4. Chapter 5 handles the attempt to determine local water levels at the study site during the flood of 2001, followed by a discussion of the effect of graded sediment of the riverbed to the scour process. The results of the calculations at the selected scour holes are presented in chapter 7. Last, chapter 8 deals with the conclusions from this study followed by a discussion.

2 Problem description

2.1 The river Allier

The river Allier is medium-sized rain-fed river in central France. It is an important tributary of the river Loire and has a length of 410 km. The river rises in the Massif Central. The upstream part of the river Allier lies in an area with a Mediterranean climate, which implies a concentration of rainfall in spring and autumn. Summers are usually dry. Hence the river has a strongly varying discharge. The water levels in the lower course of the river Allier react strongly on rainfall in the upper reaches of the river. The peak discharge is about 1200 m^3/s; the mean discharge is 140 m^3/s whereas the river transports only 12 m^3/s at minimum discharge (Wilbers, 1997). The banks of the river Allier are

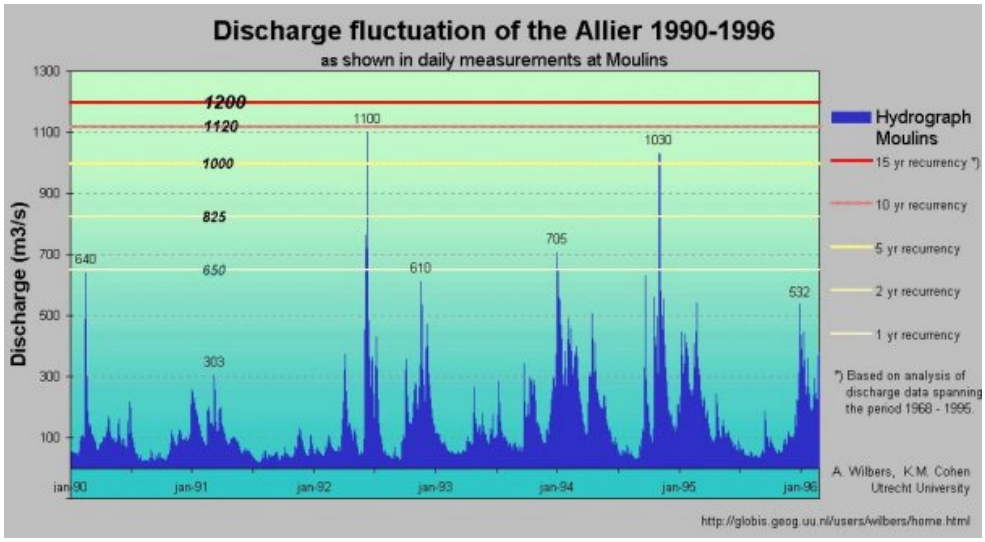

Figure 2.1: Discharge fluctuation of the Allier River (from http://globis.geog.uu.nl/users/wilbers/home.html).

mostly unprotected, which means the river has a natural character and can migrate freely. Locally, parts of the riverbanks are difficult to erode by the river due to the existence of bank protection, rock or old deposits. At the meandering section of the river, it was shown that the river could migrate up to 60 metres per year (De Kramer, 1998). So one can safely claim that the river Allier is a natural river with a dynamic character.
Research by Dutch universities on the river Allier started seven years ago. The lower coarse of the river is a gravel-bed river, which shows some resemblance to the river Grensmaas as it was hundreds of years ago. Therefore studies at the river Allier are intended to gain more knowledge about the behaviour of the river Grensmaas, which is situated at the border of Belgium and the Netherlands. The river Allier is regarded as an example for nature development on the future River Grensmaas after execution of a rehabilitation project the "Maaswerken".

Figure 2.2: Location of the river Allier. (from: Natuur Historisch Maandblad, augustus 2000)

As compared to the river Grensmaas, the river Allier shows some differences. The dimensions of the bed material is somewhat finer at the river Allier, while the bed slope is twice as steep and the discharge about twice as small as in the river Grensmaas. This means that many morphological processes are comparable in both rivers, but they will develop faster at the river Allier (Van den Berg et al., 2000).
The pattern of the river changes from the upstream to the downstream reaches. South of Moulins, the river has a meandering character, whereas a braided pattern prevails downstream of Moulins. This change in pattern can be explained from a change in characteristics of the bed material. The particle diameter becomes smaller downstream of Moulins, while the bed slope remains the same. So the transport capability of the river increases, which means that the river gradually switches to a braided pattern (Van den Berg et al., 2000).
The study site is situated South of Moulins at a meandering stretch of the river, as illustrated in figure 2.3. The area includes a double meander bend situated at Château de Lys. The western bank is locally protected at this château. It is a meandering stretch of the river and can be characterised by bend-migration and the development of large point bars. Due to this bend migration a large zone with natural vegetation can be found along the river. The vegetation type is characteristic of a natural river such as the Allier.
The bed material at the study site consists of sand and gravel. Earlier studies in this area show that there is an armoured layer at the surface. This layer has a grain size diameter d_{50} of 16 mm and d_{90} of 41 mm. Underlying this layer the sediment consist of material with a grain size diameter d_{50} of 7.7 mm and d_{90} of 34.2 mm. (Wilbers, 1997 & Cohen, 1998). The material of which this sediment consists are granite, quartz, gneiss, and basalt. At the flood plain pieces of marl can be found, which originates from a steep face at a curve

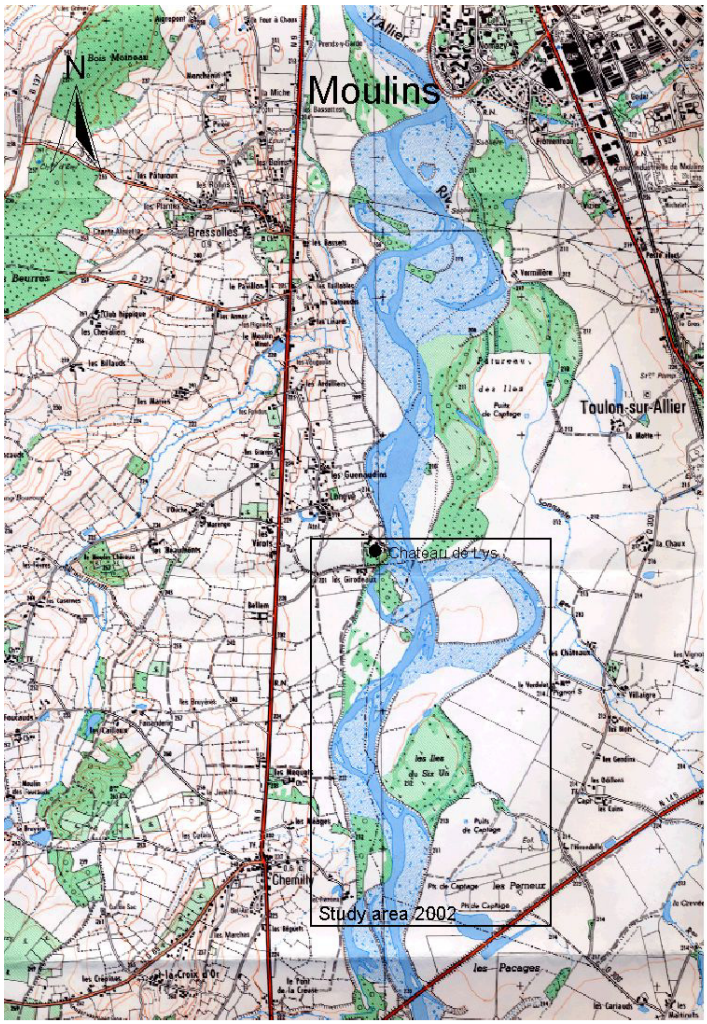

River pattern is incorrectly presented.

Figure 2.3: The study area located south of Moulins. The aerial photograph is from 2000.

upstream of this plane. At some places in the riverbed, limestone and marl reach the surface (De Kramer, 1998).

2.2 Problem statement

In order to get a better understanding of the morphological changes of the river Allier, it is important to have a good perception of the flow pattern and the flow velocities during floods. It is difficult to carry out direct measurement of the flow velocities during floods. High water levels and flow velocities restrict the possibility to do measurements and the flood comes unnoticed and the flood period lasts only a couple of days.
As mentioned before, the Allier River can migrate freely in some reaches. Trees standing along the riverbanks are being uprooted and become an obstacle in the river flow. Most of these trees are transported downstream where they are deposited at the higher point-bars. They form obstacles to the river flow. Around these obstacles scour holes develop, which may give an indication about the local current direction and the local flow velocities.
Local flow velocities during floods are unknown, but they can possibly be retrieved from the characteristics of local scour holes. The main question this thesis tries to answer is:

> *What are the local flow velocities during floods? Is it possible to determine these velocities by studying the phenomena of scouring around obstacles?*

From this main question further background questions arise:

- What is the analogy between local scour holes at bridge piers and holes that develop at uprooted trees? In other words: is it possible to model a tree stump as a bridge pier?
- In literature there are many empirical formulae available for bridge pier scouring. Which are suitable for the scour around tree trunks?
- What is the three-dimensional flow pattern around an uprooted tree? What can be concluded from this pattern?
- What are the development time scales of these local scour holes in comparison with the duration of a flood?

2.3 Problem approach

As stated above, this study aims to derive a local flow velocity during a flood from the characteristics of a scour hole. Due to the existence of large wooden debris at the riverbed, a scour hole develops around this obstacle during the flood. This study emphasizes on the flood of 2001, which was the last flood event that occurred before the start of this research. The characteristics of this scour hole may give information about these occurred local flow velocities. These characteristics could be extracted from the dimensions of the scour hole and its obstacle or the sediment properties around the scour hole. Now the question arises which characteristics could be suitable to derive the local flow velocities during a flood. The following characteristics are defined:

- Depth of the scour hole.
- Width of the scour hole compared to the width of the obstacle.
- Length and lateral position of the scour hole tail.
- The amount of accumulated sediment downstream the large wooden debris.
- The difference in sediment properties upstream and downstream the scour hole.

From the characteristics described above, the depth of the scour hole appeared to be the best indication for the occurred flow velocity. In history, the collapse of brigdes due to local scour at the bridge pier led to intensive research aiming to find a relation between the local flow conditions and the local scour depth around the pier. The necessary foundation depth of the bridge pier is dependent on the depth of scour around this pier. In literature, many emperical relationships describing the scour depth around bridge piers can be found. Some of these equations will be used. If a local scour depth is known, one can calculate the necessary flow velocity that causes this scour depth. So the outcome of the

calculations will be a flow velocity, which will cause the measured scour depth around an obstacle in the river flow.
To find an answer to the main question of this thesis the following subjects will be regarded. First it will be determined whether a large wooden debris such as a tree trunk can be regarded as a bridge pier. Next the parameters will be discussed, which are necessary to calculate with scour relations.
Besides the local scour depth, the difference in sediment characteristics upstream and downstream the obstacle will also be regarded. This difference may be a measure of the occurred flow velocity. Also the effect of the large wooden debris to the morphology of the point bar will be regarded.

3 The Process of Scouring

The research to local scour started decades ago. As a result of this research a wide variety of empirical formulae predicting local scour depths are available. Many bridges have collapsed in the past years due to damage of the bridge foundation. The main reason for this damage is local riverbed scour at the foundations of these bridges. Contrary to the structural design of bridges, which is highly advanced, local scour is a complex problem for which the unifying theory for estimating scour depths is still in an early stage. This is mainly due to the complex nature of the problem and also because river characteristics, bridge foundation geometry and soil and water interaction are different for each bridge as well as for each flood (Melville & Coleman, 2000). So, local scour around obstacles is a complex problem, which properties are not yet fully understood. The scour process is described by empirical formulae, which are based on mostly flume experiments.
This chapter will discuss the theoretical background of scouring at bridge piers. First some definitions concerning local scour will be discussed, followed by a description of the flow pattern around a bridge pier subjected to the flow. The scour process around large wooden debris may be comparable to local scour at bridge piers. The applicability of scour formulae on large wooden debris will be discussed, followed by a description of the scour formulae that are used in this study. Scour is a time dependent process, where in time different processes like erosion and sedimentation occur. This will be further explained in the last section.

3.1 Definitions in scouring

Many definitions of local scour can be found in literature. According to Schiereck (2001), scour is a special case of sediment transport that occurs when the local transport exceeds the supply from upstream. The difference in transport can be due to a difference either in flow velocity or turbulence intensity. Another definition of scour is the lowering of the level of the riverbed by water erosion. The amount of reduction below an assumed natural level is termed the scour depth. Local scour is caused by the interference of the piers and abutments (obstacles) with the water flow and is characterised by the formation of s scour hole near the bridge pier or abutment (Melville & Coleman, 2000).
From these definitions it can be concluded that the turbulence of a water flow and the local flow pattern are important factors in the scour process. Also the sediment transport conditions upstream influences the local scour depth. Local scour is a direct consequence of the interaction between the obstacle and the flow.

3.1.1 Flow patterns at obstacles

A good understanding of the flow pattern is necessary to gain insight in local scour phenomena. In recent years several papers have appeared dealing with local scour at bridge piers and abutments. Most of them are based on laboratory data and describe the behavioural pattern of scour at bridge piers. This section will describe the general flow patterns around piers and abutments.

Flow patterns around piers

Piers, when introduced to a flow, result in changes to the flow pattern. This flow pattern is complex in detail and turbulence effects cannot be neglected. The formation of a scour hole increases the complexity of this pattern. The flow pattern around an obstacle has got a three dimensional character. The principal features in the flow pattern around a pier are illustrated in Figure 3.1.

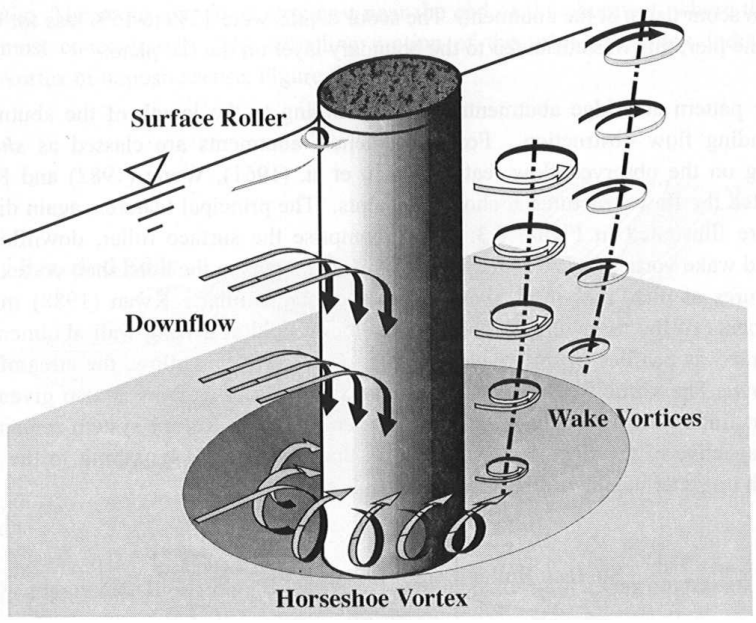

Figure 3.1: Flow pattern around cylindrical pier (from: Melville & Coleman, 2000)

The flow decelerates as it approaches the cylinder coming to rest at the face of the pier. The associated stagnation pressures are highest near the surface and decrease downwards. This resulting downward pressure gradient at the pier face generates a downflow. This downflow reaches the bed and acts like a vertical jet, which forms a trench immediately adjacent to the front of the pier. This trench initially is almost vertical and undermines the slope of the scour hole above. The slope collapses into the erosion zone, thus maintaining the slope at the local angle of repose of the sediment. The development of the scour hole creates a lee eddy, which is known as the horseshoe vortex. This vortex transports the dislodged particles in downstream direction of the pier. Raudkivi (1986) noted that the horseshoe vortex is a consequence of scour, not the cause of it. Mainly, the down flow and the horseshoe vortex are together responsible for the scour process.
The flow separates at the sides of the pier developing into wake vortices also known as the vortex street of Von Karmann. These vortices are translated downstream by the mean flow and act as vacuum cleaners transporting sediment from the bed (Melville & Coleman, 2000).

Flow pattern at short abutments

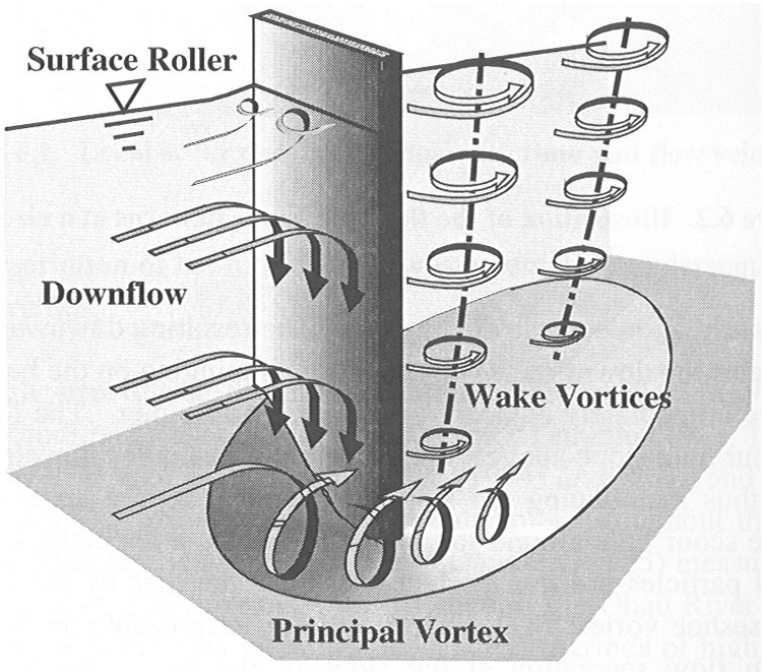

Figure 3.2: Flow pattern around abutment (from: Melville & Coleman, 2000)

The principal features of the flow pattern are very similar to those of the flow around a pier and can be found in figure 3.2. They comprise the surface roller, down flow, principal vortex and wake vortices. The principal vortex is analogous to the horseshoe vortex. The shape of the scour hole is different because the wake vortices do not influence each other, which is the case at a bridge pier.
Figure 3.3 shows the shape of the scour hole at a very wide pier. The maximum depth of scour can be found at the ends of the pier and not in the middle.

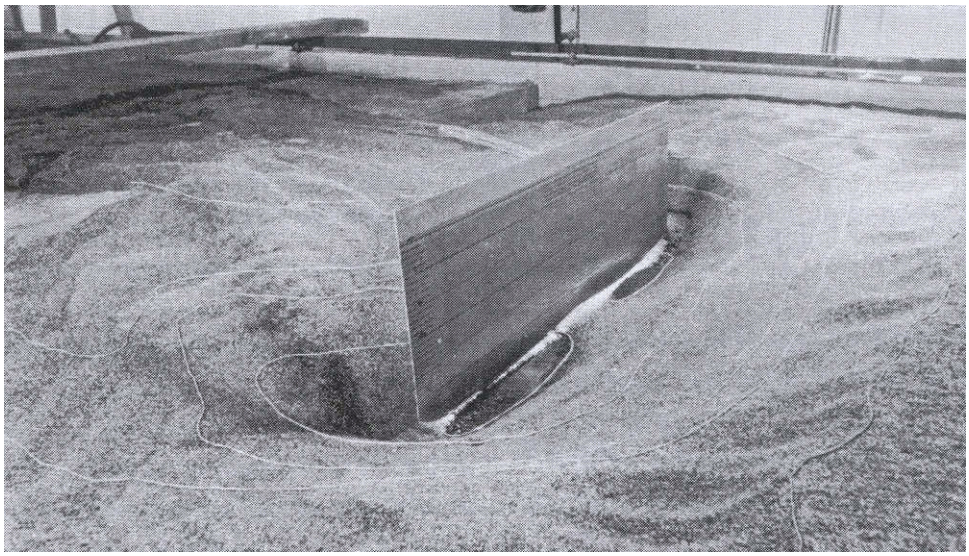

Figure 3.3: Scour at a wide pier. The maximum depth is attained at the ends of the pier (from: Melville & Coleman, 2000).

3.1.2 Geometry of a local scour hole

The main dimensions of a scour hole, which are important in local scour, are illustrated in Figure 3.4 and Figure 3.5. The obstacle, which is a detached body like a bridge pier or a tree, is hatched in grey. According to literature, the scour hole reaches its maximum depth adjacent to the obstacle. At very wide piers, maximum depth can be found at both ends of the obstacle.

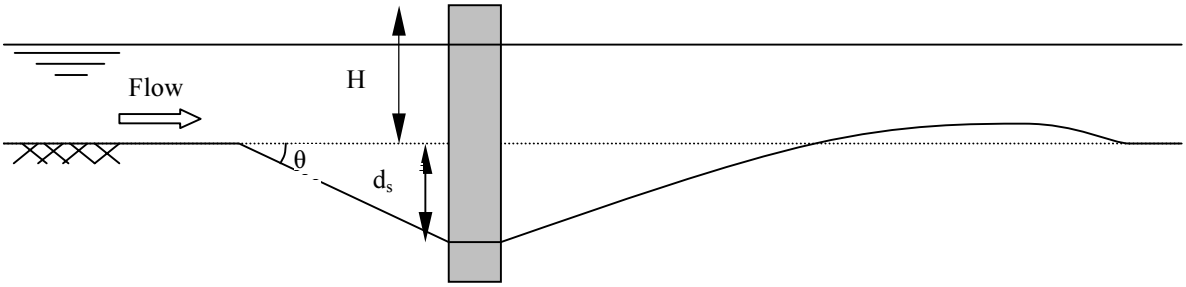

Figure 3.4: Length profile of a local scour hole

The following parameters are defined:

- H Height of the obstacle. This dimension is important when the water level at flood discharge is higher than the height of the obstacle (m).
- d_s Erosion depth in front of the obstacle measured from the ground level (m).
- θ Angle between ground level and the slope of the scour hole. This angle is close to or equals the angle of repose of the sediment.
- b Width of the obstacle (m).
- A Width of the scour hole at the obstacle (m).

The heart line (HL) defines the direction of the local flow during a flood.

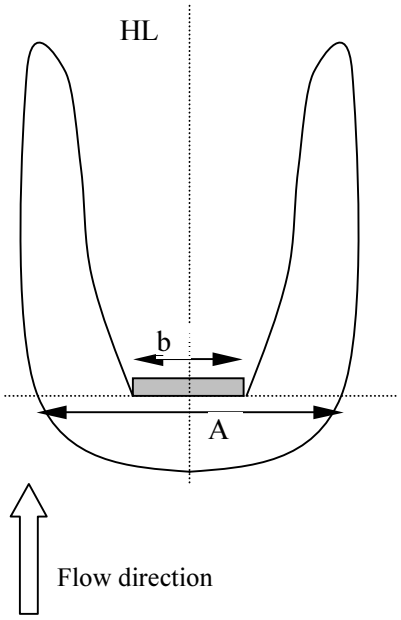

Figure 3.5: Top view of a schematised scour hole.

3.1.3 Clear-water scour and live bed scour

Local scour (and scour in general) can occur in two conditions: as clear-water scour and as live bed scour, which is illustrated in Figure 3.6. Clear-water scour is the case when there is no sediment supply from upstream while sediment is transported downstream. To predict the transition between clear-water scour and live bed scour, many formulae define a local critical velocity (U_c) for which there is no sediment supply from upstream to the scour hole. The scour depth reaches a maximum when the flow velocity is equal to the critical velocity. Further considerations regarding the definition of the critical velocity can be found in chapter 6.
As a logical consequence, live bed scour occurs for velocities larger than the critical velocity (U_c). There is sediment supply from upstream to the scour hole. Local interactions of the water flow with the obstacle cause accelerations and turbulence, which lead to a local increase in transport capacity. So more sediment is transported out of the scour hole than is supplied to the scour hole. The equilibrium scour depth under live bed conditions is attained when there is a balance between the sediment supply from upstream and that transported out of the hole (Melville & Coleman, 2000 and Schiereck, 2001).

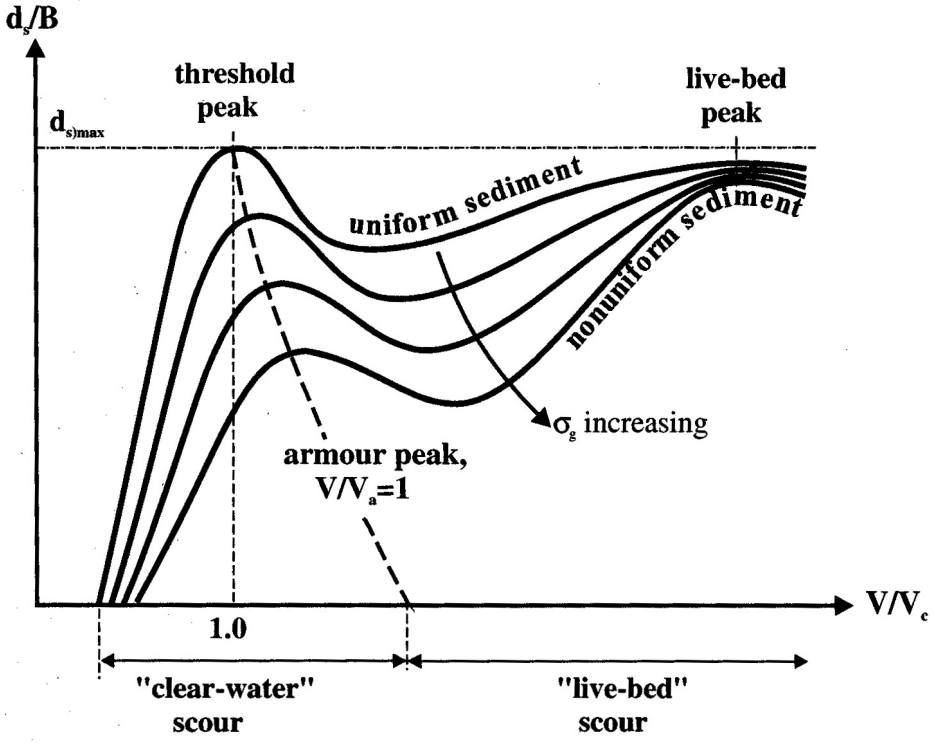

Figure 3.6: Clear-water and live-bed condition as function of the flow intensity (from: Melville and Coleman, 2000). B stands for the width of the obstacle (b). The threshold peak is when the approach velocity (U) equals the critical velocity (U_c).

3.2 Applicability of scour formulae

Now the question arises if scour relationships designed for bridge piers are able to describe the scour process at a large wooden debris such as tree trunks, which are the subjects of this study. If it is assumed that the flow pattern around a tree trunk is to a large extend similar to that around a bridge pier, scour formulae are able to describe the scour process around a tree trunk. The depth of scour and the shape of the scour hole is highly affected by the flow pattern around an obstacle. Field-work showed that the shape of the scour hole appeared to be similar to the shape of the hole around a bridge pier. This is an indication that both flow patterns can be regarded similar, but this has not been further investigated.

The shape of an obstacle also affects the flow pattern. To have similar flow patterns, the shape of the large wooden debris should be similar to that of a bridge pier. However, field study showed that sometimes the shape of the large wooden debris showed little resemblance to the shape of a bridge pier. If the shape of the obstacle results in a flow pattern that allows the existence of a downflow, scour formulae can be applied. The downflow is together with the horseshoe vortex the main scouring force.

Concluding one can say that scour formulae are applicable if the flow patterns around the wooden obstacles are similar to that around bridge piers. This is the case when the shape of these obstacles show some resemblance with the shape of a bridge pier.

3.3 Used scour formulae

There are many types of local scour formulae available in literature, which are based on experiments in laboratories or at prototypes. These formulae have an empirical background: the influence factors are presented in such way that they fit to the measurement data. As an example the influence factors according to Melville and Coleman (2000) are presented below. The relation between depth of local scour d_s and its dependent parameters can be written as:

$$d_s = f\,[\text{Flood flow, Bed sediment, Bridge geometry, Time}] \tag{3.1}$$

Among others, the flood flow is a function of:

- the fluid properties such as fluid density (ρ) and kinematic viscosity (υ)
- the mean approach flow (U)
- the flow depth (h_0).

The properties of the bed sediment can be described by:

- the median particle size (d_{50})
- the sediment density (ρ_s)

the critical mean approach flow velocity for entrainment of bed sediment (U_c).
The bridge geometry is dependent on:

- the width of the pier (b)
- the shape factor (K_s)
- the alignment of the obstacle to the flow (K_θ).

Scouring is time dependent process, which can be described by a characteristic time (t_e or T_{50}).
It can be concluded from above that the depth of local scour can be influenced by flow conditions, the riverbed sediment, the geometry of the obstacle and time. Most researches in literature use the same influence factors.
The formulae used in this study are selected on applicability: the scour formula must contain the mean approach velocity of the water because this is the unknown parameter. Secondly, the scour formulae are selected from recent publications from which it is assumed that they represent the knowledge of scour processes until now. Last the formulae should describe both clear-water scour as live bed scour.
This research uses three different types of scour formulae, which are described in appendix A. The formulae are obtained from Melville and Coleman (2000), from Richardson & Davis (2001), and from Hoffmans & Verheij (1997). The formula of Richardson & Davis is hereafter referred as HEC-18 and originates from the USA.The formula, which is referred as Hoffmans & Verheij (1997), is based on the research of Breusers et al. (1977) and find its origin in the Netherlands. Last, the formula presented by Melville and Coleman (2000) comes from the Auckland University in New Zealand.
This study tries to predict an occurred approach velocity from a certain scour depth. So a scour formula should be rewritten into the following form:

$$U = f\,[d_s, \text{Flood flow, Bed sediment, Geometry of the obstacle, Time}] \tag{3.2}$$

The influence of the approach velocity (U) to the scour depth (d_s) is mostly taken into account by a ratio between the flow velocity (U) and the critical velocity for entrainment of the bed sediment (U_c).
The formulae used in this study will be shortly discussed below, with emphasis on the relation between the flow velocity and the scour depth. A full description of the scour formulae described below can be found in appendix A.

3.3.1 Melville and Coleman

General form of the formula is:

$$d_s = K_{h_o b} * K_I * K_d * K_\theta * K_G * K_t \tag{3.3}$$

Where:

d_s = scour depth (m)
K_{h0b} = flow depth - foundation size (depth-size) factor
K_I = flow intensity factor (-)
K_d = sediment size factor (-)
K_s = pier shape factor (-)
K_θ = foundation alignment factor (=1)
K_G = approach channel geometry (=1)
K_t = time factor (-)

The general form of the formula can be rewritten as follows:

$$K_I = \frac{d_s}{K_{h_o b} * K_d * K_\theta * K_G * K_t} \tag{3.4}$$

Where K_I is the flow intensity factor specified by:

$$K_I = \frac{U - (U_a - U_c)}{U_c} \tag{3.5}$$

Where:

U = mean approach flow (m/s)
U_c = critical velocity for entrainment of sediment (m/s)
U_a = armour peak velocity (m/s)

3.3.2 HEC-18

This formula is presented by Richardson and Davis (2001) in the Hydraulic Engineering Circular no. 18 (here after referred as HEC-18). The general form of the formula is:

$$d_s = 2.0 * K_s * K_\theta * K_3 * K_4 * K_w * \left(\frac{h_0}{b}\right)^{0.35} * Fr^{0.43} * b \tag{3.6}$$

Where:

K_s = pier nose shape factor (-)
K_θ = correction factor for angle of attack of flow (-)
K_3 = bed condition factor (-)
K_4 = correction factor for armouring by bed material size (-)
K_w = correction factor for very wide piers (-)
$Fr = \frac{V}{\sqrt{g h_0}}$ = the Froude number (-)

The correction factor for armouring by the bed material uses an approach velocity. The correction factor K_4 can be written as:

$$K_4 = 0.4\left(V_R\right)^{0.15} \tag{3.7}$$

Where V_r is a function of the mean approach flow velocity, the critical velocity for incipient motion of the bed, and the approach velocity required to initiate scour:

$$V_R = \frac{U - U_{icd_{50}}}{U_{cd_{50}} - U_{icd_{95}}} > 0 \qquad (3.8)$$

Where:

U_{icdx} = the approach velocity required to initiate scour at the pier for the grain size d_x.
U_{cdx} = the critical velocity for incipient motion for the grain size d_x.
d_x = grain size for which x percent of the bed material is finer.

3.3.3 Hoffmans and Verheij

The general form of the formula is:

$$d_{se} = 1.5 K_i b \tanh\left(\frac{h_0}{b}\right) \qquad U > U_c$$

$$d_{se} = 2.0 K_i b \left(\frac{2U}{U_c} - 1\right) \tanh\left(\frac{h_0}{b}\right) \qquad 0.5 < \frac{U}{U_c} < 1 \qquad (3.9)$$

$$K_i = K_s * K_\theta * K_g$$

Where:

K_s = pier shape factor (-)
K_θ = pier alignment factor (-)
K_g = factor for the influence of gradation of the bed material (-)

According to equation (3.9), the flow velocity only influences the scour depth when there are clear-water conditions, which means that there is no sediment supply from upstream. For clear-water conditions equation (3.9) can be rewritten into:

$$U = \frac{d_{se} U_c}{4.0 K_i b \tanh\left(\frac{h_0}{b}\right)} + \frac{U_c}{2} \qquad 0.5 < \frac{U}{U_c} < 1$$

$$K_i = K_s * K_\theta * K_g \qquad (3.10)$$

Where:

b = width of pier (m)
U = approach flow velocity (m/s)
U_c = critical velocity (m/s)
h_o = flow depth (m)
d_{se} = equilibrium scour depth (m)

3.4 Effect of time on the scour process

The process of local scour is time-dependent. There are four phases in the evolution of a scour hole: an initial phase, a development phase, a stabilisation phase and an equilibrium phase. During these phases the depth of the scour hole increases until equilibrium scour depth has been reached. The development of a local scour hole around a cylindrical bridge pier is discussed below.
Local scour is a direct consequence of the flow obstruction caused by the obstacle. Scour begins when the local flow pattern is strong enough to remove bed material. The development of a scour hole is being initialised at the sides of a pier. These two shallow holes, which are adjacent to the cylinder, rapidly propagate upstream reaching the centreline of the pier. In an early stage of development, the downflow acts like a jet eroding a trench in front of the pier. The lip of this trench is often very sharp and the face almost vertical. When scouring proceeds the trench undermines the scour hole slope above. This slope collapses until the slope angle is maintained. The shape of the scour hole creates the horseshoe vortex, which intensifies the scour process. In the stabilisation phase the upstream slope of the scour hole collapses until a more or less straight slope is maintained. The scour hole has almost

reached its maximum depth (Kamil & Othman, 2002). In the equilibrium phase the trench becomes very shallow or disappears completely. The scour process stops when the local transport of sediment equals the upstream supply (live bed scour) or when the flow pattern is not able to transport material from the hole anymore (clear-water scour). The equilibrium scour depth is reached asymptotically, which is shown in Figure 3.7.

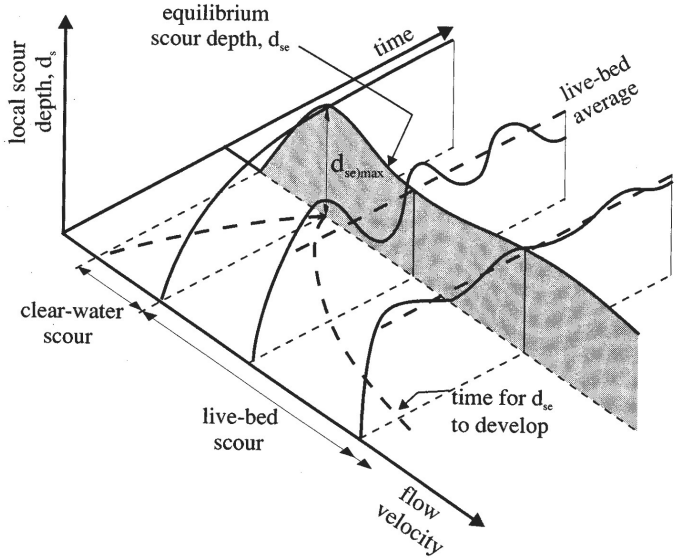

Figure 3.7: Local scour depth compared to time and flow velocity (from Melville and Coleman, 2000).

The scour process at large wooden debris in the Allier river can possibly be compared to the scour process at an obstacle in a tidal area. Because the flow velocity and the water depth vary in time in a way that half tidal cycle equals to a flood wave. Several approaches are known from literature, which describe time phenomena: the approach from Breusers (Hoffman & Verheij, 1997), from Melville & Coleman (2000), and the approach of Escarameia and May (1999). The methods use a characteristic time scale, which depends on:

- The depth averaged flow velocity (U).
- The depth of flow (h_0).
- The particle size of the bed sediment (e.g. d_{50}) and/or the critical velocity U_c, for initiation of sediment movement.

A comparison showed that the method by Escarameia and May (1999) appeared to be the best suitable. It can be applied to all obstacles, while the method from Breusers only applies for scour holes that are deeper than the width of the obstacle. Secondly the approach of Breusers uses flow parameters like turbulence intensity and characteristic velocity, which are unknown and show a wide range. So more assumptions should be made to work with this method. The approach of Escarameia and May (1999) will be described below.

Approach of Escarameia and May

The core of this method lies in the determination of a characteristic time scale. The approach to determine time effects is based on obstacles that are subjected to tidal flows. Their report describes a time scale (T_{50}), which is defined as the time taken for the scour depth to reach 50% of the final equilibrium scour value.

The relation between scour depth and time is:

$$\frac{2d_s}{d_{se}} = \left(\frac{t}{T_{50}} \right)^{\alpha} \tag{3.11}$$

where:

t = time (s).
d_s = maximum scour depth at t (m).
d_{se} = equilibrium scour depth (m).
T_{50} = characteristic time scale at which the scour depth is 50% of the equilibrium scour depth (s).
α = coefficient (-), α=0.165 for rectangular objects and α=0.327 for circular structures.

From experiments the characteristic time T_{50} scale is defined as:

$$T_{50} = \frac{5500b}{(\beta U - U_c)} \tag{3.12}$$

where:

b = width of pier (m).
U = mean approach velocity (m/s).
U_c = critical mean velocity (m/s).
β = coefficient (-), for rectangular structure β=2.67, for circular structure β=1.92.

The coefficient β is the local velocity intensification factor due to the presence of the structure. Thus βU is the effective flow velocity occurring at the obstacle when the upstream flow velocity is U. Values of β can be determined by assuming that local scouring of the bed will start to occur if $\beta U = U_c$.

3.5 Conclusions

The scour of sediment around an obstacle is being caused by the changes in the flow pattern, due to the introduction of this obstacle to the flow. The flow pattern has got a three dimensional character. The main characteristics of the flow pattern that urge the scour process are the downflow in front of the obstacle and the horseshoe vortex. Local scour can be split up in two conditions: clear-water scour and live bed scour. The first condition applies when there is no sediment supply from upstream. The latter is valid when there is general transport of the bed material upstream of the obstacle.
Scour formulae are applicable to describe the scour process around large wooden debris if the shape of the wooden obstacle can be schematised as a bridge pier. If the shape shows similarity to that of a pier, the flow pattern, which causes the scour, corresponds with the flow pattern at bridge piers.
Three different scour formulae will be used in this study, which all use the approach flow velocity to predict a local scour depth. The formulae will be used in a reverse order: the approach flow velocity will be predicted on the basis of measured scour depths at large wooden debris. The scour process is time dependent. The approach of Escarameia and May (1999) will be used to take the time effect into account because of its simplicity and general applicability.

4 Data collection

The calculations with scour formulae require the dimensions of the large wooden debris, the sediment characteristics, and also the dimensions of the scour hole. A field-work was executed in the summer of 2002 to partly obtain this data. This section will describe which information is available to proceed with this study and which methods have been used to obtain this information. The processed data will be discussed on the basis of a datasheet, which contains all necessary data to calculate with scour formulae. Last, the results of this processing, which are not related to the calculation of the flow velocities, will be presented in paragraph 4.2 and 4.3.

4.1 Description of the field-work

From July 5th to August 4th a field-work has been executed at the river Allier. The field-work had two main goals, to acquire a terrain model of the study site located near Chateau de Lys and to gather information about the dimensions of the large wooden debris with the adjoining scour holes. Moreover, the sediment characteristics of the armour layer were determined near each obstacle.
The field-work started with an investigation of suitable obstacles within the study site. Most scour holes were found at the western banks of the river because these flood plains were situated at a lower level and therefore covered a larger area. Fifteen scour holes were found suitable for further research. They were numbered, starting at the most upstream obstacle. A handheld GPS marked the positions of these holes to trace them back later on.

Figure 4.1: Measurements in progress.

Information obtained from field-work

All the data obtained at the field-work have been summarised in data sheets. The data sheets of all holes are included in appendix B. An example of a data sheet can be found below. On the basis of this sheet the way in which the field data has been obtained and processed will be explained.

Table 4.1: Example of the datasheet of hole 1. Other datasheets can be found in appendix B.

Data sheet	Hole 1						
Dimensions tree stump			**Hole visible on aerial photograph 2000?**		No		
Width of rootwad	2.36	m	**Flow direction**	Flood	42	degrees	
Height of rootwad	2.2	m		Falling Flood	87	degrees	
Surface rootwad	5.1	m^2	**Water depth when obstacle start floating:**				
Length of tree	21.3	m		dw		m	
Diameter of bore	0.65	m					

Remarks:

- Probable chance that tree was situated along the river bank in 1998
- Clear signs of different flow directions during flood stages
- After obstacle, bank level is visibly higher for about 100 metres.
- At the right side, scour is more developed than at the left side

Vegetation growth:

- Right of obstacle: line of pioneer vegetation in downstream direction
- Vegetation growth where sandy sediment has been deposited.

Grid data

Interpolation method: kriging

Residuals:				**Reference plane:**		
Minimum	-0.03878	m		Minimum	210.35	m
Maximum	0.07354	m		Maximum	210.68	m
Mean	0.00113	m		Mean	210.54	m
Standard deviation	0.02006	m		Standard deviation	0.12853	m

Scour Hole:				**Obstacle:**					
	Point #	Height			Point #	Height			
Deepest point	13059	209.28	m	Highest point rootwad	11002	212.01	m		
point for rootwad	13056	209.59	m	From highest point rootwad to edge scour hole:					
Depth of scour hole		1.26	m	Length	5.12	m	dZ	-1.42	m
Width of scour hole at obstacle		20.2	m	Left	5.2	m	Right	9.6	m

Calculated Volumes: ground surface to reference plane		
Volume above reference plane (cut)	504.2	m^3
Volume below reference plane (fill)	110.7	m^3
net Volume (cut-fill)	393.5	m^3

Sediment characteristics						
where	Before scour hole (armour layer)		After scour hole (armour layer)		average over study site (from: Driesprong, 2001)	
d_{16}	8.3	mm	7.5	mm	0.63	mm
d_{50}	17.2	mm	17.4	mm	8.40	mm
d_{80}	32.7	mm	26.2	mm	23.26	mm
d_{84}	35.4	mm	28.2	mm	25.97	mm
d_{90}	40.0	mm	31.4	mm	30.65	mm
σ_g	2.06		1.94		6.40	

Dimension of the trees

The main dimensions such as width and height of the obstacle were being measured by hand using a measuring rod or beacon. Because the root wad of the obstacle mostly had an irregular shape, the width and height of the object represent the dimensions of the root wad that are fully exposed to the flow. Photographs were taken from different angles for additional information.
The dimensions of the obstacles were measured more accurately by a real time kinetic DGPS system, which has an accuracy of 3 centimetres in the horizontal plane. Certain characteristic points of the obstacle itself were measured to outline the shape of the object. Some characteristic points are: top of root wad (highest point), end of the tree's bore and the width of the root wad. By calculating the distance between these characteristic points, the dimensions of the large wooden debris are obtained

The calculated dimensions of the tree are: width and height of root wad or obstacle, length of tree bore (if possible), diameter of the bore, and elevation of the highest point of the root wad.
The dimensions of the drifting wooden debris adjacent the main tree, which was pushed against the obstacle during the flood, have been measured separately. Drifting wooden debris is defined as wood that is not part of the main tree and that is not part of the area of the main object exposed to the water flow. The small wooden debris affects the shape of the obstacle and therefore influences the flow characteristics.
Most of these dimensions were obtained by both the GPS system as the beacon. If there appears to be a difference between the two measured values, the value from the GPS system will be used.

Flow directions

Part of this study deals with the determination of the flow directions that occurred during flood. Two points were measured at the site of each tree, which characterise the flow direction. Sometimes two different flow directions were visible: one at a flood and one when the water level was falling. Both have been measured during the field-work. The flow direction during the main part of the flood is assumed to coincide with the orientation of the tail of sediment deposition downstream of the scour hole. In most cases, the direction of the tree's bore is the same as the direction of the sediment deposition.
When the flow direction changes during a part of the flood and the new flow direction continues long enough, marks will be visible at the riverbed. In most cases these marks are streaks of fine sediments, such as sand, which orientation is in line with the flow direction. Sometimes the current was strong enough to move the coarser part of the bed material, but not strong enough to change the orientation of the large wooden debris. This resulted in an asymmetrical scour hole and the deposition of a sediment tail with the same orientation as the flow direction (see section 4.3). It turned out that the measured flow directions at the falling stage were generally more directed to the main channel.

Water depth when obstacle starts floating

The calculation of the water depth when a log starts to float is based on a force balance. In still water, a log starts to float when the gravitational forces on the log equal the buoyant force. More information about the movement of logs in a river can be found in Baudrick and Grant (2000). Their study predicted a threshold of motion for logs in rivers. Wood entrainment has been considered in relation to the force balance model acting on wood in streams. A log starts to move when its downstream forces (gravitational and drag force) and upstream force (frictional force) are balanced. The bore has been schematised as a cylinder and its root wad as a larger disk attached to this cylinder.
This study made an attempt to determine the water level at which a tree starts to float. Because the large wooden debris at the study site mostly had an irregular shape, this calculation could only be applied to a few objects.

Profile measurements

The dimensions of the scour hole have been measured more accurately by a real time kinetic DGPS system with an accuracy of 3 centimetres in the horizontal plane. First a point just in front of the edge of the scour holes was selected to represent the place of the obstacle at the point-bar. Four points in the vicinity of the scour hole were measured to represent the reference plane. Within this imaginary rectangle, the measured points represent the shape of the scour hole created by the obstacle.
An interpolation method uses these points to create a digital elevation model (DEM) of the scour hole. Different interpolation techniques have been compared in order to find the most suitable method. The best method showed the smallest difference in elevation between the measured points and the calculated points. The Kriging method was found to be the best suitable.
The calculated dimensions of the scour hole are the following:

- Scour hole depth (d_s).
- Elevation just in front of the obstacle (Z, IGN 69)
- Total width of the scour hole at the tree stump (A)

- The horizontal distance and height difference from the highest point of the obstacle to the edge of the scour hole (*H*).

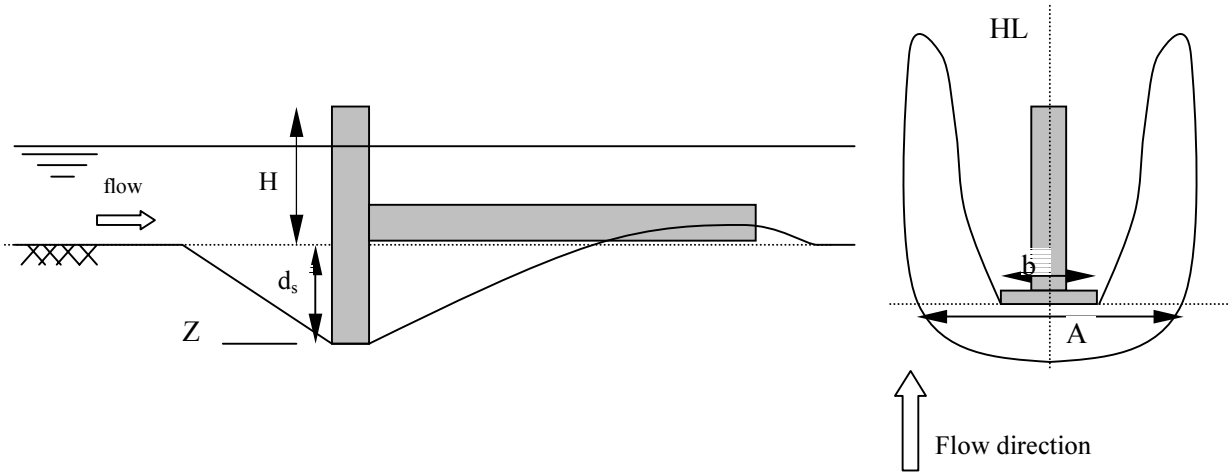

Figure 4.2: Schematised length profile and top view of a scour hole around a tree.

The scour hole depth is the difference between the elevation of the reference level and the elevation of the deepest point in the scour hole. This point lies not necessarily just before the obstacle because fine sediment fills the scour hole during the last part of the flood. These fine sediments also hinder the measurements of the maximum depth of the scour hole. The horizontal distance between the root wad and the edge of the scour hole may give an indication of the occurred maximum scour depth assuming there may be a relation between the maximum scour depth and this horizontal distance. This relation has not been further investigated and is only valid on the condition that the scour hole has been fully developed and the angle of repose under water is constant.
The elevation just in front of the root wad gives information about the elevation of the tree compared to the reference level. When the scour hole deepens, the elevation of the tree also lowers. The tree 'digs' itself into the riverbed during the scour process. So the lowest point of the tree differs from the elevation of the reference plane. The height of the obstacle is defined as the level difference between the highest point of the root wad and the reference plane. The total width of the scour hole compared to the width of the obstacle may also give information about the flow velocity. It may result in a constant factor. This assumption has not been further elaborated.

Calculated volumes

During the field-work it was noticed that the bed level downstream of the tree stump was higher than the level upstream of the obstacle. For this reason the volumes above and below the reference level have been calculated. This negative fill represents the volumes eroded by the scour process while the positive volume stands for the volume of sediment deposited downstream of the obstacle. Further information can be found in paragraph 4.2.

Grid sampling

The grid sampling method determined the sediment characteristics of the local armoured bed. This method is only suitable for coarse gravel (d>8 mm) or pebbles and has the advantage that it gives a good representation of the particle distribution of the surface layer without using much necessary equipment. A minimum of two samples was taken at each scour hole: one directly upstream of the scour holes and one downstream of the scour holes. If there was a large difference visible in particle size downstream of the scour hole two samples were taken (one of the coarser part and one of the finer part). The results of the grid sampling method together with the other sources of sediment characteristics will be discussed in section 4.4.

4.2 Calculated volumes of eroded and deposited sediment

The deposition of tree trunks on the floodplains is assumed to have morphological effects to the point-bars. The water flows around an obstacle and erodes sediment in front of the tree and deposits the sediment downstream of the tree. Now the question arises whether a tree trunk on a floodplain has a net eroding or accumulating effect to the sediment on the point-bar. Because a digital elevation model has been made, it is possible to calculate the volumes below and above a certain reference level. The outcome of this calculation can be found in Table 4.2. The volume below the reference level stands for the eroded volume in front of and at both sides of the obstacle. The volume above this level represents the accumulated bank downstream of the tree. Figure 4.3 shows a schematised view of the defined volumes.

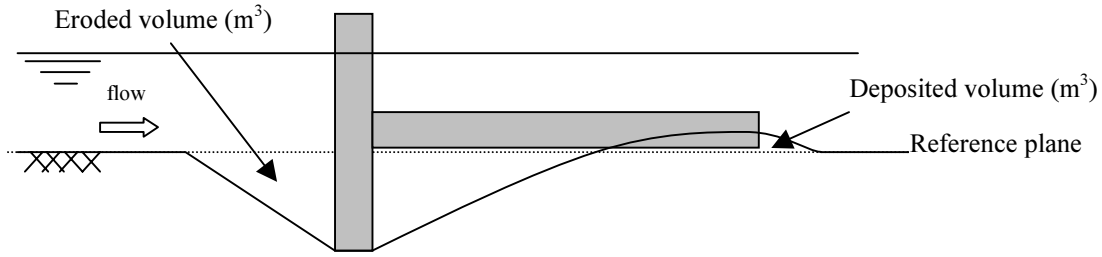

Figure 4.3: Schematised length profile of a scour hole around a tree.

Table 4.2: Calculated cut and fill volumes from reference level.

	Volume below reference level (m^3)	*Volume above reference level (m^3)*	*Net volume (m^3)*	*Place*
Hole 1	111	504	394	
Hole 2	188	464	276	southern point-bar
Hole 3	119	54	-65	
Hole 4	67	250	183	
Hole 5	134	218	84	middle point-bar
Hole 6	337	288	-49	
Hole 7	65	185	121	
Hole 8	46	140	94	
Hole 9	57	48	-9	
Hole 10	14	16	2	
Hole 11	36	73	37	northern point-bar
Hole 12	17	16	-2	
Hole 13	13	17	4	
Hole 14	99	5	-94	
Hole 15	57	94	37	
		average	67.5	m^3
		standard deviation	127.75	m^3

The figures presented above can be regarded as an indication whether an obstacle on a flood plain has a net eroding or accumulating effect. A positive net volume means that more sediment was deposited downstream of the obstacle than was eroded due to the obstacle. At larger obstacles a bank form was still visible beyond the measured area of these scour holes. This implies that the existence of wooden debris on a flood plain can have an even larger effect to the sediment deposition than presented in Table 4.2, because the measurement area does not cover the whole bank formation downstream. Figure 4.4 shows a photo of the first and most upstream obstacle, which illustrates the formation of a bank downstream of the obstacle.
During the field-work it was visually estimated that the accumulated volume of sediment downstream of the tree was usually larger than the eroded volume. This estimation seems to be correct regarding the results of this calculation, allthough the results presented in the table above show a wide range.

Also, it should be noted that some obstacles may have influence to each other: the position of hole 5 is upstream of hole 6. So the change in flow pattern at hole 5 also affects the scouring process at hole 6. Also most obstacles are small compared to the size of the point-bar. Looking at the northern point-bar near "Chateau de Lys" for example, the change in local morphology due to the wooden debris is small compared to the effects of the large scale morphological processes such as bend migration and point-bar development. If the obstacle is relatively large to the size of the point-bar and the local flow velocities are relatively high, the effects on the morphology of the point-bar can be much larger, which is illustrated by hole 1 and hole 5.

Figure 4.4: Front view of the firstan most upstream obstacle of the southern point-bar.

4.3 Local flow directions at the study area

A calculation of a local flow velocity has less meaning if the local direction of flow is unknown. So one of the aims of the field-work was to derive the local flow directions at the obstacles. Two points recorded the local flow direction. In most cases the direction of the tree's bore corresponds to the direction of the current. However, the flow directions change during a flood. Especially in the last phase of the flood when water levels are already decreasing. Measurements show that the local flow directions are slightly more directed to the main channel. The water flows from the point-bar to the main channel. The flow direction changes, but the current is not strong enough to change the direction of the tree's bore. The scour process is still active, which results most probably in an asymmetrical scour hole. The flow still moves the fine sediment, which settles at the lee side of the tree. The direction in which these mostly fine sediment are deposited stands for a second flow direction at decreasing discharges. If two directions were visible, both have been recorded. Table 4.3 shows the measured flow directions at the study site and Figure 4.5 shows the position of the scour holes with their flow direction during flood. Both measured flow directions are compared to each other in Figure 4.6.

Another sign of changing flow directions during a flood can be found in the dimensions of the scour holes. The current was strong enough to erode the bed material near the obstacle, but not strong enough to change the orientation of the large wooden debris. This results in an asymmetrical scour hole (see for example hole 1 in appendix B) and the deposition of a sediment tail with the same orientation as the flow direction. Unfortunately, flow directions cannot be derived from the dimensions of an asymmetrical scour hole, because the shape of the scour hole yields ambiguous flow directions. However, it may be an indication that flow directions have changed during the flood. It also may indicate that the flow velocities at the left and right side of the scour hole differ. This can be the case when a tree is situated at the edge of a second gully on the point-bar.

Table 4.3: Local flow directions at all obstacles in the study area.

	Flow direction (degrees from North)	
Hole NR	Flow direction during flood	Flow direction at decreasing water levels
1	42	87
2	55	
3	27	
4	284	299
5	290	305
6	322	
7	55	63
8	40	65
9	39	20
10	22	
11	10	
12	349	333
13	322	
14	267	
15	289	

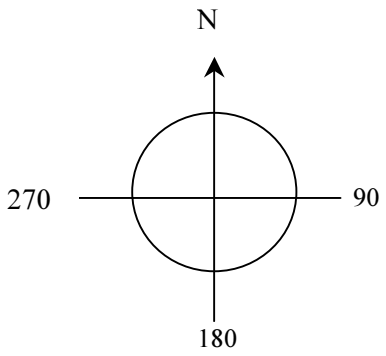

Figure 4.5: Measured flow directions at the study site. Aerial photograph originates from 2000, implying that the river course has changed since and is presented incorrectly. The numbers stand for the numbering of the investigated scour holes.

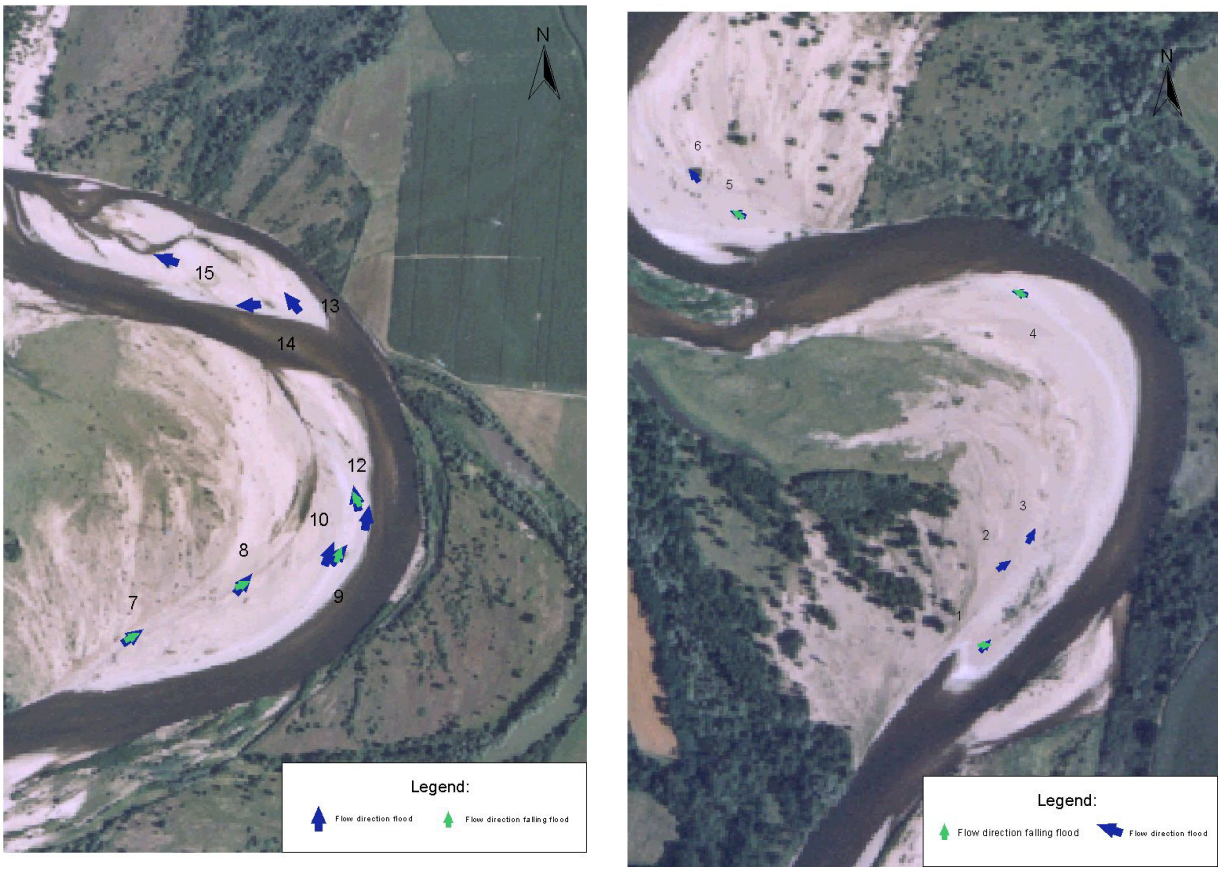

Figure 4.6: Flow directions during the flood and during the falling stage of the flood. The northern point-bar is presented on the left, while the right figure shows the southern and middle point-bar.

4.4 Particle size distributions at the obstacles

As stated before, the scour process also depends on the sediment characteristics of the riverbed. Neessen (2000) and Driesprong (2001) conducted earlier studies from which results of the latter are presented below. As a result, the averaged particle size distribution of the study area is known. Furthermore, the sediment characteristics of the local armoured bed were determined by means of grid sampling. This method gives an indication of the particle size distribution of the upper part of the armoured bed. Together with earlier measurements of the sediment in the study site, it forms a good impression of the particle size distribution in the vicinity of the scour holes.

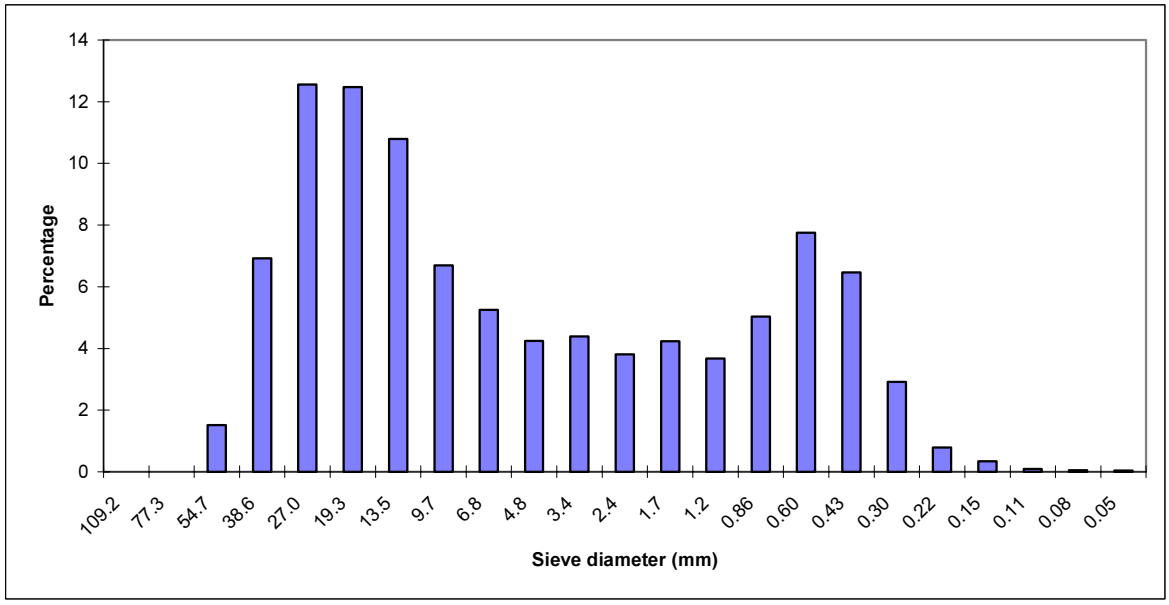

Figure 4.7: Averaged particle size distribution of the study area (from: Driesprong (2001)).

As stated before, the grid sampling method determined the sediment characteristics of the local armoured riverbed. This method is only suitable for coarse gravel (d>8 mm) or pebbles and has the advantage that it gives a good representation of the particle distribution of the surface layer without using much necessary equipment. Grid sampling needs a square net to provide an unbiased picking of the particles and a template to classify the particles. In theory, the sample size is 100 stones, but in practice the samples had a smaller size of 90 to 95 stones. It was assumed that these "missing" particles were most likely part of the smallest class (d< 8 mm) of the distribution. Most samples were corrected to fill the sample size to 100. Therefore these samples can only predict the d_{50} and d_{84} particle sizes of the gravel bed. Other sources of errors in the grid sample method are the operator error and the statistical error due to the sample size. The operator error comes from the assumption that different persons yield different particle size distributions at the same location. The statistical error due to the sample size can be estimated using the student's t test, which will be discussed in chapter 7.

Minimums of two samples were taken at each scour hole: one directly upstream of the scour hole and one downstream of the scour hole. When there was a great difference visible in the particle size of the riverbed downstream of the scour hole, two samples were taken (one of the coarser part and one of the finer part). The characteristics of the armoured bed can be found in Table 4.4.

Table 4.4: Characteristics (d_{50} and d_{90}) of the local armoured upper layer upstream and downstream of the scour holes. The last two columns state the characteristics when there was a large difference visible in the particle size of the armoured bed. The averaged particle size distribution yielded d_{50}= 8.40 mm and d_{90}= 30.65 mm (Driesprong, 2001).

	Upstream		*Downstream*		*Downstream*	
	d50 (mm)	*d90 (mm)*	*d50 (mm)*	*d90 (mm)*	*d50 (mm)*	*d90 (mm)*
Hole 1	17.2	40.0	17.4	31.4		
Hole 2	15.6	28.7	13.6	26.7	8.2	14.4
Hole 3	18.4	31.2	10.0	17.0		
Hole 4	10.8	19.1	10.0	17.0		
Hole 5	15.1	32.0	14.3	26.9		
Hole 6	14.6	26.1	15.6	29.3	12.5	20.7
Hole 7	20.8	36.1	13.4	21.0		
Hole 8	15.8	33.4	18.6	30.1		
Hole 9	15.8	28.1	13.0	21.7		
Hole 10	15.6	30.3	13.5	21.5		
Hole 11	13.8	23.4	10.9	21.4		
Hole 12	14.8	26.6	11.3	18.5		
Hole 13	13.8	22.6	15.4	26.1		
Hole 14	11.9	18.6	15.7	27.0		
Hole 15	13.5	25.4	13.4	29.7		

It was assumed that the river bed upstream of the obstacle had a coarser particle distribution than the downstream river bed. This assumption appeared to be correct at the scour holes situated at the upstream part of the point-bar. The armoured bed downstream of the obstacle was sampled because the difference in sediment size could be an indication for the difference between the occurred bed shear stress upstream and downstream of the obstacle. So, this assumption could possibly say something about the occurred flow velocities. In most cases the mean particle size was coarser at the upstream side of the tree, but local flow velocities could not be derived from this observation. Mainly because the assumption of the difference in sediment size was not generally valid.

5 Determination of water levels

5.1 Avaible water level data

The process of scour around obstacles is dependent to the depth of flow. Therefore it is important to have information about the occurring flow depths during a flood. This section deals with the determination of the occurred water levels during the flood of 2001. Finally, these water levels are used to deduct a relation between the discharge (Q) and the flow depth (h) at the designated cross-sections. To find this Q-h relation the following data are available: measured water levels at positions upstream and downstream of the river Allier and water levels deducted from photographs. These data will be discussed below.

Water levels along the river Allier

Water levels have been measured upstream and downstream of the study area. These water levels are acquired by levelling from known points along the river. Because the measurement took place in a short time period, the discharge is assumed to be constant. Table 5.1 shows these water levels. The study site is situated between Toulons sur Allier Pont R.C.E.A. and Bressolles "Les Guenaudins".

Table 5.1: Measured water level at the Allier River. The column PK indicates the distance from the confluence of the river Allier with the river Loire.

	date:	8/31/2000	12/6/2000
	discharge (m^3/s)	43.3	234
Site	PK (km)	Z (IGN 69, m)	Z (IGN 69, m)
Bessay sur Allier "Par les Rigaudets"	72.60	214.44	215.52
Bessay sur Allier "La Beaune"	70.10	212.77	214.11
Toulons sur Allier Pont R.C.E.A.	67.80	211.53	212.51
Bressolles "Les Guenaudins"	63.50	207.8	209.02
Moulins "Limnigraphe"	57.50	205.3	205.86
Moulins "Pont de Regemorte"	57.4	205.27	205.72

Water levels from photographs

The only sources of information of water levels at higher discharges are photographs from the study site. Figure 5.1 is an example of the photograph used to derive a water level from. There are two suitable pictures available of this flood, which viewpoints are illustrated in figure 5.3. These photographs were taken during a site visit in May 2001. The discharge of the river at the moment the photos were taken was not precisely known. It can only be estimated from a gauge in Moulins, which is situated downstream of the study area. The available data series of this gauge show only one value a day and it is unknown at which time these measurements took place. The time series of the discharges during in the first half of May are presented in figure 5.2.
Thus, the discharge at the time the photos were taken is unknown but is estimated to be 700 m^3/s. This value is quite arbitrary chosen. The photographs taken in May 2001 show the point where the waterline was at the time the photo was taken. The height of this point can be extracted from the digital elevation model of the study area.

Figure 5.1: Point-bar of Chateau de Lys at the 7th May 2001 (photo: J. de Kramer)

The water levels that are found in this way are subjected to errors. Furthermore, it appeared to be difficult to point the waterline on the photograph and translate this point to the digital elevation model. So it can be concluded that the water levels deducted from photographs should be regarded with care.

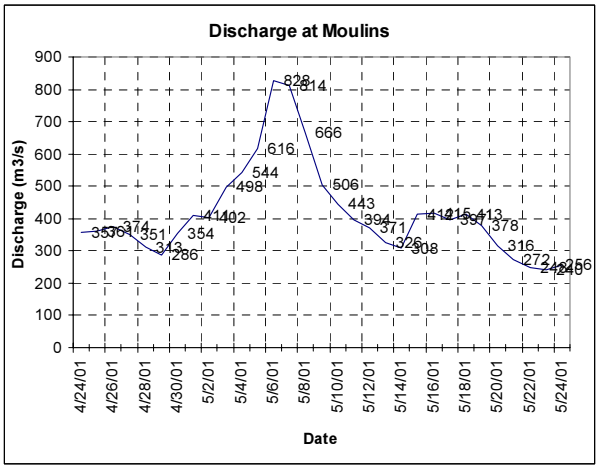

Figure 5.2: Time series of the discharge at Moulins in from April 24 to May 24 of 2001.

Cross-sections of the Allier River

During the field-work the level of the terrain has been measured by a DGPS system. Because the equipment was not suitable for wet conditions, the profile of the main channel has been levelled at characteristic points. Together with the digital elevation model, it is possible to derive the profile of a cross-section of the river. The positions of these cross-sections are shown in figure 5.3. Four cross-sections have been defined: one at the point-bar of "Chateau de Lys" (northern point-bar), one at the point-bar of "Le Verdelet" (middle point-bar), and two at the southern point-bar named South 1 and South 2. The profiles of these cross-sections can be found in appendix C.

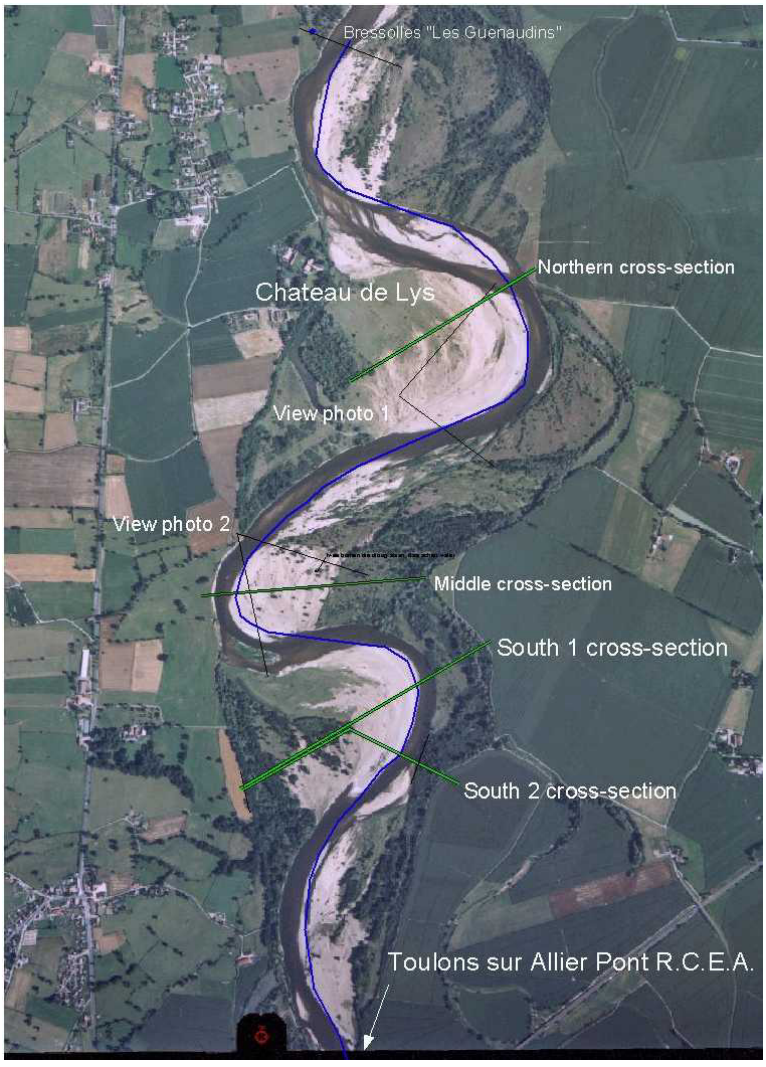

Figure 5.3: Aerial picture of the study site with the locations of the cross-sections and viewpoints of the used photographs.

Water level gradients

As stated earlier, the water levels are known for two discharges at a point upstream and a point downstream of the study site. To be able to calculate the water levels at the different cross-sections, a water level gradient must be defined. The calculation of this water level gradient requires a definition of the distance between the two points of measurement. An imaginary line represents this distance. This line can be found in figure 5.3. Because few data is available, the water level gradient is assumed to be constant along this line. The imaginary line has been positioned in such way that it should represent the water level gradient at moderate to high discharges. It must be noted that it is a very rough way to deduct these water levels. A line drawn at another place could just as well represent the places at which the water level gradient is constant. Therefore the results of these simple linear calculations should be regarded with great care and adaptions should be applied when they appear to be

necessary. The water levels at different cross-sections, which are used in the calculation, are presented in Table 5.2. The water levels at discharges 43.3 and 234 m^3/s are calculated from the measurement points upstream and downstream of the study site. At 700 m^3/s, the water levels of the northern and middle cross-sections are estimated from photos and then extrapolated to the southern cross-sections. The estimated water levels at this high discharge should be regarded with care because the water levels at the northern and middle cross-section have a great deal of uncertainty. The uncertainty at the southern cross-sections is even higher because errors in the water levels at the northern and middle cross-sections add up to the error in the southern cross-sections. Of all calculated water levels at the different cross-sections, those at a discharge of 43.3 and 234 m^3/s are assumed to be the most accurate of the data set.

Adaption of data set

With the original data set the Q-h relations were determined at each cross-section and the water levels were polated to the scour holes. It appeared that the obstacles close to the river were flooded more often than assumed on beforehand. This gave rise to further investigations. Figure 5.4 shows a photo of hole 14, which was taken during a short visit in May 2002. According to the time series of the daily discharges at Moulins, the discharge that particular day was estimated to be 55 m^3/s. According to the derived Q-h relations, the water depth at hole 14 at a discharge of 55 m^3/s should be 0.3 metres. But the picture prooves otherwise. So the water levels at the low discharge of 43.3 m^3/s have been adapted in such way that hole 14 was dry during a discharge of 55 m^3/s. Table 5.2 shows the adapted data set of the water levels. Reason that this change in the data set was a right one came from the second approach described in section 5.3.2. Before the adaption, the fit-factors of the schematised Q-h relations differ 1.5 to 2.0 times the fit-factor at a discharge of 43.3 and 234 m^3/s. After the revision both factors have become more equal to each other, which is an indication that the adaption is justified.

Figure 5.4: Scour hole number 14 at the northern point-bar. The background shows "Chateau de Lys". Photo was taken in May 2002.

Table 5.2: Data set of water levels at different discharges.

Date	8/31/2000	12/6/2000	5/5/2001
Discharge (m^3/s)	43.3	234	700 m3/s
Calculated gradient	6.48E-04	6.06E-04	7.62E-04
Cross-section:	Z (IGN 69, m)	Z (IGN 69, m)	Z (IGN 69, m)
Northern	208.34	209.80	210.80 m
Middle	209.44	210.84	212.20 m
South 1	209.98	211.34	212.73 m
South 2	210.16	211.50	212.94 m

5.2 Q-h relations

The water level data are used to derive a relation of the discharge (Q) and the flow depth (h) at each cross-section. The water depth is defined as the absolute water level minus the elevation of the lowest point of the profile. First these points are set out into graphs, which are shown in Figure 5.5. From this graph a relation between the flow depth (h) and the discharge (Q) can be derived. This relation has the following form:

$$Q = a\left(h\right)^{b} \tag{5.1}$$

where:
Q = discharge through a cross-section (m^3/s)
h = flow depth (m) from the deepest point of the profile
a,b = fit factors (-)

Because the data presented in Table 5.2 are inaccurate and because only three points are available to fit a Q-h relation, these relations do not represent the exact relation between the water depth and the discharge at each cross-section. Other relations could just as well be right. Therefore a range of relations has been defined in the following way. Assume that at a certain water level the discharge can vary. So there is an arbitrary range of discharges at each water level. Yet the magnitude of this range is unknown but the range will increase at higher discharges. So this range is proportional to the magnitude of the discharge and is assumed to be 10% of the discharge. At the southern cross-sections, the uncertainty in the discharge is even larger. Therefore that range is assumed to be 15% of the discharge. Table 5.3 shows the data used to fit the Q-h relation, which is described above.

Table 5.3: Data used to fit Q-h relation

Profile	*Lowest point profile Z (IGN, m)*	*Error in discharge (%)*	*Water depth h (m)*	*Discharge Q (m^3/s)*	*Discharge upper range (m^3/s)*	*Discharge lower range (m^3/s)*
Chateau de Lys	206.91	10 %	1.43	43.3	47.6	39.0
			2.89	234	257	211
			3.89	700	770	630
Middle point-bar	207.42	10 %	2.02	43.3	47.6	39.0
			3.42	234	257	211
			4.78	700	770	630
South 1, straight	208.28	15 %	1.70	43.3	49.8	36.8
			3.06	234	269	199
			4.45	700	805	595
South 2, bended	208.77	15 %	1.39	43.3	49.8	36.8
			2.73	234	269	199
			4.17	700	805	595

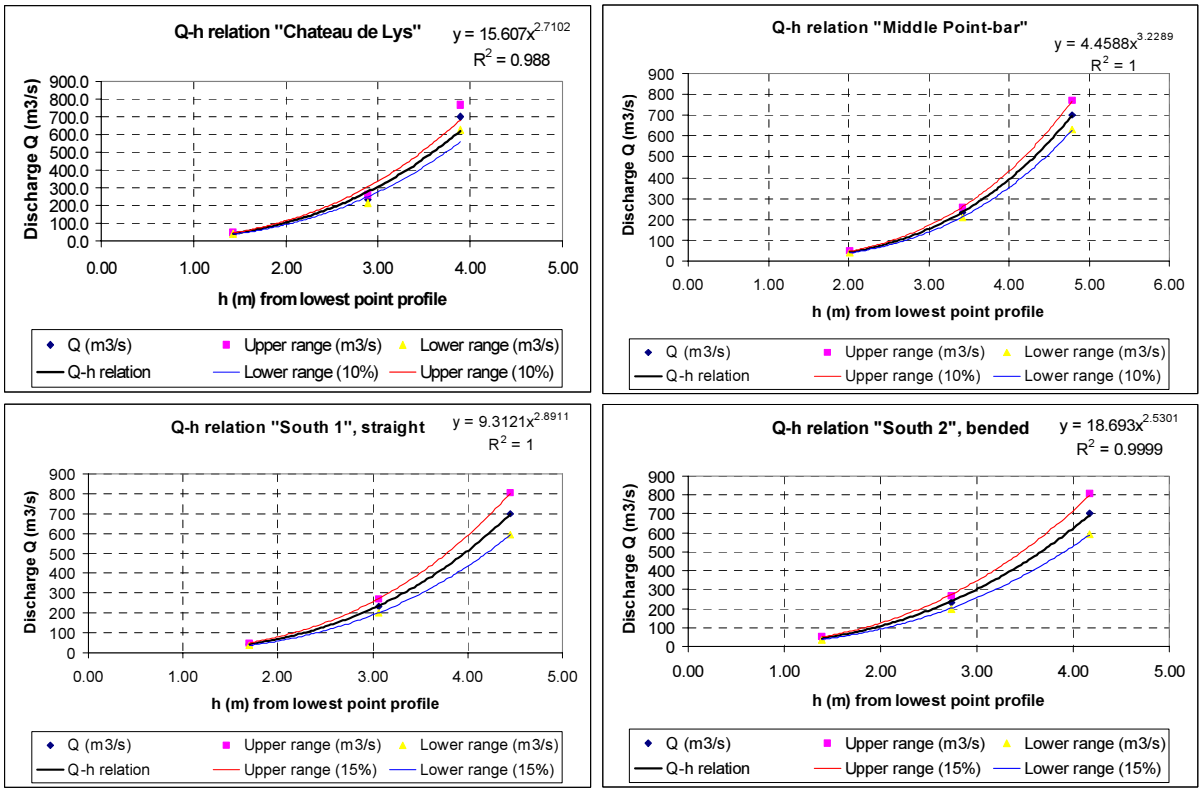

Figure 5.5: Q-h relations of different cross-sections.

From the graphs presented in Figure 5.5, the Q-h relations are deducted, which are illustrated in Table 5.4.

Table 5.4: Q-h relations of all cross-sections.

Profile	*Q-h relation*		*range of fit factor a*	
Northern point-bar "Chateau de Lys"	$Q = 15.61(h)^{2.71}$	(5.2)	lower range: upper range:	*a*= 14.05 *a*= 17.17
Middle point-bar "Le Verdelet"	$Q = 4.46(h)^{3.23}$	(5.3)	lower range: upper range:	*a*= 4.013 *a*= 4.905
South 1, straight	$Q = 9.31(h)^{2.89}$	(5.4)	lower range: upper range:	*a*= 7.915 *a*= 10.71
South 2, bended	$Q = 18.7(h)^{2.53}$	(5.5)	lower range: upper range:	*a*= 15.89 *a*= 21.50

5.3 Approach to gain confidence in the Q-h relation

The presented dataset contains the minimum required amount of dat. So an independent check of the Q-h relations is not possible. Therefore two approaches have been used to get a grip on the Q-h relations, which are presented above. It is not possible to do an independent check on these relations, because the same data set has been used. Therefore these approaches only are useful to estimate whether these Q-h relations make sense. The first approach distributes the discharge over the cross-section whereas the second approach schematises the cross-sections to derive a Q-h relation, which will be fitted to the available data. The found Q-h relation will then be compared to the relation described in section 5.2.

5.3.1 Approach 1: distribution of discharge over cells

The core of this approach lies in the distribution of the discharge over the profile of the cross-section. The profile has been split up in a number of cells. Each cell has a width, a depth and a roughness coefficient. Then the discharge through each cell can be calculated as:

$$Q_i = \frac{C_i B_i i^{1/2} h_i^{3/2}}{\sum_{j=1}^{N} C_j B_j i_j^{1/2} h_j^{3/2}} Q_{tot} \qquad (5.6)$$

where:

Q_i = discharge in cell i (m^3/s)
h = water depth (m)
N = total number of cells (-)
Q_{tot} = total discharge (m^3/s)
C = Chézy roughness ($m^{1/2}/s$)
B = grid cell width (m)
i = bottom slope (-)

The water level gradient in the formula can be discarded because these gradients are assumed to be constant over the cross-section. This distribution is only valid for prismatic channels with no secondary flows present. Appendix C shows these cross-sections and the used roughness coefficients and cell widths. This method makes it possible to get a feel of the validity of Q-h relations. At each cross-section, a possible maximum flow velocity can be calculated, which is likely to occur at various discharges. These calculated flow velocities can be compared to the visual estimated flow velocities of the flood 0f 2001. Although this method is not very scientific, it still filters the exceptions of the available data. Table 5.5 shows the possible maximum flow velocities of the various discharges at each cross-section.

Table 5.5: Possible maximum flow velocities at various discharges

	Maximum flow velocity (m/s)					
Discharge: (m^3/s)	*100*	*234*	*500*	*600*	*700*	*800*
Northern point-bar "Chateau de Lys"	1.1	1.3	1.6	1.6	1.6	1.6
Middle point-bar "Le Verdelet"	1.1	1.6	2.0	2.1	2.1	2.0
South 1, straight	1.0	1.3	1.5	1.5	1.5	1.4
South 2, bended	1.3	1.7	1.9	1.9	1.8	1.7

It must be emphasised that these data presented in the table above have no real meaning. As stated before, equation (5.6) is only valid for prismatic cross-sections. However, it mut be noted that most defined cross-sections are positioned in bends where secondary flows are assumed to exist. So the results of this method present most likely wrong values, which means that conclusions cannot be drawn from these calculations. They only indicate in what range the flow velocities could occur in a situation with given discharge and water level. From this table it can be concluded that the derived Q-h relations do not show any exceptions.

5.3.2 Approach 2: Schematisation of cross-sections

The second approach schematises the cross-section of each profile into a triangle and rectangle, which is illustrated in Figure 5.6.

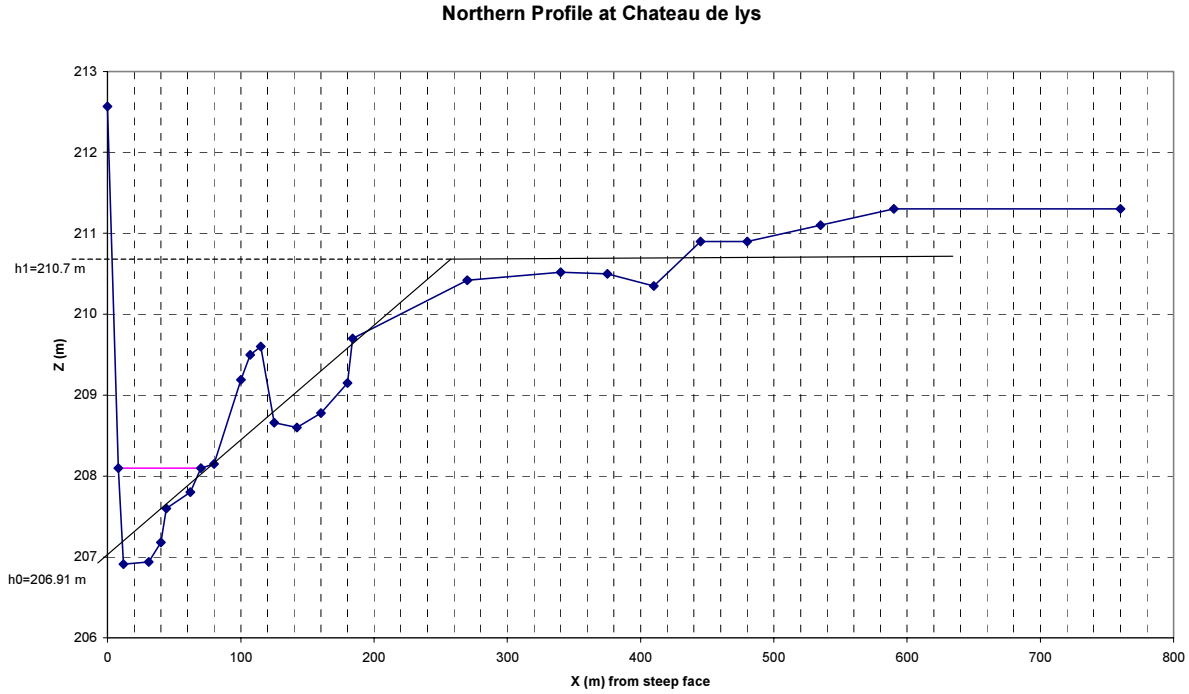

Figure 5.6: Profile of Northern cross-section at Chateau de Lys with schematisation

Below a certain flow depth h_1, the cross-section has got a triangular shape. When $h>h_1$, the cross-section is a combination of a triangular and a rectangular shaped profile. Because the width of the rectangular section is much larger than the width of the triangular section, the profile is schematised as a rectangular profile. Again the Q-h relation has the form of:

$$Q = a(h)^b \tag{5.7}$$

where:

Q = discharge through a cross-section (m3/s)
h = flow depth (m) above the water level of the summer discharge
a,b = fit factors (-)

The factor b follows from the shape of the cross-section, while the constant a is a parameter to fit the relation to the data set. For a triangular profile the value of b=2.5, which is further explained in appendix D. A rectangular cross-section has got a value of b=1.5. This results in equation (5.8) and (5.9).

For $h<h_1$ the Q-h relation is:

$$Q = a(h)^{2.5} \tag{5.8}$$

And for $h>h_1$ the Q-h relation is:

$$Q = a(h)^{1.5} \tag{5.9}$$

Now the value of a can be calculated using the water levels at different discharges, which can be found in Table 5.6.

Table 5.6: Parameters used to fit the Q-h relation.

Profile:	h_1 (m)	Q (m^3/s)	h (m)	$h>h_1$	a (-)
Northern point-bar "Chateau de Lys"	3.79	43.3	1.73	no	17.71
		234	2.89	no	16.41
		700	3.89	yes	91.24
Middle point-bar "Le Verdelet"	4.58	43.3	2.32	no	7.47
		234	3.42	no	10.84
		700	4.78	yes	66.98
South 1, straight	4.12	43.3	2.00	no	11.49
		234	3.06	no	14.31
		700	4.45	yes	74.59
South 2, bended	3.63	43.3	1.69	no	19.01
		234	2.73	no	18.93
		700	4.17	yes	82.24

The second column shows the water depth h_1 from where the Q-h relation with factor b= 1.5 should be valid. Furthermore Table 5.6 shows that there are two discharge-water level relations available to fit the Q-h relation below the water depth h_1. If a triangular profile can be justified, both fit factor should be equal. Table 5.6 also shows that the rectangular schematisation can only be fitted to one relation between discharge and water depth. As a result, this fit factor is not verifiable. So the conclusion may be that the profiles could be schematised as a triangle at lower discharges. These relations may be valid in a range around the fitted discharge. Figure 5.7 shows graphs of each profile together with the Q-h relation from paragraph 5.2.

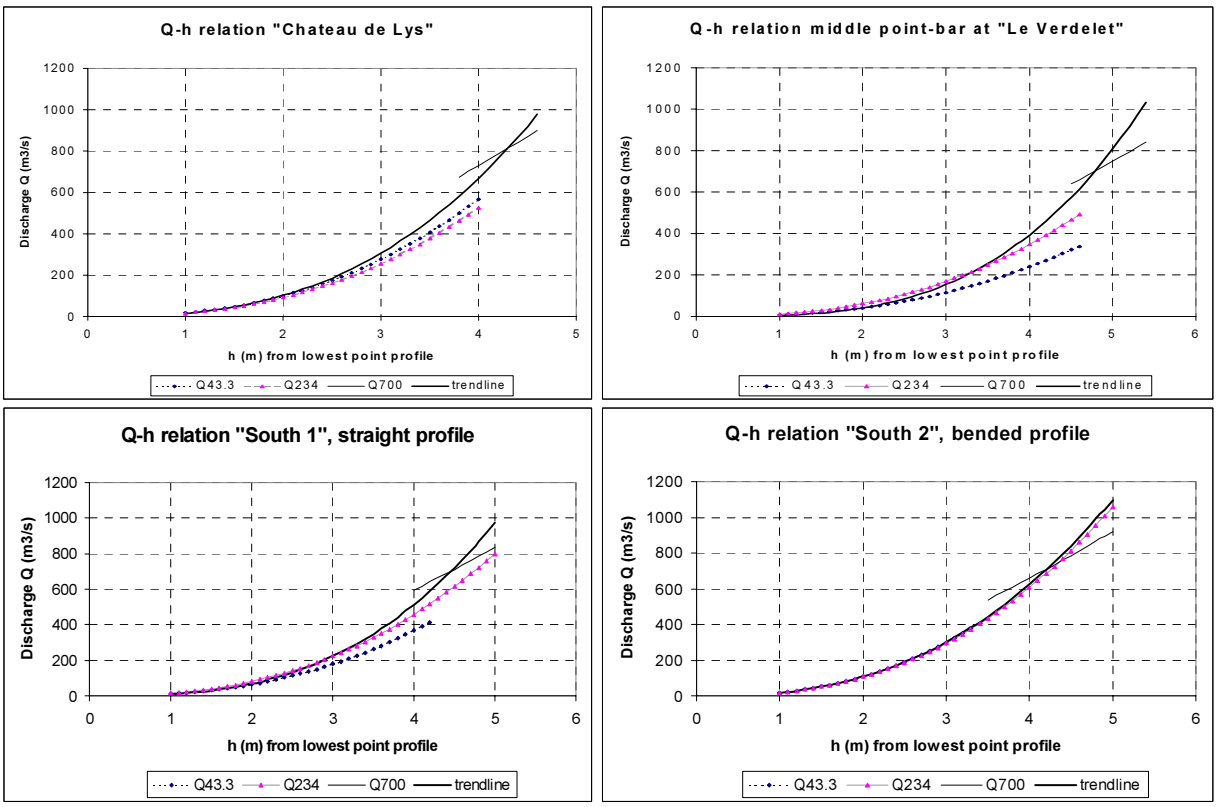

Figure 5.7: Q-h relation derived from schematisation of all cross-sections. Q43.3 stands for the fit to the discharge of 43.3 m^3/s, Q234 fits to the discharge of 234 m^3/s, and Q700 fits to the discharge of 700 m^3/s. The trend line represents the Q-h relation found in paragraph 5.2.

Now the question arises what can be concluded from these graphs in Figure 5.7? They compare the schematised profiles to the trend line fitted to the available data. Because the same data set has been used, the trend line will cross the other relations at about 43.3, 234, and 700 m^3/s. Looking at the graph of the cross-section of "Chateau de Lys" and "Le Verdelet", there is a gap between the fit to 234 m^3/s and to 700 m^3/s. The trend line connects both fits, which may be an indication that the trend line is able to represent the Q-h relation of each cross-section. But this proposition is not more than logical because the same data set has been used. At discharges above 700 m^3/s, the trend line is steeper than the schematised profile. This implies that when the discharge increases the water level increases more according to the schematised profile than according to the trend line. At these high discharges, a rectangular profile could well be assumed because the whole profile is under water. So, the schematised rectangular profile may give a better relation between the discharge and water depth. Regarding the difference between the trend line and the Q-h relations of the schematised cross-sections, one can say that the water depths are estimated somewhat too low at high discharges.

5.3.3 Conclusions

First of all one can conclude that it appeared to be possible to derive Q-h relations from a minimum of available data. These Q-h relations might not be very accurate, but they give a good indication of possible water levels at the study site. The strong point of these relations is that they provide reasonable water levels at discharges from 234 to 700 m^3/s, although the lack of intermediate data. Therefore these Q-h relations are useful because this is the range at which the scour process is assumed to be active or starts.
The few data available also implies that a good verification of the Q-h relation is impossible. Therefore one can only estimate whether these Q-h relations make sense using the techniques described above. The relations will not lead to "impossible" flow velocities when the discharge has been distributed over the cross-sections. However, it should be noted that the relations might yield too low water levels at discharges larger than 700 m^3/s. So, the relations have better predictions in the range from 200 to 700 m^3/s than at discharges larger than 700 m^3/s.

5.4 Water levels during the flood of 2001

With the Q-h relations, which are described above and the time series of the discharge at Moulins, it is possible to derive water levels at the study site. If we assume that the amount of water added to the river between the study site and Moulins is relatively small, and that the shape of the flood wave will be undeformed, the discharge in 2001 is presented in Figure 5.8. Only the discharges of 2001 will be regarded because the data of 2002 show no peaks in discharge until the field-work started. So the last major flood event occured in 2001.

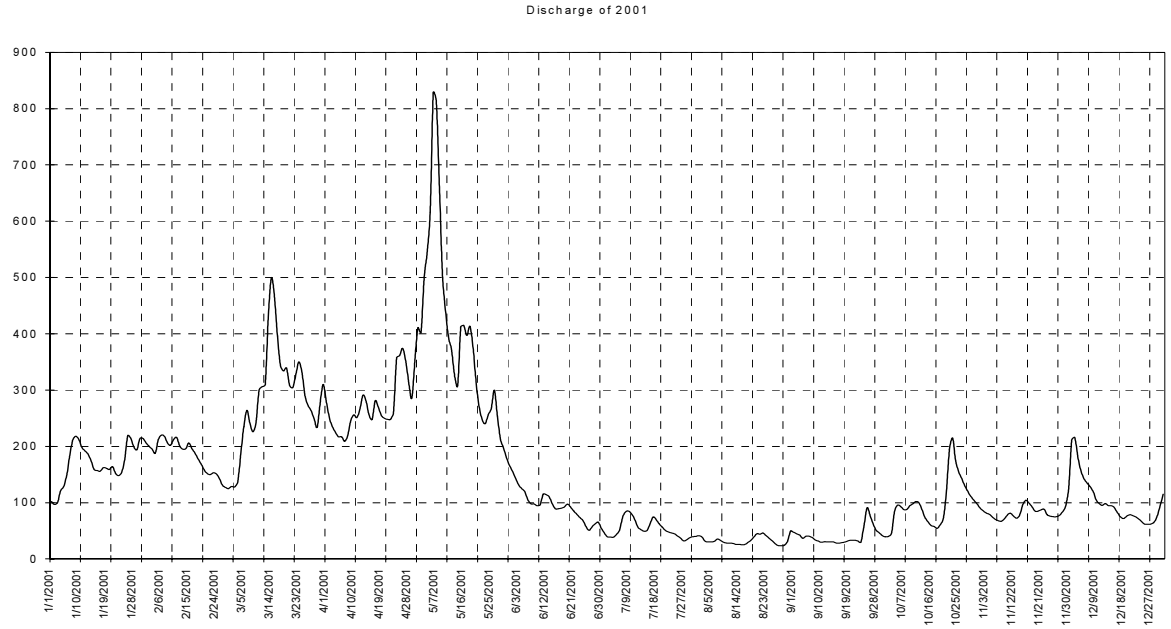

Figure 5.8: Time series of the discharge at Moulins. The flood wave reaches a maximum of 828 m^3/s at Mai 6^{th}. The summer discharge is about 40 m^3/s.

The Q-h relations in section 5.2 are only valid at the defined cross-sections. The water levels at the different scour holes are computed using a uniform gradient and a distance between the scour hole and the nearest cross-section. The gradient follows from the data set in Table 5.3. The distance is calculated along the line to which these gradients are valid. See paragraph 5.2.
Once the water levels are known at all the cross-sections, it is possible to calculate at what discharge the scour holes are flooded. Table 5.7 shows the discharges at which the scour holes are flooded. The gradient used for these calculations equals $6.2*10^{-4}$, which is somewhere between the measured gradients at a discharge of 43.3 and 234 m^3/s. This gradient has no physical meaning because it is based on a imaginary line only used to set the distance between two points.

Table 5.7: Discharges at which the scour holes are flooded. The second part of the table shows the percentage of the year 2001 at which the water depths exceeds 0,20, or 40 centimetres.

	Discharge (m^3/s) when:			Percentage of the year at which:		
	h>0 m	h>0.20 m	h>0.40 m	h>0 m	h>0.20 m	h>0.40 m
Hole 1	68	91	120	71%	57%	47%
Hole 2	195	235	280	32%	21%	13%
Hole 3	230	280	330	21%	13%	8%
Hole 4	145	180	220	41%	34%	22%
Hole 5	85	110	140	59%	47%	42%
Hole 6	215	260	310	27%	16%	11%
Hole 7	215	260	310	27%	16%	10%
Hole 8	355	425	500	7%	3%	2%
Hole 9	140	175	215	42%	35%	24%
Hole 10	195	240	290	30%	21%	12%
Hole 11	150	185	225	41%	33%	22%
Hole 12	200	240	290	31%	21%	12%
Hole 13	55	80	105	77%	65%	49%
Hole 14	55	75	100	77%	67%	50%
Hole 15	135	165	205	42%	35%	27%
			average:	42%	32%	23%

The discharge described in the table above should be regarded with care. During our stay in the summer of 2002, the discharge was estimated to be 40 to 50 m^3/s and none of the obstacles were flooded, although some scour holes were filled with ground water. Another reason to be careful is the very limited data set, which is used to calculate the water levels. So, the meaning of the second column and the fifth column can be questioned. Which conclusions can then be drawn from Table 5.7? The scour holes are flooded at a lower discharge than estimated beforehand. Also it can be concluded that the obstacles have been subjected to water for about 40 to 50 percent of the year 2001.
Now the question arises at which point the scour process starts. It is unlikely that the scour process immediately starts when the obstacle are flooded, because the local flow velocity will be small at the start of flooding of an obstacle. With increasing discharge, also the flow velocity and water level will increase until a condition will be reached that the scour process starts. This flow condition is unknown, so the point at which scour starts will be mostly arbitrary chosen. Unfortunately, there is no relation available, which predicts at which discharge the scour process starts. But with the knowledge that the scour holes are flooded for a long period, one can say that the time effect might be neglected for the larger part of the obstacles.

Maximum water depths

Also it is possible to estimate the maximum occurred water depths at each scour hole. The range of maximum water depths can be found in Table 5.8. The used gradient in these calculations is $7.5*10^{-4}$. The effect of the gradient on the water levels is small compared to the effect of the range of Q-h relations discussed in paragraph 5.2. So the effect of an inaccurate chosen water level gradient can be neglected.

Table 5.8: Estimated maximum water depths at each scour hole. The upper and the lower value follows from the range in the Q-h relations. The last columns shows the height of the obstacles above the ground level.

	Mean h (m)	*Lower value* h (m)	*Upper value* h (m)	*Height of obstacles* (m)
Hole 1	2.82	2.58	3.12	1.47
Hole 2	1.96	1.72	2.26	2.25
Hole 3	1.76	1.51	2.05	0.58
Hole 4	2.11	1.89	2.39	1.32
Hole 5	2.56	2.41	2.72	2.18
Hole 6	1.75	1.60	1.92	1.46
Hole 7	1.81	1.66	1.98	1.67
Hole 8	1.24	1.09	1.41	2.20
Hole 9	2.13	1.98	2.31	0.64
Hole 10	1.83	1.68	2.01	0.59
Hole 11	2.08	1.93	2.26	1.60
Hole 12	1.82	1.67	1.99	0.47
Hole 13	2.71	2.56	2.88	0.78
Hole 14	2.72	2.57	2.89	0.73
Hole 15	2.09	1.94	2.26	1.03

The last column in Table 5.8 shows the height of the various obstacles above the local ground level. When these values are compared to the maximum water depths, the conclusion is that water levels are higher than the height of the tree. So either water flows over the tree during the occurance of a flood or either the tree was not run aground at the moment of the maximum flood levels. When water is flowing over the tree the scour formulas may not be valid. This problem will be discussed in chapter 7.

6 Critical Velocity

Beside the water depths, a critical velocity is also necessary to calculate with scour formulae. This section deals with the different definitions of the critical velocity, which distinct the transition between clear-water scour conditions to live-bed conditions. Because the maximum scour depth and the time to attain this differ for the clear-water and live bed conditions, it is important to identify the conditions of movement (Melville & Coleman, 2000). The critical velocity marks the transition between these conditions and is defined as the flow depth averaged velocity at which there is incipient motion of the bed material. There are different approaches to calculate this critical velocity. These schemes are stated below and originate from Melville and Coleman (2000), from Hoffmans (2002), and from Richardson and Davis (2001) (referred as HEC-18).

6.1 Approaches to critical velocity

6.1.1 Concept of Shields

Shields (1936) chose the bottom shear stress as the active force of erosion. The critical bed shear stress is defined as:

$$\tau_c = \rho u_{*c}^{\ 2} \tag{6.1}$$

or in dimensionless form:

$$\Psi_c = \frac{u_{*c}^{\ 2}}{\Delta g d_{50}} \tag{6.2}$$

where:

ρ = fluid density (kg/m^3)

Δ = relative density: $\frac{\rho_s - \rho_w}{\rho_w}$

d_{50} = median particle size (m)

u_{*c} = critical bed shear velocity (m/s)

Ψ_c = critical mobility parameter (-)

For a uniform flow (logarithmic profile) over a hydraulically rough bed the depth averaged critical velocity U_c is:

$$U_c = u_{*c} \frac{C}{\sqrt{g}} \tag{6.3}$$

with C as the Chézy constant, which is defined as:

$$C = \frac{\sqrt{g}}{\kappa} \ln \frac{12R}{k_s} \tag{6.4}$$

where:

k_s = equivalent roughness of Nikuradse (m), hydraulically rough flow: 3*d_{90}, hydraulically smooth flow: 2*d_{50}.

R = hydraulic radius (m)

κ = Von Kármán constant = 0.4 (-)

Hydraulically rough conditions apply when the dimensions of the particle sizes of the bed are larger than the thickness of the viscous sub-layer. For hydraulically smooth flow the thickness of the viscous sub-layer is large compared to the particle sizes.

If the width B is much larger than the flow depth h_0, the hydraulic radius R can be replaced by h_0. Equation (6.3) can then be written as:

$$U_c = 2.5\sqrt{\Psi_c \Delta g d_{50}} \ln\left(\frac{12h_0}{k_s}\right) \tag{6.5}$$

where:

h_0 = water depth (m)

The critical mobility parameter Ψ_c range from 0.03 to 0.055. At values of 0.03, occasional movement of single particles may occur. There is general movement of particles at a value of 0.055. Van Rijn (1993) gives an empirical relationship between the critical mobility parameter Ψ_c and the mean particle size. The critical Shields parameter is related to the sedimentological diameter D_* and can be given by:

$$D_* = d_{50}\left(\frac{\Delta g}{\upsilon^2}\right)^{1/3} \tag{6.6}$$

where:

ν = kinematic viscosity (m2/s): $\upsilon = \dfrac{40*10^{-6}}{20+\theta}$

θ = temperature (°C.)

For all holes it can be calculated that D_*>150, which means that according to Van Rijn the critical mobility parameter Ψ_c is equal to 0.055.
The equivalent roughness of the bed is usually related to the largest particles of the bed. According to Van Rijn (1993), the equivalent roughness of a plane movable bed varies from about 1 to 10 times d_{90} of the bed material. These values, which are rather large, indicate that a completely plane bed does not exist for conditions with active sediment transport (Hoffmans & Verheij, 1997). The assumption of k_s=2d_{50} is valid if no transport occurs (Ψ_c << 0.03). When particles are transported, the roughness of the bed will increase (Hoffmans, 2002).

6.1.2 Melville and Coleman

Melville and Coleman (2000) give an emperical relationship between the d_{50} of the bed and the critical shear stress velocity u_{*c}. This relation is:

$$u_{*c} = 0.0305 d_{50}{}^{0.5} - 0.0065 d_{50}{}^{-1} \tag{6.7}$$

where:

d_{50} = median particle size (m)

This formula is valid for quartz sand with 3<d_{50}<100 mm and a water temperature of 20 °C. It is based on the concept of Shields. Equation (6.2) can be rewritten to:

$$u_{*c} = \sqrt{\Psi \Delta g d_{50}} \tag{6.8}$$

With a Shields parameter Ψ_c of 0.055 this relation yields:

$$u_{*c} = 0.9435\sqrt{d_{50}} \tag{6.9}$$

Equation (6.9) yields the same result as (6.7). So the u_{*c} corresponds with the u_{*c} of Shields for Ψ=0.055. The depth averaged critical flow velocity is then calculated by:

$$U_c = 5.75 u_{*c} \log\left(5.53 \frac{h_0}{d_{50}}\right) \tag{6.10}$$

where:

h_0 = water depth (m)

This formula equals the formula stated at the Shields concept, with the use of an equivalent roughness of k_s=2.2*d_{50}.

6.1.3 HEC-18

In the HEC-18 formula, the critical velocity is defined as:

$$U_{cd_{50}} = 6.19 \left(h_0\right)^{1/6} \left(d_{50}\right)^{1/3} \tag{6.11}$$

where:

U_{cd50} = the critical velocity for incipient motion of particle size d_{50} (m/s).
d_{50} = median particle size (m)
h_0 = water depth (m)

The critical flow velocity defined above presents the same results as the Shield concept using a critical mobility parameter (Ψ_c) of 0.043 and the assumption of a hydraulic smooth bed (k_s= 2*d_{50}).
This relation has the same form as a formula given by Neill (1968), which is used as an example by Melville and Coleman (2000):

$$U_c = 1.41 \sqrt{\Delta g d_{50}} \left(\frac{h_0}{d_{50}}\right)^{1/6} \tag{6.12}$$

The form of (6.12) can be obtained by using the Manning and Strickler equations and the Shields parameter. With Δ=1.65 equation (6.12) becomes:

$$U_c = 5.67 \left(h_0\right)^{1/6} \left(d_{50}\right)^{1/3} \tag{6.13}$$

So equation (6.11) is similar to (6.13). The HEC-18 formula only uses a slightly larger constant.

Conclusions

Concluding one can say that both the formulas of Melville and HEC-18 are based on the concept of Shields. So it is possible to determine the equal Shields parameters for these formulas. The formula of Melville uses a critical mobility parameter (Ψ_c) of 0.055 and an equivalent roughness of Nikuradse k_s=2.2d_{50}. The other formula, HEC-18 produces the same results compared to the Shields concept with a Ψ_c of 0.043 and also an equivalent roughness of Nikuradse k_s=2d_{50} (hydraulically smooth flow).

6.2 Graded sediment

The effect of graded sediment is also an important factor in predicting the hydraulic conditions at which live bed scour occurs. The bed sediment in the river Allier consists of a mixture of sand and gravel, which is illustrated in Figure 6.1. Due to the distribution of the sediment, an armouring of the bed occurs. In principle armouring is an erosive phenomenon. The water flow erodes the smaller particles from the bed but leaves the larger particles behind. As a result, the riverbed consists of a coarser upper layer, which protects the sub-layer.
The armouring leads to an increase in the critical shear stress velocity of the riverbed. The depth averaged critical velocity increases, which delays the transition to live-bed scour. An armour layer only breaks up when the bottom shear stress is high enough to erode the larger particles of the bed. If during a flood the bottom shear stress exceeds a critical bottom shear stress for the larger particles one speaks of a dynamic armour layer. There is an exchange between the coarse particles of the bed and the coarse particles from the sediment supply upstream. At this point, also the fine sediment of the bed is being transported from the bed. As a characteristic of the occurrence of a dynamic armour layer, the riverbed shows a large spatial differentiation in sediment particle sizes. The existence of a dynamic armour layer is characteristic for rivers with a considerable supply of coarse sediment such as the river Allier (Kleinhans et al., 2000).

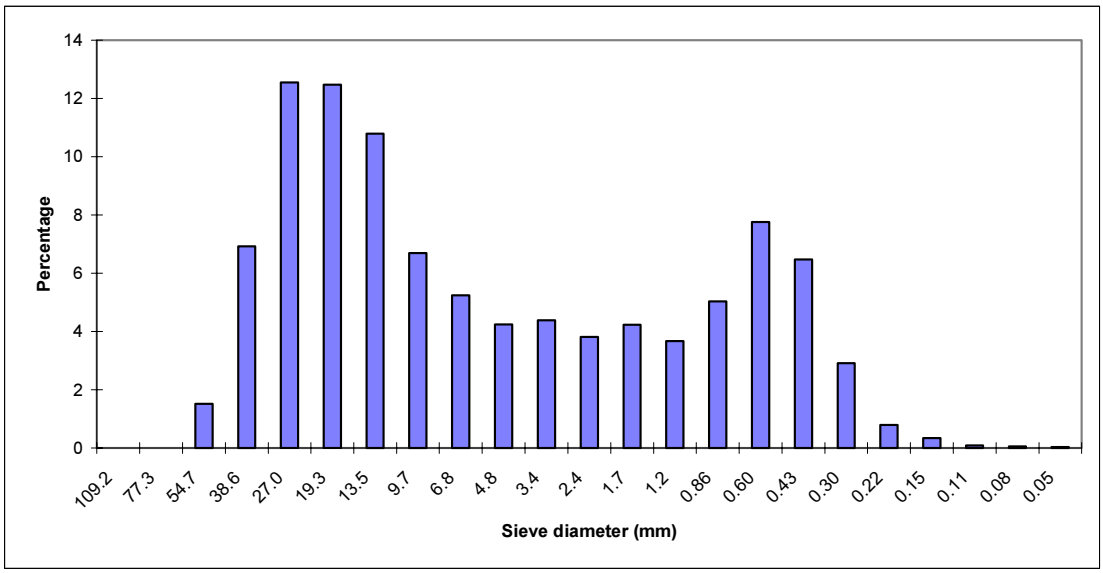

Figure 6.1: Averaged particle size distribution at the study area (from Driesprong, 2001).

For this research the following data of the riverbed sediment distributions are available. Earlier study from Driesprong (2001) presents an averaged sediment distribution at the study site, which is shown in Figure 6.1. The particle size distribution of the armoured bed upstream and downstream of each obstacle has been measured in the summer of 2002. These distributions show spatial variations of the particle sizes, which is an indication of the existence of a dynamic armour bed in the river Allier. Table 6.1 shows the variation in the mean particle diameter.

Table 6.1: d_{50} and d_{90} of the particle size distributions at the study site.

	d50 (mm)	d90 (mm)	
General	8.40	30.65	from Driesprong (2001)
Hole 1	17.23	40.04	southern point-bar
Hole 2	15.62	28.68	
Hole 3	18.43	31.16	
Hole 4	10.79	19.14	
Hole 5	15.05	32.00	middle point-bar
Hole 6	14.59	26.14	
Hole 7	20.83	36.13	northern point-bar
Hole 8	15.80	33.42	
Hole 9	15.81	28.10	
Hole 10	15.58	30.34	
Hole 11	13.77	23.35	
Hole 12	14.81	26.64	
Hole 13	13.85	22.63	
Hole 14	11.92	18.56	
Hole 15	13.45	25.40	

The first row indicated as "general" shows the d_{50} and d_{90} of the particle size distribution obtained by Driesprong (2001). Hole 1, 5 and 7 are situated at the upstream part of each point-bar. Hole 4, 14, and 15 lie at the downstream side of the point-bars. It can be concluded that the sediment of the riverbed becomes smaller in the downstream direction at each point-bar.

Transition to live bed scour

As stated above there are different methods to calculate the critical velocity. This section deals with the question in which way these methods will be applied to this study. The used scour formulae present different ways in which the transition to live bed scour is implemented. The critical velocity marks the transition between clear-water and live bed scour. According to Melville & Coleman (2000), live bed scour occurs when sediment is continuously supplied to the scour hole. The equilibrium depth is attained when there is a balance between the sediment supply and that transported out of the scour hole. So at live bed conditions, the equilibrium scour depth also depends on the sediment transport rate rather than being influenced by the flow characteristics alone. Therefore the sediment must be transported at a reasonable rate in order to have influence to the depth of the scour hole.
Now the question arises what the effect is of an armour layer on the sediment transport and on the value of the critical velocity. Each formula used in this study shows a different approach to take the effect of armoured riverbed into account. The formula of Melville and Coleman (2000) uses the following flow intensity parameter (see also appendix A):

$$K_I = \frac{U - (U_a - U_c)}{U_c} \tag{6.14}$$

In which U_a represents the effect of armouring of the bed. If $U/U_a<1$ armouring of the bed occurs as scour proceeds and clear water conditions are considered to exist. The value of U_a is calculated by:

$$\begin{aligned} d_{50a} &= \frac{d_{\max}}{1.8} \\ u_{*ca} &= 0.0305 d_{50a}{}^{0.5} - 0.0065 d_{50a}{}^{-1} \\ \frac{U_{ca}}{u_{*ca}} &= 5.75 \log\left(5.53 \frac{h_0}{d_{50a}} \right) \\ U_a &= 0.8 U_{ca} \end{aligned} \tag{6.15}$$

The calculations executed in chapter 7 will use the averaged particle size distribution of the study area, because the effect of armouring is taken into account.
The formula of from Richardson and Davis (2001), named HEC-18, has a different approach to take the effect of armouring into consideration, which is also explained in appendix A. This formula defines a parameter V_R:

$$V_R = \frac{U - U_{icd_{50}}}{U_{cd_{50}} - U_{icd_{95}}} > 0 \tag{6.16}$$

U_{icdx} = the approach velocity required to initiate scour at the pier for the grain size d_x.

$$U_{icd_x} = 0.645\left(\frac{d_x}{b}\right)^{0.053} U_{cd_x} \tag{6.17}$$

U_{cdx} = the critical velocity for incipient motion for the grain size d_x.

$$U_{cd_x} = 6.19\left(h_0\right)^{\frac{1}{6}}\left(d_x\right)^{\frac{1}{3}} \tag{6.18}$$

d_x = grain size for which x percent of the bed material is finer.
Equation (6.16) is substituted in a factor K_4. The correction factor K_4 equals:

$$K_4 = 0.4\left(V_R\right)^{0.15} \tag{6.19}$$

This factor K_4 decreases scour depth for armouring of the scour hole. It is applicable for bed materials that have a d_{50} equal to or larger than 2.0 mm and d_{95} equal to or larger than 20 mm. Both the mean particle size distribution as the distribution of the armour bed will be used in the calculations described in chapter 7. The results of Equation (6.18) are about 10 percent larger than the results of equation (6.13) by Neill (1968). The use of the critical velocity defined by HEC-18 leads to lower values of K_4 compared to the use of the definition of Neill (1968). Lower values of K_4 lead to larger results of the approach velocity because the predicted scour depth decreases when K_4 decreases.
The formula presented by Hoffmans and Verheij (1997) only defines a critical flow velocity in which the effect of armouring is taken into account. Now the question arises which flow conditions should be used to set this critical flow velocity (U_c). To answer this question first the available sediment data will be considered that will be used in the calculation of the critical velocity. Earlier studies give an averaged particle size distribution of the study area. This distribution also shows the finer sand fraction of the bed sediment. Secondly, a particle size distribution of the armour layer upstream and downstream of each scour hole has been measured in the field-work related to this research. The method used to yield this distribution is only valid for particles larger than medium gravel (>8 mm). The advantage of the use of the d_{50} of the armour bed is that it takes the spatial variations of the sediment into account. According to Melville and Coleman (2000) the critical velocity is approximately equivalent to competent velocity for a sediment, where the latter is the averaged (possibly including a safety margin) for a channel flow that does not erode the bed. Melville and Coleman (2000) gives a reference to Harris (1988), who recommends to adopt the competent velocity based on the d_{80} of sediment size for an armouring effect. The d_{80} particle size of the averaged sediment distribution is 23.3 mm, which is somewhat larger than the d_{50} of the armour bed. Hence, the particle size distributions of the armour bed at each scour hole will be used to calculate the critical velocity.
Next the flow conditions at which live bed scour starts should be determined. The critical mobility parameter (Ψ_c) related to the sediment characteristics of the armour bed has to be defined, as well as the equivalent roughness (k_s). The specific behaviour of an armour bed under flow is yet to be discovered, so a well-considered choice of these parameters is preferred. We regard an armour bed together with a certain flow condition. The bed shear stress velocity (u_*) is strong enough to move the finer part of the particle sediment distribution, but leaves the coarser particles at their places. Increasing flow velocities will lead to higher bed shear stresses until there is a moment at which the armour bed starts to erode. All sizes in the sediment distribution are now in motion. The occurring bed shear stress velocity (u_*) will be equal or higher than the critical shear stress velocity of the armour bed (u_{*ca}). This moment can be regarded as the threshold of movement for the armour bed. It is possible to calculate the critical flow velocity for the armour bed (U_{ad90}) using a critical mobility

parameter (Ψ_c) of 0.03 and the d_{90} of the particle size distribution of the armour bed. Results of this computation can be found in Table 6.2.

Table 6.2: Calculation of the critical flow velocity of the armoured bed. The first row of the table represents the overall sediment distribution in the study field area. The sixth column shows the critical velocity using a d50 and Ψ_c =0.055. The last column shows a calculation of U_{ad90} with the critical bed shear stress of the d90 and with a Ψ_c of 0.03.

water depth:	1.5 m		Psi 0.055			Psi 0.03		
			Hydraulic rough: k_s=3d$_{90}$			**Hydraulic rough:** k_s=3d$_{90}$		
	d_{50} (mm)	d_{90} (mm)	u_{*c} d_{50}	k_s (m)	U_c (m/s)	u_{*ca} d_{90}	k_s (m)	U_{ad90} (m/s)
General	8.40	30.65	0.0865	0.092	1.14	0.1220	0.092	1.61
Hole 1	17.23	40.04	0.1239	0.120	1.55	0.1394	0.120	1.75
Hole 2	15.62	28.68	0.1179	0.086	1.58	0.1180	0.086	1.58
Hole 3	18.43	31.16	0.1281	0.093	1.68	0.1230	0.093	1.62
Hole 4	10.79	19.14	0.0980	0.057	1.41	0.0964	0.057	1.39
Hole 5	15.05	32.00	0.1158	0.096	1.51	0.1247	0.096	1.63
Hole 6	14.59	26.14	0.1140	0.078	1.55	0.1127	0.078	1.53
Hole 7	20.83	36.13	0.1362	0.108	1.74	0.1325	0.108	1.69
Hole 8	15.80	33.42	0.1186	0.100	1.54	0.1274	0.100	1.65
Hole 9	15.81	28.10	0.1186	0.084	1.59	0.1168	0.084	1.57
Hole 10	15.58	30.34	0.1178	0.091	1.56	0.1214	0.091	1.60
Hole 11	13.77	23.35	0.1107	0.070	1.54	0.1065	0.070	1.48
Hole 12	14.81	26.64	0.1148	0.080	1.56	0.1137	0.080	1.54
Hole 13	13.85	22.63	0.1110	0.068	1.55	0.1048	0.068	1.46
Hole 14	11.92	18.56	0.1030	0.056	1.49	0.0949	0.056	1.37
Hole 15	13.45	25.40	0.1094	0.076	1.50	0.1111	0.076	1.52

The columns U_c and U_{ad90} represent a range of flow velocities at which the armour bed upstream of the scour hole may start to erode. Generally speaking the value of U_{ad90} is slightly higher than U_c. Regarding the definition of the critical velocity at the formulas of Melville and HEC-18, the use of a Ψ_c of 0.055 seems to be more appropriate to calculate the critical velocity. On the other hand the smaller part of the sediment is not represented in the particle size distribution of the armour bed. This fine fraction is logically already in motion at the flow conditions when the armour bed starts to erode. It is assumed that the finer particles do not contribute to the deepening or sedimentation of the scour hole. Because the local flow conditions around the obstacle are assumed to have a greater erosive power than the upstream flow conditions, the finer sediment is readily transported out of the scour hole. So the finer particles have no effect on the choice of the critical mobility parameter (Ψ_c). Therefore a critical velocity (U_c) calculated with a critical mobility parameter (Ψ_c) of 0.055 is the most appropriate indication for the transition to live bed scour. Because there is already some sediment transport at these flow conditions, the resistance of the riverbed increases. So the assumption of a hydraulically rough condition will be used.

6.3 Conclusions

A critical mean velocity marks the transition from clear-water scour to live bed scour conditions and is defined as the depth averaged flow velocity at which there is incipient motion of the bed material. Many definitions of the critical velocity can be found in literature. The scour formulae presented by Melville and Coleman (2000) and HEC-18 define a critical velocity, which can be converted to the concept of Shields (1936). Both formulae use the assumption of a hydraulic smooth bed, which use can be questioned regarding graded sediment. Still both definitions will be used unaltered, because change in the critical velocity results in a change in the scour depth. As a result, the scour depth will not match to the laboratory conditions under which the experiments were executed

The effect of graded sediment is an important factor in predicting the hydraulic conditions at which the transition to live bed scour occurs. Due to this graded sediment, an armouring of the bed occurs, which lead to a higher critical bed shear stress velocity (u_{c*}). The method from Melville and Coleman (2000) and HEC-18 reckon with this armour effect. The method presented by Hoffmans and Verheij (1997) does not define the critical velocity precisely. This critical velocity will be calculated using a critical mobility parameter (Ψ_c) of 0.055 and the assumption of a hydraulically rough condition. The local particle size distribution of the armour bed will be used to take the spatial variations of the riverbed sediment into account.

7 Calculations of the occurred flow velocities

This chapter describes the way in which the flow velocities are calculated and presents the results of the computation. First the calculation method to compute the occurred flow velocities will be discussed. The next section describes the way in which all necessary input parameters are determined. The calculation considerations at each obstacle together with the results will be discussed, subsequently all the results of the calculations will be summarised.

7.1 Calculation method

The empirical formulae used in this research have a number of input parameters. According to Melville and Coleman (2000) the relation between depth of local scour d_s and its dependent parameters can be written as a function of the characteristics of flood flow, bed sediment, bridge geometry, and time. The most important parameters are:

b = width of pier or obstacle (m)
U = mean approach flow (m/s)
h_0 = mean approach flow depth or representative flow depth (m)
d_{50} = median size of the sediment particle size distribution (mm)
U_c = critical mean approach flow velocity for entrainment of bed sediment, depends on h_0 and d_{50} (m/s)
t = time (hours)
t_e = time fore the equilibrium depth of scour to develop (hours)

As can be found in chapter 3, the used formulae are presented in a form in which characteristic parameters are used, e.g. U/U_c. The method to calculate the effect of time is also influenced by the approach velocity. This method presents the time effects in a ratio between the scour depth and the equilibrium scour depth (d_s/d_{se}). Therefore it is difficult to rewrite these formulae in such form that U= f[b,h_0,d_{50},U_c,t,t_e]. To deal with this problem the following calculation method has been used, which is explained in the figure below:

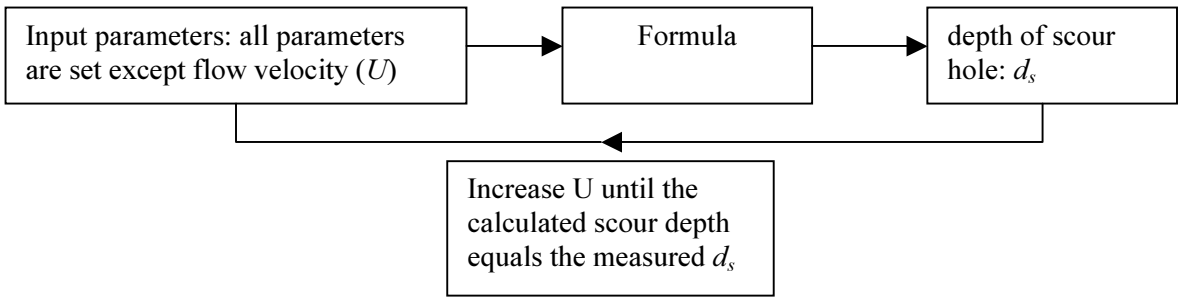

Figure 7.1: Calculation method.

All the necessary input parameters are kept fixed, only the approach velocity (U) varies. Now it is possible to calculate the occurring scour depths. The approach velocity increases with steps of 0.01 m/s and varies from 0.1 m/s to 3.0 m/s. Next the calculated scour depths are sorted in an ascending order. A routine returns the flow velocity at which the calculated scour depth equals the measured scour depth.

7.2 Input parameters in scour formulae

7.2.1 Water depth

The effect of water depth to scouring is represented by a representative water depth h_0. The question arises what the magnitude of the water depth h_0 must be, because the water levels vary in time during the flood. This variation of the water depth at each scour hole should be reduced to one representative water depth, which represent this variation. Beforehand it is necessary to mention the large uncertainty in the history of a scour hole. A tree could stay in the same position during the flood, but it could as well moved downstream. Even if it is assumed that a tree has been deposited during the last flood, it is difficult to determine the water level at which the tree touched the ground. This uncertainty also affects the determination of a representative water depth calculated from the data set of water levels. There are two ways to predict this water depth:

- The average water depth calculated from the given data of water depths at the time period when scour is assumed to occur.
- The averaged influence of the water depth used in the different formulae to the depth of scour. The water depth is usually represented by a ratio between the width of the obstacle and the water depth. This ratio is different for each scour formula. The formula of Melville and Coleman yields the following influence factor:

$$K_{h_0 b} = 2\sqrt{h_0 b} \tag{7.1}$$

Which is valid for all cases. The representative water depth h_0 is the calculated from the averaged influence factor:

$$h_0 = \left(\frac{\sum_{i=1}^{i=n} \sqrt{h_i b}}{n} \right)^2 \frac{1}{b} \tag{7.2}$$

The influence factor of the water depth to the scour depth is in the formula of HEC-18 represented by:

$$f_{HEC-18} = \left(\frac{h_0}{b} \right)^{0.35} \tag{7.3}$$

The representative water depth is then defined as:

$$h_0 = \left(\frac{\sum_{i=1}^{i=n} \left(\frac{h_i}{b} \right)^{0.35}}{n} \right)^{1/0.35} b \tag{7.4}$$

The formula of Hoffmans and Verheij yields the following ratio between the water depth and the width of an obstacle:

$$f_{H\&V} = \tanh\left(\frac{h_0}{b} \right) \tag{7.5}$$

The definition of a representative water depth h_0 for the formula of Hoffmans and Verheij is as follows:

$$h_0 = \tanh^{-1}\left(\frac{\sum_{i=1}^{i=n}\tanh\left(\frac{h_i}{b}\right)}{n}\right)b \qquad (7.6)$$

Water depth larger than height of obstacle

As can be seen in paragraph 5.3, the maximum local water levels often exceed the height of the tree trunk. As a consequence, the flow pattern changes and scour formulae may not be valid. The question arises how to deal with this situation. The ratio between the water depth and the height of the tree is an important factor. There are examples of similar cases such as pipelines at the sea bottom known in literature, which will be discussed below.

The case can be compared to a pipeline at the bottom of a sea. The (tidal) current flows against this tube and creates a scour hole at each side of the pipeline. Unfortunately this knowledge cannot be applied to this case because it is assumed that the pipeline has an infinite length. Therefore the flow pattern can be schematised as two dimensional, whereas the flow pattern around and obstacle with certain width has a three dimensional character.

Another comparison could come from the case of a bridge pier based on a wide caisson foundation. According to Melville and Raudkivi (1996), the width of the wider caisson becomes more important to the scour depth than the pier width if the caisson comes above the local bed level. Also the width of the caisson becomes more important if the ratio between the pier diameter and the width of the caisson becomes smaller.

In principle, the application of a smaller water depth has got a diminishing effect to the scour depth. So the supposed flow velocity should be higher to attain the same scour depth. When the water level exceeds the height of an obstacle, this will lead to a smaller scour depth compared to the situation that the height of an obstacle is equal to the same water depth. Regarding a case that the water depth is kept constant, the depth of scour will be larger at the obstacle, which rises above water level, compared to an obstacle that lies entirely flooded. If the ratio between the water depth and the height of the tree is smaller than 1.2, it is assumed that this excess of water level does not affect the scour depth. For ratios larger than 1.2, the representative water depth should be reduced until the ratio decreases to 1.2. This is an arbitrary assumption because the flow pattern may change in such way that the scour formulae cannot be applied to the wooden obstacles for which h_0/H is larger than 1.2. Thus, when the ratio between the representative water depth h_0 and the height of the obstacle H initially exceeds 1.2, the results of the computation are meaningless, because the maximum water depth is much larger than the height of the obstacle.

7.2.2 Time period estimation

The factor time plays an important role in the development of a scour hole. It takes a certain time before the scour process stops and the scour hole has reached its equilibrium depth. Therefore it is important to determine a time period in which the scour process was active.

The first step is to determine at which point the scour process starts. Scour begins when the local hydraulic conditions (water depth and flow velocity) are strong enough to move particles close to the obstacle. But these hydraulic conditions are unknown; there are only time series of discharges from which water levels have been derived. The start of scour can be predicted by:

- An estimation of the discharge or water levels at which scour starts. This manner is subjected to arbitrary choices, but is always better than to select the moment of flooding.
- A comparison between the cell averaged flow velocity at a cross-section and the calculated velocity at which scour initiates. Section 7.3 describes this method. It only applies to some obstacles. Results of hole 2, 6 and 13 can be found in section 7.4.

- If the case was considered that a tree run aground after the peak of the flood, it is possible to predict the water level when the tree touches ground. This is the point from which scour starts.

The prediction of the time at which scour ends can be estimated in a similar way. It can be reasoned that flow velocities are higher after the peak of the flood when water levels are descending. A second tail of sediment at an obstacle indicates that these velocities were high enough to move particles from the bed. This second, less-defined tail has a direction more to the main channel, indication that water flows from the point-bar to the main channel. This indicates that the scour process continues longer at decreasing water levels. Secondly, water levels are assumed to descend more quickly at the main channel than at the point-bar, which leads to steeper water level gradients and higher flow velocities. So, it is assumed that the scour process continues longer at decreasing water levels. Because it is unknown at which water level the scour process stops and the water level decreases at a rapid rate, it is assumed that the scour process stops at the same water level as it starts. Figure 7.2 explains these considerations more clearly.

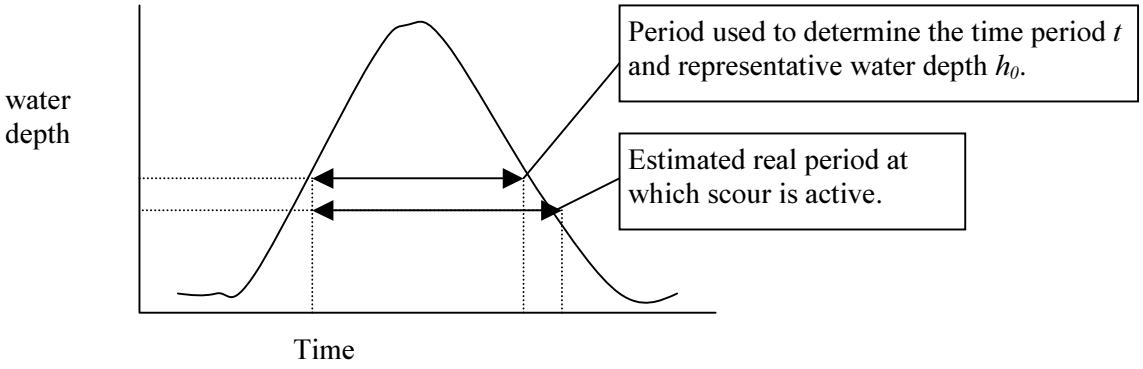

Figure 7.2: Schematisation of the time period estimation.

7.2.3 Scour depth

The scour hole depth is the difference between the elevation of the reference level and the elevation of the deepest point in the scour hole. Literature showed that the maximum scour depth is attained in front of and at either side of the obstacle. This point lies not necessarily just before the obstacle because fine sediment fills the scour hole during the last part of the flood. The elevation just in front of the root wad gives information about the elevation of the tree compared to the reference level. When the scour hole deepens, the elevation of the tree also becomes lower. So the bottom of the tree lies not necessarily at the same level as the reference level.
The GPS system has an error in the vertical plane of 6 cm. Also the depth could be wrongly measured when the scour hole was filled with fine sediment. The total error range is estimated to be ± 15 cm.

7.2.4 Width of the obstacle

The width of the obstacle has been measured by hand and by the GPS system. The root wad with the adjacent debris has mostly an irregular shape, so it turned out to be difficult to estimate the representative width of the obstacle. Therefore the error in the estimation of the width is much larger than the error in the measurement device. So the error range depends on the shape of the tree's root wad and is determined separately at each obstacle.

7.2.5 Sediment parameters

The scour process also depends on the sediment characteristics of the riverbed. The calculation method of Melville and Coleman (2000) uses the mean particle size distribution from Driesprong (2001). The results from the formula of HEC-18 will be presented using both the averaged sediment distribution as the particle distribution of the armour bed in the calculations. The formula presented by Hoffmans and Verheij (1997) makes use of the particle size distribution of the armour bed, as described in chapter 6.
During the field-work of 2002, the sediment characteristics where determined by the grid sampling method, which is explained in chapter 4. The used sample size was 100. According to Bunte & Abt (2001) the absolute error around the mean given in ϕ-units is computed from:

$$e_{\pm\phi m} = \left(\frac{t_{1-\alpha/2,n-1}}{\sqrt{n}} S_I \right) \tag{7.7}$$

where:

$e_{\pm\phi m}$ = absolute error around the mean in ϕ-units

$$S_I = \left| \frac{\phi_{84} - \phi_{16}}{2} \right|$$

$t_{1-\alpha/2,n-1}$ = Student's t statistical numerical value. For a confidence level of 95 % (α=0.05) and a sample size n=100, $t_{1-\alpha/2,n-1}$= 1.987. The numerical value of Student's t depends on two parameters: confidence level and sample size.
If a t-value for a 95% confidence level is used, a sample size is computed for which there is a 95% chance that the absolute difference (positive or negative) between the estimated sample mean and the true population mean is less than the specified acceptable error. Because the sample size is known, the original equation is rewritten in such way that it expresses the error belonging to the sample size with the required confidence level. The error in the mean particle size differs at each scour hole.

7.2.6 Shape of the obstacle

The effect of the shape of the obstacle is presented by a factor K_s. Various values for the factor K_s have been found in laboratory conditions. These so-called pier shape factors have a range from 0.65 to 1.2. Rectangular piers have K_s=1.1. It is difficult to project the shape of a bridge pier to the irregular shape of a root wad with wooden debris at the sides. Also because a root wad might be partly permeable at the sides, which influences the flow pattern around the obstacle. The error range for this shape factor is 0.1 for ill-defined root wads and 0.05 for the well-defined ones.

7.2.7 Angle of attack

This describes the influence of the orientation of the pier to the scour depth. When piers are aligned with the flow direction then $\theta = 0^o$ and K_θ=1.0. If the orientation of a pier is oblique to the flow and the full length of the pier is subjected to the flow, a formula describes this effect. This formula does not apply to the situation of a tree with its root wad. The tree usually aligns with the local flow direction, when the tree runs aground because the root wad touches ground first. Even in a possible situation that the tree's direction is oblique to the flow, water flows over or under the smaller bore of the tree. So the effect of an ablique orientations of the obstacle to the scour depth is estimated to be small and can be discarded. Therefore this factor will be kept fixed at a value of 1.0.

7.3 Expected range of results in the calculated flow velocities

Before the calculation of the flow velocities starts, it appeared to be possible to define a probable range of flow velocities. In this range the results from the scour formulae might be expected. First the lower value of the range will be defined, followed by considerations about the upper range.

7.3.1 Lower range: flow velocity at which scour starts

The initiation of scour marks the lower boundary for the calculations of the occurred flow velocities during a flood. According to Hoffmans & Verheij (1997), scour at an obstacle starts when the occurring flow velocity is larger than half the critical velocity (U>0.5*U_c). The HEC-18 formula gives a relation for the approach velocity required to initiate scour at an obstacle for a particle size d_x. This relation is:

$$U_{icd_x} = 0.645\left(\frac{d_x}{b}\right)^{0.053} U_{cd_x} \tag{7.8}$$

where:

U_{icdx} = the approach velocity required to initiate scour at the obstacle for particle size d_x.
b = width of the obstacle (m).
U_{cdx} = the critical velocity for incipient motion of particle size d_x (m/s), defined as:

$$U_{cd_{50}} = 6.19\left(h_0\right)^{1/6}\left(d_{50}\right)^{1/3} \tag{7.9}$$

where:

U_{cd50} = the critical velocity for incipient motion of particle size d_{50} (m/s).
d_{50} = median particle size (m)
h_0 = water depth (m)

The formula described above leads to higher values of the flow velocities compared to the value of 0.5*U_c. The HEC-18 formula will be used to calculate the initiation of scour for the following reasons: the tree trunks are assumed to run aground at places where an armour layer already exists, which means that the flow velocity should be high enough to break through this armour layer. Therefore the use of the critical velocity defined in HEC-18 can be justified. As stated in section 6.1.3, this formula uses a mobility parameter of 0.043. Secondly, local conditions at the tree trunks are taken into account, which follows from the use of the ratio between the width of the tree trunk and the particle diameter. This leads to an increase of the velocity at which scour initiates.
So the lower boundary is only dependent on the water depth, width of the tree trunk, and mean particle diameter of the bed. Because water levels are estimated from the daily discharges of 2001, it is possible to calculate the velocity for the initiation of scour at each discharge. The result is a data set, from which conclusions can be drawn. The averaged flow velocities at which scour starts are presented in Table 7.1.

Table 7.1: Estimated flow velocities at which scour starts.

	U (m/s)	Lower range U (m/s)	Upper range U (m/s)	Maximum U (m/s)
Hole 1	0.72	0.71	0.74	0.96
Hole 2	0.62	0.63	0.66	0.87
Hole 3	0.66	0.65	0.68	0.92
Hole 4	0.58	0.57	0.60	0.77
Hole 5	0.67	0.67	0.69	0.89
Hole 6	0.55	0.55	0.57	0.77
Hole 7	0.69	0.70	0.72	0.98
Hole 8	0.61	0.60	0.64	0.84
Hole 9	0.66	0.64	0.67	0.87
Hole 10	0.63	0.62	0.65	0.87
Hole 11	0.63	0.62	0.65	0.84
Hole 12	0.62	0.61	0.65	0.86
Hole 13	0.68	0.67	0.69	0.88
Hole 14	0.67	0.66	0.69	0.88
Hole 15	0.61	0.59	0.61	0.79

The last column shows the maximum values of the flow velocity of the data set. These values occur at the peak of the flood of 2001, which had a discharge of about 828 m^3/s. The other columns present the averaged lower boundaries of the occurred flow velocities. If an obstacle was flooded, the flow velocity should be higher than this value to initiate scour. The lower and upper ranges indicate the effect in the uncertainty of the estimated water levels.

7.3.2 *Upper value: maximum flow velocity at a point in the cross-section*

The upper value of the occurred flow velocity is difficult to estimate and therefore has a higher uncertainty. The core in the estimation of this upper value is the assumption of a point in the defined cross-section at which the same flow velocity occurs as at the nearest scour hole. Some scour holes have positions fairly close to the defined cross-sections, which is illustrated in 7.3.

The cross-sections are divided in a number of cells, as described in paragraph 5.2.1. Assume that flow conditions are the same along a streamline. Then there is a point in a

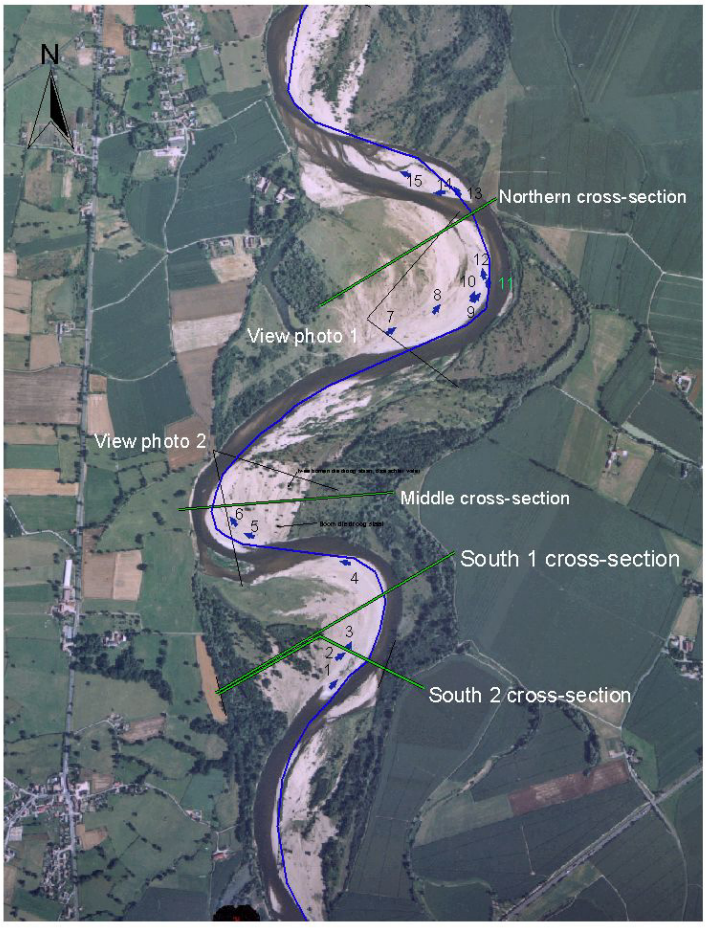

Figure 7.3: Positions of the scour holes together with the defined cross-sections.

cross-section at which the flow conditions should be equal to the nearest scour hole. This can only reasonably assumed if the location of the scour hole is close enough to the cross-section. Therefore not all scour holes are suitable. The obstacles, which appeared to be suitable, are hole 2, 3, 6 and 13. Next step is to calculate the flow velocities at the designated cell in 2001. To achieve this the water levels of different discharges have been divided over the cell. Then the development in time of the cell averaged flow velocity at the representative cell can be calculated. So a relation between the discharge Q and the cell averaged flow velocity can be deduced. Next it is possible to calculate the flow velocities at the designated cell applying this relation to the occurred discharges in 2001. Figure 7.4 shows the results together with the flow velocity at which scour is assumed to start (lower boundary).

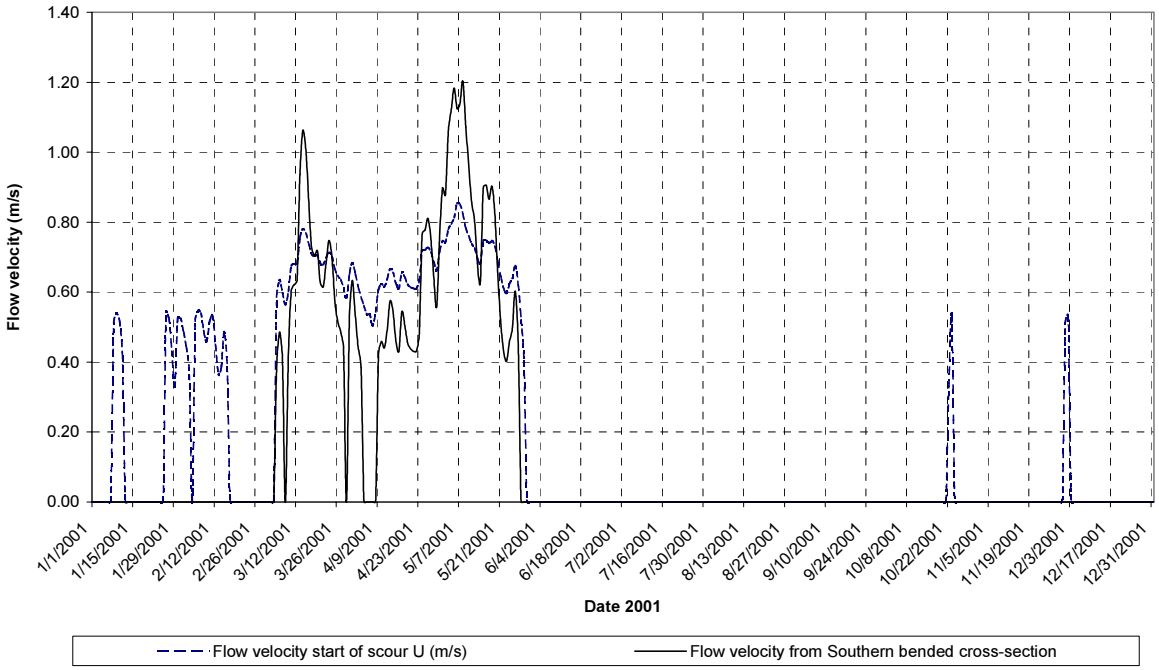

Figure 7.4: Begin of scour at hole 2. The mean U stands for the minumum velocity at which scour is active.

These graphs are useful to estimate the time period at which scour is active. This estimation only applies if the tree was already on the point-bar before the flood occurred and stayed in the same position during the flood. As shown in Figure 7.4, a flow velocity is calculated at which scour starts while the flow velocity from the southern cross-section is still assumed to be non-existent. The reason for is that the designated cell uses an averaged surface level that is different from the local surface level at hole 2. The maximum flow velocity showed in the graphs is in all cases close to 1.2 m/s. However, the value of this cell averaged flow velocity is dependent on the correctness of the roughness coefficients, cell depths, and the Q-h relation. Also the schematisation of the cross-section in cells can only be applied to prismatic channels. The conclusion is that this value can be considered as meaningless, but the procedure may be suitable to estimate the time period at which scour is active.

7.4 Calculation of flow velocities at the obstacles

The way in which the input parameters are determined, is discussed in the previous section. This paragraph presents the results of the computations at each obstacle, together with the calculation considerations. Further information of all obstacles can be found in appendix B, where a more extensive description of scour hole can be found. The positions of all scour holes are again illustrated in Figure 7.5.

Figure 7.5: Positions of all scour holes in the study area. The arrows point de direction of the local flow direction during the flood. The aerial photograph is from 2000.

Hole 1: large tree close to main channel

This is the most upstream scour hole of the southern point-bar. During the field-work the scour hole was largely filled with ground water. It has an asymmetrical scour hole with the largest scour at the side of the main channel. The left side of the hole is not fully developed. This could imply that the obstacle worked as an abutment at some discharges. The large tree could possibly stand at the riverbank in 1998, so an equilibrium scour depth has been assumed. The shape of this obstacle has been largely formed by small wooden debris entangled in the root wad of the main tree. Downstream of the obstacle, a deposition of sediment can be found, which level is visibly higher than the surrounding point-bar level for about 100 metres. There are clear signs that show different flow directions during the flood. The shape of the obstacle is well-defined and can be schematised as a bridge pier. First the input parameters are discussed and subsequently the range of results are given.

Table 7.2: Input parameters of hole 1.

Value: / *Parameter:*	*original*	*lower range*	*upper range*	*remarks*
b (m)	2.36	2.26	2.46	Well measurable
d_s (m)	1.26	1.11	1.41	Scour hole was flooded at measuring
h_0 Melville & C. (m)	1.42	1.25	1.63	Water levels at discharges higher
h_0 HEC-18 (m)	1.42	1.25	1.62	than 230 m^3/s are regarded in the
h_0 Hoffmans &Verheij (m)	1.41	1.25	1.61	calculation
d_{50} (mm) general	8.40	6.95	9.85	Average over the area
d_{50} (mm) armour	17.23	16.08	18.38	In front of scour hole
t (hour)	1872			Equilibrium depth is always attained
K_s	1.1	1.05	1.15	Fairly regular shape, rectangle
Discharge begin of scour	230	m^3/s		Arbitrary chosen, water depth at this discharge is about 1.0 m
aground when:	X	m^3/s		

Table 7.3: Results of the computation of hole 1

Flow velocity (m/s)	*Melville and Coleman*	*HEC-18* *with general sediment characteritics*		*HEC-18* *using characteristics of the armour layer*		*Hoffmans and Verheij*
Critical velocity	**1.50**	**1.34**		**1.70**		**1.53**
Original	**0.88**	**1.17*)**	**1.57**	**1.36*)**	**1.91**	**1.11**
b+	0.87	1.16	1.54	1.34	1.86	1.11
b-	0.89	1.18	1.60	1.37	1.95	1.11
d_s+	0.93	1.27	1.76	1.46	2.14	1.15
d_s-	0.82	1.07	1.37	1.24		1.07
h_0+	0.86	1.16	1.54	1.35	1.88	1.10
h_0-	0.89	1.18	1.59	1.37	1.93	1.12
d_{50}+	0.77	1.22	1.66	1.37	1.93	1.14
d_{50}-	1.00	1.09	1.42	1.34	1.87	1.07
K_s+	0.86	1.13	1.49	1.31	1.82	1.09
K_s-	0.90	1.21	1.65	1.40	2.00	1.12

The results are presented with an accuracy of centimetres/second. This accuracy has only been used to show a better distinction between the influence of the various parameters.
Second row presents the results of the computation using the original input parameters. Below this row the effect of the parameter variations are shown.E.g. $b+=b+\Delta b$, which is equal to the upper range of *b* in the table of the input parameters.
*): The scour depth occurred at both clear-water as live bed conditions. The right side of the column shows the computed flow velocities at live bed conditions.

The formula of HEC-18 has been split up in two columns. The left column shows the results of a calculation using the averaged particle size distribution of the study area. The right one shows the calculation with the sediment characteristics of the local armoured upper layer. The period of the peak of the flood in May 2001 is small compared to the scour period, which was assumed to be 78 days. As a result, the representative water level (h_0) is small compared to the estimated maximum water depth (h_{max}=2.82 m). This is probably the reason that the results of hole 1 are larger than the critical velocity.

Hole 2: large bare bore with large root wad. Much debris in front of root wad

The calculation at this tree can be divided in two cases: the tree survived the entire flood of 2001 or it runs aground during the flood. Both cases will be discussed. The shape of the root wad is similar to a rectangular pier, allthough the root wad has an irregular shape, which hampers the determination of the appropiate width. A large amount of wooden debris can be found in front of the tree. This wooden debris in front of the root wad has not been considered in the calculation because the history and position of this debris during the flood is unknown. If the debris was in the same position during the flood, it could affect the flow pattern in such way that scour formulae cannot be used. Thus the suitability of this object representing a bridge pier can be questioned and is dependent of the history of the debris in front of the main tree. Therefore the results presented below can be questioned, but act as a case to show the effect of time on the calculated flow velocities.
The tree has small effects to the local morphology of the point-bar. The deepest part of the scour hole can be found at the right side of the tree. Behind the obstacle, a sharp separation of a coarse and fine sediment distribution can be found. Both have been measured: the coarse part has a d_{50} of 13.6 mm and the fine part has a d_{50}=8.2 mm. This difference is clearly visible but it is unknown where this difference originates from. Some grasses can be found at the sandy deposits around the tree. The tree itself is also a fertile soil for vegetation. It has been calculated that the bore probably will start to float at a water depth of about 0.9 metres.

Case 1: obstacle stayed at the same position during the flood

Table 7.4: Input parameters of 2nd hole, case 1.

Value: / *Parameter:*	*original*	*lower range*	*upper range*	*remarks*
b (m)	2.5	2.3	2.7	Irregular shape, width not accurate.
d_s (m)	0.82	0.67	0.97	asymmetrical scour hole, more depth at right side.
h_0 Melville & C. (m)	0.93	0.74	1.16	Water levels at discharges higher than 330 m^3/s are considered in the calculation.
h_0 HEC-18 (m)	0.92	0.73	1.16	
h_0 Hoffmans &Verheij (m)	0.94	0.76	1.16	
d_{50} (mm) general	8.40	6.95	9.85	
d_{50} (mm) armour	15.62	14.51	16.73	In front of scour hole
t (hour)	744	(case 1)		
K_s	1.1	1.05	1.15	Clear rectangular shape
Discharge begin of scour	330	m^3/s		Case 1
aground when:	X	m^3/s		

Table 7.5: Results of the computation of hole 2, using the parameters of case 1.

Flow velocity (m/s)	*Melville and Coleman*	*HEC-18* *with general sediment characteritics*	*HEC-18* *using characteristics of the armour layer*	*Hoffmans and Verheij*
Critical velocity	**1.40**	**1.24**	**1.53**	**1.44**
Original	**0.73**	**0.88**	**1.04**	**1.01**
b+	0.71	0.87	1.03	1.01
b-	0.74	0.89	1.06	1.01
d_s+	0.79	0.99	1.16	1.07
d_s-	0.66	0.78	0.92	0.96
h_0+	0.72	0.87	1.03	1.00
h_0-	0.74	0.89	1.05	1.03
d_{50}+	0.64	0.92	1.05	1.05
d_{50}-	0.85	0.82	1.02	0.98
K_s+	0.71	0.86	1.01	1.00
K_s-	0.74	0.91	1.07	1.03

The results are presented with an accuracy of centimetres/second. This accuracy has only been used to show a better distinction between the influence of the various parameters.

Case 2: tree runs aground during the flood of 2001

Table 7.6: Input parameters of the 2nd hole, case 2.

Value: *Parameter:*	*original*	*lower range*	*upper range*	*remarks*
b (m)	2.5	2.3	2.7	Irregular shape, width not accurate.
d_s (m)	0.82	0.67	0.97	asymmetrical scour hole, more depth at right side.
h_0 Melville & C. (m) h_0 HEC-18 (m) h_0 Hoffmans &Verheij (m)	0.85 0.85 0.85	0.67 0.67 0.67	1.07 1.07 1.07	Water levels at discharges higher than 330 m^3/s are considered in the calculation.
d_{50} (mm) general d_{50} (mm) armour t (hour) K_s	8.40 15.62 192 1.1	6.95 14.51 (case 2) 1.05	9.85 16.73 1.15	 In front of scour hole Clear rectangular shape
Discharge end of scour aground when: 	330 450	m^3/s m^3/s		 Case 2

Figure 7.6: Side view of hole 2 at the southern point-bar.

Table 7.7: Results of the calculations of 2nd case of hole 2.

Flow velocity (m/s)	*Melville and Coleman*	*HEC-18* *with general sediment characteritics*	*HEC-18* *using characteristics of the armour layer*	*Hoffmans and Verheij*
Critical velocity	**1.38**	**1.22**	**1.51**	**1.41**
Original	**0.77**	**0.91**	**1.04**	**1.02**
b+	0.77	0.91	1.03	1.02
b-	0.78	0.91	1.06	1.02
d_s+	0.83	1.00	1.17 1.51*)	1.08
d_s-	0.72	0.82	0.94	0.97
h_0+	0.77	0.91	1.04	1.01
h_0-	0.78	0.91	1.05	1.04
d_{50}+	0.70	0.95	1.05	1.06
d_{50}-	0.87	0.86	1.03	0.98
K_s+	0.76	0.89	1.01	1.01
K_s-	0.79	0.93	1.08	1.03

The results are presented with an accuracy of centimetres/second. This accuracy has only been used to show a better distinction between the influence of the various parameters.
*): The scour depth occurred at both clear-water as live bed conditions. The right side of the column shows the computed flow velocities at live bed conditions.

The difference between the results of the first and the second case can be neglectable. The representative water depth h_0 is comparable, so the critical velocity also differs not much. The difference between both cases lies within the used time period. The results of the first case may give information about a longer time period than was used in the second case. The time period of the first case contains the peak of the flood whereas the second case's time period is after the peak when water levels were already decreasing. The highest water levels at the flood's peak have not significant influence on the representative water depth. So a conclusion is that the calculations at the first case do not provide information about the flow velocities during the peak of the flood. Unfortunately, the morphological processes are assumed to be the most active during this period. Nevertheless, the results may present the averaged flow conditions that are necessary to create the measured scour depth in the designated time period. This assumption leads to the conclusion that the results of the second case should be representative for the averaged flow velocity at the falling stage of the flood.

Hole 3: three bores with adjoining debris

This hole is composed of three bores, probably connected to one root wad. There are some small trees positioned at each side. It is assumed that the obstacle stayed at the same place during the flood of 2001, because the obstacle is composed out of several trees. The front of the obstacle can be schematised as a round pier, but the shape is not well defined. Vegetation grows at the lee sides of the object. Scour hole is partially filled with small wooden debris and has a symmetrical shape. There is a long tail of fine sediment downstream of the tree. The height of the tree is low compared to the maximum occurred water depths, implying that scour formulae could possibly be inapplicable. Even the representative water depth h_0 exceeds the height of the tree, thus the representative water depths are adjusted to a ratio of water depth/height=1.2. This is another reason to question the results presented in Table 7.9

Table 7.8: Input parameters of hole 3.

Parameter: / *Value:*	*original*	*lower range*	*upper range*	*remarks*
b (m)	2.23	2.03	2.43	Large uncertainty in representative width.
d_s (m)	0.79	0.64	0.94	Measured under the adjoining small debris, which was not considered in the calculations
h_0 Melville & C. (m)	0.72	0.53	0.96	Ratio too large. $h_{0,max}$=0.69 m
h_0 HEC-18 (m)	0.71	0.52	0.95	Calculation of water levels starts for
h_0 Hoffmans &Verheij (m)	0.73	0.55	0.96	Q > 330 m^3/s
d_{50} (mm) general	8.40	6.95	9.85	
d_{50} (mm) armour	18.42	17.31	19.53	In front of obstacle.
t (hour)	744			
K_s	1.0	0.9	1.1	Assumed round shape, not well-defined.
Discharge begin of scour	330	m^3/s		Same as Hole 2
aground when:	X	m^3/s		

Table 7.9: Results of the computations of hole 3.

Flow velocity (m/s)	*Melville and Coleman*	*HEC-18* *with general sediment characteritics*		*HEC-18* *using characteristics of the armour layer*		*Hoffmans and Verheij*
Critical velocity	**1.34**	**1.18**		**1.54**		**1.44**
Original	**0.79**	**0.95**		**1.14**		**1.14**
b+	0.77	0.94		1.12		1.13
b-	0.81	0.97		1.17	1.57*)	1.14
d_s+	0.87	1.08		1.29	1.79	1.22
d_s-	0.71	0.83		1.00		1.06
h_0+						
h_0-	0.82	1.20		1.16	1.53	1.18
d_{50}+	0.70	0.99		1.15		1.17
d_{50}-	0.90	0.89		1.13		1.10
K_s+	0.75	0.89		1.07		1.10
K_s-	0.84	1.03	1.31*)	1.23	1.66	1.18

The results are presented with an accuracy of centimetres/second. This accuracy has only been used to show a better distinction between the influence of the various parameters.
*): The scour depth occurred at both clear-water as live bed conditions. The right side of the column shows the computed flow velocities at live bed conditions.

The time period at which the scour process was assumed to be active equals 31 days. Therefore the results do not provide information about the occurred flow velocities during the peak of the flood. The maximum water depth (h_{max}) at hole 3 is assumed to be 1.76 m, while the wooden obstacle only rises 0.58 m above the surface level. Assuming that the debris was at the same position during the flood, it can only be concluded that this hole does not provide information about the occurred flow velocities because scour formulae cannot be applied.

Hole 4: large object at the end of the southern point-bar

This obstacle consists of a tree with its crown still attached to the bore. As at hole 1, the shape of the obstacle is mainly formed by small wooden debris adjoining the root wad. The brim of the scour hole shows sandy deposits where grasses can be found. The hole shows extended scouring and has vegetation growth at lee parts, which are marks that the tree was at the same position during the flood of 2001. The particle size distribution of the armoured bed is relatively small compared to the particle size at the upstream part of the point-bar. This is similar to the northern point-bar near "Chateau de Lys". The scour hole is clearly defined. There is little debris deposited in the scour hole, which implies that the flow pattern is similar to that around bridge piers. Only small debris drifted against the tree could change the shape of the obstacle during the flood. The shape of the tree trunk is assumed to be rectangular. The period at which the scour process is assumed to be active equals 65 days, which means that this hole does not provide information about the peak of the flood. The maximum water depth is estimated at 2.1 metres, while the height of the root wad is only 1.32 m.

Table 7.10: Input parameters of hole 4.

Value: / *Parameter:*	*original*	*lower range*	*upper range*	*remarks*
b (m)	2.41	2.21	2.61	Clearly defined width, but edges are permeable
d_s (m)	0.98	0.83	1.13	Max. depth at left side of tree
h_0 Melville & C. (m)	0.90	0.73	1.10	Water levels at discharges higher than 250 m^3/s are considered in the calculation.
h_0 HEC-18 (m)	0.89	0.72	1.09	
h_0 Hoffmans &Verheij (m)	0.90	0.74	1.10	
d_{50} (mm) general	8.40	6.95	9.85	
d_{50} (mm) armour	10.79	9.69	11.89	In front of tree
t (hour)	1560			Equilibrium depth attained
K_s	1.1	1.05	1.15	Clearly defined
Discharge begin of scour	250	m^3/s		
aground when:	X	m^3/s		

Table 7.11: Results of the calculations of hole 4.

Flow velocity (m/s)	*Melville and Coleman*	*HEC-18* *with general sediment characteritics*		*HEC-18* *using characteristics of the armour layer*		*Hoffmans and Verheij*
Critical velocity	**1.40**	**1.23**		**1.34**		**1.28**
Original	**0.80**	**1.01**	**1.24*)**	**1.15**	**1.50*)**	**0.97**
b+	0.79	0.99		1.13	1.44	0.97
b-	0.82	1.02	1.30	1.17	1.57	0.97
d_s+	0.87	1.11	1.45	1.27	1.75	1.02
d_s-	0.74	0.90		1.02		0.92
h_0+	0.79	0.99		1.13	1.47	0.95
h_0-	0.82	1.02	1.27	1.16	1.53	1.00
d_{50}+	0.70	1.05	1.32	1.16	1.52	1.02
d_{50}-	0.92	0.94		1.13	1.47	0.92
K_s+	0.79	0.97		1.11	1.43	0.95
K_s-	0.82	1.04	1.31	1.18	1.57	0.98

The results are presented with an accuracy of centimetres/second. This accuracy has only been used to show a better distinction between the influence of the various parameters.
*): The scour depth occurred at both clear-water as live bed conditions. The right side of the column shows the computed flow velocities at live bed conditions.

Hole 5: old tree close to main channel

This large tree was possibly visible on an aerial photograph of 2000, because of the extensive vegetation growth downstream of the obstacle. Due to the large deposits of sediment behind this scour hole, small poplars could survive the period after the flood of 2001. This implies that the tree gives rise to a new line of pioneer vegetation. The shape of the root wad is rectangular and is largely affected by small wooden debris accumulated in front of the tree. Therefore K_s=1.05 has been chosen. The flow pattern is assumed to be comparable to the pattern around a bridge pier. The scour hole lies partly below the ground water level and is partly filled with sandy deposits at the right side of the obstacle. At the side of the main channel, the occurring flow velocities at decreasing water levels hampered the deposition of fine sediments. Like hole 4, the scour period is assumed to be 65 days. This implies that time effects can be neglected. The maximum water depth is about 2.5 metres, which is comparable to the height of the tree (2.2 m). So the scour formulae can be applied to this obstacle. The results presented in Table 7.13 are the largest of all computations in this study.

Table 7.12: Input parameters of hole 5.

Value: / *Parameter:*	*original*	*lower range*	*upper range*	*remarks*
b (m)	2.49	2.29	2.69	Width not clearly defined
d_s (m)	1.35	1.20	1.50	measured through sandy deposits
h_0 Melville & C. (m)	1.33	1.21	1.46	Water levels at discharges higher
h_0 HEC-18 (m)	1.32	1.21	1.45	than 250 m^3/s are considered in the
h_0 Hoffmans &Verheij (m)	1.32	1.21	1.45	calculation.
d_{50} (mm) general	8.40	6.95	9.85	
d_{50} (mm) armour	15.05	13.92	16.18	In front of tree
t (hour)	1560			Equilibrium depth attained
K_s	1.1	0.95	1.15	Clearly defined
Discharge begin of scour	250	m^3/s		
aground when:	X	m^3/s		

Table 7.13: Results of the calculations of hole 5.

Flow velocity (m/s)	*Melville and Coleman*	*HEC-18* *with general sediment characteritics*		*HEC-18* *using characteristics of the armour layer*		*Hoffmans and Verheij*
Critical velocity	**1.48**	**1.32**		**1.60**		**1.51**
Original	**0.91**	**1.22**	**1.65*)**	**1.41**	**2.01*)**	**1.11**
b+	0.89	1.21	1.59	1.39	1.93	1.10
b-	0.93	1.24	1.73	1.43	2.10	1.11
d_s+	0.96		1.86	1.52	2.25	1.15
d_s-	0.85	1.13	1.46	1.30	1.70	1.07
h_0+	0.89	1.21	1.64	1.40	1.99	1.10
h_0-	0.92	1.23	1.67	1.42	2.03	1.12
d_{50}+	0.80	1.27	1.75	1.42	2.04	1.15
d_{50}-	1.02	1.14	1.50	1.39	1.98	1.07
K_s+	0.88	1.18	1.57	1.36	1.91	1.09
K_s-	0.98		1.94	1.56	2.36	1.17

The results are presented with an accuracy of centimetres/second. This accuracy has only been used to show a better distinction between the influence of the various parameters.
*): The scour depth occurred at both clear-water as live bed conditions. The right side of the column shows the computed flow velocities at live bed conditions.

Hole 6: two living trees with wooden debris

This is the second most downstream scour hole at the middle point-bar near the farm "le Verdelet". The obstacle consists of two trees, which are still alive, and it is clearly visible on the aerial photograph of 2000. Wooden debris has been accumulated between both trees, which all together form the obstacle. The width is 8.55 m, so it can be questioned if scour formulae apply to such width. As a result of this width, an extensive bank is visible downstream. This bank gives shelter to all types of vegetation. There is a sharp separation in the size of the sediment visible at this bank, just as can be found at hole 2. The tree is flooded at a small discharge, allthough the point-bar is rather high. The maximum water level equals 1.8 metres, which is not much larger than the assumed height of the composed obstacle H=1.5 m. It is assumed that the scour starts at Q=250 m^3/s (case 1). At case 2 this discharge will be 300 m^3/s.

Case 1: discharge starts and ends at a discharge of 250 m^3/s

Table 7.14: Input parameters at hole 6, first case.

Value: / *Parameter:*	*original*	*lower range*	*upper range*	*remarks*
b (m)	8.55	8.25	8.85	Very wide obstacle
d_s (m)	0.94	0.79	1.09	Maximum depth at left side obstacle
h_0 Melville & C. (m)	0.51	0.39	0.64	Water levels at discharges higher
h_0 HEC-18 (m)	0.50	0.37	0.63	than 250 m^3/s are considered in the
h_0 Hoffmans &Verheij (m)	0.55	0.46	0.68	calculation.
d_{50} (mm) general	8.40	6.95	9.85	
d_{50} (mm) armour	14.59	13.50	15.68	In front of tree
t (hour)	1560			Equilibrium scour depth is attained.
K_s	1.1	1.0	1.15	
Discharge begin of scour	250	m^3/s		
aground when:	X	m^3/s		

Table 7.15: Results of the computation at hole 6, first case.

Flow velocity (m/s)	*Melville and Coleman*	*HEC-18* *with general sediment characteritics*	*HEC-18* *using characteristics of the armour layer*	*Hoffmans and Verheij*	
Critical velocity	**1.27**	**1.12**	**1.35**	**1.26**	
Original	**0.82**	**0.79**	**0.90**	**1.12*)**	**1.3-3.0*²)**
b+	0.82	0.78	0.89	1.12	1.3-3.0
b-	0.82	0.79	0.91	1.12	1.3-3.0
d_s+	0.90	0.87	0.99	1.20	1.3-3.0
d_s-	0.75	0.70	0.81	1.04	
h_0+	0.75	0.78	0.89	1.07	
h_0-	0.92	0.80	0.91	1.16	1.3-3.0
d_{50}+	0.73	0.82	0.91	1.16	1.3-3.0
d_{50}-	0.92	0.75	0.89	1.07	1.3-3.0
K_s+	0.80	0.76	0.88	1.10	
K_s-	0.87	0.84	0.96	1.17	1.3-3.0

The results are presented with an accuracy of centimetres/second. This accuracy has only been used to show a better distinction between the influence of the various parameters.
*): The scour depth occurred at both clear-water as live bed conditions. The right side of the column shows the possible flow velocities at live bed conditions.
*²): Scour depth becomes independent of the flow velocity at live bed conditions.

Regarding the results of these computations, the discharge at which scour starts may be estimated too low. If a larger discharge is chosen, the averaged water levels will be higher and therefore also the critical velocities. A calculation with higher water depths will be showed in case 2.

Case 2: Scouring starts at Q=300 m^3/s

Table 7.16: Input parameters of hole 6, second case.

Value: / *Parameter:*	*original*	*lower range*	*upper range*	*remarks*
b (m)	8.55	8.25	8.85	Very wide obstacle
d_s (m)	0.94	0.79	1.09	Maximum depth at left side obstacle
h_0 Melville & C. (m)	0.70	0.57	0.83	Water levels higher than 300 m^3/s
h_0 HEC-18 (m)	0.69	0.57	0.82	are considered in calculation.
h_0 Hoffmans &Verheij (m)	0.73	0.61	0.86	
d_{50} (mm) general	8.40	6.95	9.85	
d_{50} (mm) armour	14.59	13.50	15.68	In front of tree
t (hour)	984			Equilibrium scour depth is attained.
K_s	1.1	1.0	1.15	
Discharge begin of scour	300	m^3/s		
aground when:	X	m^3/s		

Table 7.17: Results of the calculation of hole 6, second case.

Flow velocity (m/s)	*Melville and Coleman*	*HEC-18* *with general sediment characteritics*	*HEC-18* *using characteristics of the armour layer*	*Hoffmans and Verheij*
Critical velocity	**1.34**	**1.18**	**1.42**	**1.34**
Original	**0.75**	**0.79**	**0.89**	**1.06**
b+	0.75	0.78	0.88	1.06
b-	0.75	0.79	0.90	1.06
d_s+	0.80	0.86	0.98	1.12
d_s-	0.70	0.72	0.81	1.00
h_0+	0.72	0.78	0.88	1.04
h_0-	0.79	0.79	0.90	1.09
d_{50}+	0.68	0.81	0.90	1.10
d_{50}-	0.85	0.75	0.88	1.02
K_s+	0.73	0.77	0.87	1.04
K_s-	0.77	0.83	0.94	1.10

The results are presented with an accuracy of centimetres/second. This accuracy has only been used to show a better distinction between the influence of the various parameters.

Only the dicharge at which the scour process starts is the difference between both cases. The time period of the first case equals 65 days, whereas this period reduces in the second case to 41 days, which is still rather long. As a result, the representative water depth h_0 is about 20 centimetres higher in the second case. This leads to smaller results of the approach flow velocities in the second case. Due to the long period of scour, the equilibrium depth is assumed to be attained in both cases. The representative water depth h_0 is smaller than the measured scour depth in both cases, which leads to results in the live bed range at the first case. Both cases show the importance of a rightly chosen water level at which scour starts. Unfortunately the discharge at which scour starts is arbitrary chosen and thus subjected to a large uncertainty.

Hole 7: large tree at the upstream side of the northern point-bar

This hole is situated at the beginning of the northern point-bar. Here the size of the sediment is the coarsest of this point-bar. The obstacle is clearly visible on a photograph taken during the flood of 2001, which is illustrated in Figure 7.7. The hole has no large-scale morphological effects on the shape of the point-bar, which was the case at hole 5 and 6. This tree stood most probably at a riverbank, regarding the roots originating from the lower trunk and the crack in the trees bore. The obstacle can be schematised as a round bridge pier. Vegetation growth is scarce. It is assumed that the scour hole originates from the flood of 2001, because an object is visible 45 metres upstream of the position of the object on the aerial photograph of 2000. The tree trunk might have moved during the last flood, but this assumption has not been taken into account at the computations.
The time period at which scour is assumed to be active equals 26 days. The maximum water depth is assumed to be equal to 1.8 m while the height of the tree equals to 1.7 metres. Furthermore the shape of the obstacle is similar to a round bridge pier. The scour formulae can be applied to this obstacle because of the similarity in flow patterns.

Table 7.18: Input parameters used for calculations at hole 7.

Value: / *Parameter:*	*original*	*lower range*	*upper range*	*remarks*
b (m)	1.3	1.15	1.45	Well-defined
d_s (m)	0.93	0.78	1.08	Measured at the right side of the bore
h_0 Melville & C. (m)	0.83	0.71	0.97	Water levels calculated from a discharge of 350 m^3/s
h_0 HEC-18 (m)	0.83	0.70	0.97	
h_0 Hoffmans &Verheij (m)	0.82	0.70	0.95	
d_{50} (mm) general	8.40	6.95	9.85	
d_{50} (mm) armour	20.83	19.73	21.93	measured in front of the hole
t (hour)	624			
K_s	1.0	0.95	1.05	good similarity to round pier
Discharge begin of scour	350	m^3/s		
aground when:	X	m^3/s		

Table 7.19: Results of the calculation at hole 7.

Flow velocity (m/s)	*Melville and Coleman*	*HEC-18* *with general sediment characteritics*		*HEC-18* *using characteristics of the armour layer*		*Hoffmans and Verheij*
Critical velocity	**1.38**	**1.22**		**1.65**		**1.53**
Original	**0.99**	**1.17**	**1.80*)**	**1.43**	**2.35*)**	**1.25**
b+	0.96	1.15	1.70	1.40	2.22	1.24
b-	1.03	1.20	1.91	1.47	2.52	1.27
d_s+	1.09		2.12	1.59	2.78	1.33*[2])
d_s-	0.89	1.04	1.48	1.28	1.96	1.17
h_0+	0.97	1.16	1.76	1.42	2.31	1.24
h_0-	1.02	1.18	1.83	1.45	2.40	1.27
d_{50}+	0.91	1.23	1.93	1.44	2.37	1.29
d_{50}-	1.10	1.07	1.57	1.42	2.33	1.22
K_s+	0.96	1.13	1.70	1.38	2.23	1.23
K_s-	1.03	1.21	1.90	1.48	2.48	1.28

The results are presented with an accuracy of centimetres/second. This accuracy has only been used to show a better distinction between the influence of the various parameters.
*): The scour depth occurred at both clear-water as live bed conditions. The right side of the column shows the computed flow velocities at live bed conditions.
*[2]): The computed scour depth for live bed conditions is d_s=1.09 m.

Figure 7.7: The northern point-bar at Chateau de Lys at the 7th of May 2001 (photo: J. de Kramer). The tree of hole 7 is visible at this photograph. It is the most right tree that is fully covered in the water flow.

Hole 8: large tree far on point-bar

There is no accumulation of small debris at this obstacle: it is only composed of a root wad and a bore. It is assumed that the tree starts to float at a water depth of 0.8 m, so the bore must be run aground at decreasing water levels. Two cases will be regarded: first case describes a situation where the tree ran aground at a discharge of 666 m^3/s. In the second case the tree ran aground at a discharge of 814 m^3/s.The shape of the root wad is irregular, but can be presented as a rectangular pier. The flow pattern can be influenced due to this irregular shape of the root wad, but it is assumed that the scour formulae are applicable. The representative width is subjected to uncertainty because the width of the root wad largely varies. There is no vegetation growth at this location. This hole has only local morphological impact. The assumed maximum waterdepth equals 1.2 metres while the height of the tree's root wad comes to 2.2 m. The scour hole has not been fully developed during the flood of 2001, which is an indication that the equilibrium depth has not been attained yet. The estimated time period *t* is short and leads to an occurrence of a time effect in both cases, which underlines the last assumption.

Case 1: run aground at a discharge of 666 m^3/s.

Table 7.20: Input parameters for the first case of hole 8.

Value: / *Parameter:*	*original*	*lower range*	*upper range*	*remarks*
b (m)	2.27	1.97	2.57	Irregular shape
d_s (m)	0.42	0.27	0.57	In front of the tree
h_0 Melville & C. (m)	0.63	0.50	0.78	Calculated from water levels
h_0 HEC-18 (m)	0.62	0.49	0.78	occurring at a discharge higher than
h_0 Hoffmans &Verheij (m)	0.64	0.51	0.79	500 m^3/s.
d_{50} (mm) general	8.40	6.95	9.85	
d_{50} (mm) armour	15.80	14.68	16.92	In front of tree
t (hour)	48			
K_s	1.1	1.05	1.15	clearly defined
Discharge end of scour	500	m^3/s		
aground when:	666	m^3/s		h=0.84 m

Table 7.21: Results of hole 8, first case.

Flow velocity (m/s)	*Melville and Coleman*	*HEC-18* *with general sediment characteritics*	*HEC-18* *using characteristics of the armour layer*	*Hoffmans and Verheij*
Critical velocity	**1.32**	**1.16**	**1.43**	**1.29**
Original	**0.66**	**0.73**	**0.84**	**0.89**
b+	0.66	0.73	0.83	0.89
b-	0.68	0.74	0.85	0.89
d_s+	0.75	0.85	0.97	0.97
d_s-	0.58	0.62	0.57	0.81
h_0+	0.66	0.73	0.85	0.89
h_0-	0.67	0.73	0.84	0.90
d_{50}+	0.60	0.76	0.85	0.92
d_{50}-	0.76	0.69	0.83	0.86
K_s+	0.65	0.72	0.83	0.88
K_s-	0.68	0.75	0.86	0.90

The results are presented with an accuracy of centimetres/second. This accuracy has only been used to show a better distinction between the influence of the various parameters.

Figure 7.8: Side view of hole number 8.

Case 2: tree touches ground at Q=814 m^3/s.

Table 7.22: Input parameters for the second case at hole 8.

Value: / *Parameter:*	*original*	*lower range*	*upper range*	*remarks*
b (m)	2.27	1.97	2.57	Irregular shape
d_s (m)	0.42	0.27	0.57	In front of the tree
h_0 Melville & C. (m)	0.78	0.64	0.94	Calculated from water levels
h_0 HEC-18 (m)	0.78	0.63	0.94	occurring at a discharge higher than
h_0 Hoffmans &Verheij (m)	0.80	0.66	0.95	500 m^3/s.
d_{50} (mm) general	8.40	6.95	9.85	
d_{50} (mm) armour	15.80	14.68	16.92	In front of tree
t (hour)	72			
K_s	1.1	1.05	1.15	clearly defined
Discharge end of scour	500	m^3/s		
aground when:	814	m^3/s		h=1.14 m

Table 7.23: Results of the calculation using parameters of the second case of hole 8.

Flow velocity (m/s)	*Melville and Coleman*	*HEC-18* *with general sediment characteritics*	*HEC-18* *using characteristics of the armour layer*	*Hoffmans and Verheij*
Critical velocity	**1.37**	**1.21**	**1.49**	**1.35**
Original	**0.65**	**0.71**	**0.83**	**0.87**
b+	0.64	0.71	0.82	0.88
b-	0.66	0.72	0.84	0.87
d_s+	0.72	0.82	0.94	0.94
d_s-	0.50	0.62	0.56	0.81
h_0+	0.65	0.72	0.70	0.88
h_0-	0.65	0.71	0.71	0.87
d_{50}+	0.46	0.74	0.71	0.90
d_{50}-	0.75	0.67	0.81	0.84
K_s+	0.64	0.70	0.82	0.87
K_s-	0.66	0.73	0.73	0.88

The results are presented with an accuracy of centimetres/second. This accuracy has only been used to show a better distinction between the influence of the various parameters.

Figure 7.9: Front view of hole 8.

Hole 9: large obstacle composed of several trees and debris

This obstacle can also be traced on the aerial photograph from 2000, so it is assumed that equilibrium scour depth is attained. The scour process starts at a discharge of 260 m^3/s. The deepest point can be found at the left side of the obstacle. The tree dug itself into the point-bar during the scour process. The edge of the scour hole is clearly visible but the inner slope does not continue to the deepest point of the scour hole: there is horizontal surface just in front of the small wooden debris. Probably, first a scour hole was formed and then the hole filled with debris, which caused an another hole in front of this debris. The scour formulae are not applicable at this obstacle because of the following reasons. Small debris filled the scour hole, which most probably changed the flow pattern. Due to all the debris, the shape of the obstacle is not clearly defined and shows little similarity to a bridge pier, which leads to an uncertainty in the shape factor K_s and the flow pattern. Last, the maximum water depth of 2.1 metres is much larger than the height of the obstacle H=0.6 m. Even the ratio between the representative water depth h_0 and the height of the tree H was larger than 1.2. Hence, the results presented below can be regarded meaningless.

Table 7.24: Input parameters of hole 9.

Value: / *Parameter:*	*original*	*lower range*	*upper range*	*remarks*
b (m)	2.89	2.60	3.00	both sides are permeable, difficult to define
d_s (m)	0.70	0.55	0.85	measured at the left side of the obstacle
h_0 Melville & C. (m)	0.93	0.82	1.06	Calculated from water levels
h_0 HEC-18 (m)	0.92	0.81	1.05	occurring at a discharge higher than
h_0 Hoffmans &Verheij (m)	0.94	0.83	1.07	260 m^3/s.*)
d_{50} (mm) general	8.40	6.95	9.85	
d_{50} (mm) armour	15.81	14.72	16.90	in front of scour hole
t (hour)	1392			equilibrium depth attained
K_s	1.0	0.9	1.1	
Discharge begin of scour	260	m^3/s		
aground when:	X	m^3/s		

*): the ratio between the water depth and the height of the obstacle was larger than 1.2. So the representative water depth has been reduced to h_0= 0.77 m in this calculation.

Table 7.25: Results of the calculations of hole 9.

Flow velocity (m/s)	*Melville and Coleman*	*HEC-18* *with general sediment characteritics*	*HEC-18* *using characteristics of the armour layer*	*Hoffmans and Verheij*
Critical velocity	**1.36**	**1.20**	**1.49**	**1.39**
Original	**0.69**	**0.83**	**0.98**	**1.02**
b+	0.69	0.83	0.98	1.02
b-	0.71	0.85	1.00	1.02
d_s+	0.76	0.95	1.11	1.09
d_s-	0.73	0.72	0.86	0.95
h_0+	*)	*)	*)	*)
h_0-				
d_{50}+	0.59	0.87	0.99	1.05
d_{50}-	0.81	0.78	0.97	0.98
K_s+	0.66	0.78	0.93	0.99
K_s-	0.72	0.89	1.05	1.05

The results are presented with an accuracy of centimetres/second. This accuracy has only been used to show a better distinction between the influence of the various parameters.
*): In the calculations a ratio of 1.2 has been applied. Therefore the results of the range of the water depth are not given.

Hole 10: small tree next to hole 9

Hole 10 is a small tree situated next to hole 9. Because the obstacle consists of one relatively small tree without much small debris, it is assumed that this tree ran aground during the flood of 2001. The tree is estimated to run aground at a discharge of about 500 m^3/s after the peak of the flood has passed. The scour process is assumed to stop at Q=300 m^3/s. The time period of scouring is 288 hours, which is equal to 12 days. In this period the equilibrium depth has almost been attained. Some vegetation growth can be found at this site. The scour hole has little effect to the large-scale morphology of the point-bar. Sand has been deposited just behind the root wad during the flood. The scour hole is partly filled with small wooden debris. The armoured layer surrounding the scour hole is relatively coarse. The shape and width of the wooden obstacle are not clearly defined but the form of the scour hole indicates that the assumed flow pattern may be similar to that around bridge piers. The height of the tree's root wad equals 0.6 metres. The representative water depth h_0 is larger than the height of the obstacle *H.* However, the height of the obstacle *H* may initially be larger because the scour process may dug the tree into the surface during the flood.

Table 7.26: Input parameters of hole 10.

Value: / *Parameter:*	*original*	*lower range*	*upper range*	*remarks*
b (m)	1.76	1.66	1.86	Width only of root wad
d_s (m)	0.52	0.37	0.67	Measured at the left side of scour hole
h_0 Melville & C. (m)	0.72	0.61	0.85	Calculated from water levels
h_0 HEC-18 (m)	0.72	0.60	0.85	between Q=300 m^3/s and Q=506
h_0 Hoffmans &Verheij (m)	0.73	0.61	0.85	m^3/s.
d_{50} (mm) general	8.40	6.95	9.85	
d_{50} (mm) armour	15.58	14.17	16.69	in front of scour hole
t (hour)	288			
K_s	1.0	1.1	0.9	not clearly defined
Discharge end of scour	300	m^3/s		h= 0.44
aground when:	506	m^3/s		h= 1.07 m

Table 7.27: Results of the calculations of hole 10.

Flow velocity (m/s)	*Melville and Coleman*	*HEC-18* *with general sediment characteritics*	*HEC-18* *using characteristics of the armour layer*	*Hoffmans and Verheij*
Critical velocity	**1.35**	**1.19**	**1.46**	**1.34**
Original	**0.68**	**0.76**	**0.91**	**0.92**
b+	0.67	0.75	0.89	0.92
b-	0.69	0.76	0.91	0.92
d_s+	0.77	0.89	1.05	0.99
d_s-	0.59	0.64	0.78	0.85
h_0+	0.67	0.76	0.90	0.92
h_0-	0.67	0.76	0.90	0.93
d_{50}+	0.58	0.79	0.91	0.95
d_{50}-	0.80	0.70	0.88	0.88
K_s+	0.67	0.72	0.86	0.90
K_s-	0.73	0.81	0.96	0.95

The results are presented with an accuracy of centimetres/second. This accuracy has only been used to show a better distinction between the influence of the various parameters.

Hole 11: obstacle composed of several trees with wooden debris

This object is composed of one tree with a large root wad, and of several bores adjacent to this tree. Vegetation like grasses and blackberries grow at the sandy deposits in the scour hole. This obstacle has a complicated structure. Only the width of the main root wad is considered in the calculation because this was the part of the obstacle that may have produced the downflow in the flow pattern around this obstacle. The deepest point of the scour hole can be found at the left side of the object whereas the other side is to a great extent filled with debris. Therefore the flow pattern may not be comparable to that around a bridge pier. It can be doubted if the scour formulae are applicable to this case. Furthermore, h_{max} equals to 2.1 metres where as the highest point of the obstacel only rises 1.6 metres above the local surface.
The equilibrium situation is considered to exist, because it is unlikely that one flood formed this structure as it was during the field-work of 2002. The shape of the root wad of the main tree can be regarded as circular, but has a deal of uncertainty. It is assumed that the scour process starts at about Q=260 m^3/s, which is equal to a water depth of about 0.5 m. Contrary to the dimensions of the obstacle, the morphological effects of the tree to the surrounding point-bar are negligable.

Table 7.28: Input parameters of hole 11.

Value: / *Parameter:*	*original*	*lower range*	*upper range*	*remarks*
b (m)	2.14	1.94	2.34	Width not clearly defined
d_s (m)	0.55	0.40	0.70	At the side of the object
h_0 Melville & C. (m)	0.89	0.78	1.02	Calculated from water levels
h_0 HEC-18 (m)	0.88	0.77	1.01	occurring at Q>260 m^3/s
h_0 Hoffmans &Verheij (m)	0.89	0.78	1.01	
d_{50} (mm) general	8.40	6.95	9.85	
d_{50} (mm) armour	13.77	12.68	14.86	in front of tree
t (hour)	1392			Equilibrium depth attained
K_s	1.0	0.9	1.1	shape not clear
Discharge start of scour	260	m^3/s		h= 0.5 m
aground when:	X	m^3/s		

Table 7.29: Results of the computations at hole 11.

Flow velocity (m/s)	*Melville and Coleman*	*HEC-18* *with general sediment characteritics*	*HEC-18* *using characteristics of the armour layer*	*Hoffmans and Verheij*
Critical velocity	**1.39**	**1.23**	**1.45**	**1.39**
Original	**0.66**	**0.75**	**0.88**	**0.92**
b+	0.65	0.74	0.87	0.92
b-	0.67	0.76	0.90	0.92
d_s+	0.72	0.87	1.03	0.98
d_s-	0.58	0.56	0.56	0.86
h_0+	0.65	0.74	0.73	0.92
h_0-	0.71	0.75	0.89	0.92
d_{50}+	0.55	0.79	0.90	0.95
d_{50}-	0.79	0.69	0.87	0.88
K_s+	0.63	0.71	0.85	0.90
K_s-	0.69	0.80	0.94	0.94

The results are presented with an accuracy of centimetres/second. This accuracy has only been used to show a better distinction between the influence of the various parameters.

Hole 12: small tree close to hole 11

This obstacle consists of a tree with a small root wad. It is relatively small sized and has a slightly different orientation than hole 11. Two cases can be considered. First case assumes that this scour hole run aground during the last flood. Calculations predict that the tree starts to drift at a water level 0.4 m. The second case assumes that the tree stayed at the same position during the flood of 2001. The application of the scour formulae can be questioned in both cases. Reason for this is that the representative water depth at the first case is approximately equal to the measured scour depth. In the second case the maximum water levels are large compared to the height of the tree: h_{max}= 1.8 m while H= 0.5 m. So the results at case 2 are the most disputable of the two. Compared to the size of the tree, large quantities of fine sediment are deposited around it. The shape of the object is represented as a circular pier. Deepest point of the scour hole is at the left side of the tree.

Case 1: tree runs aground at 316 m^3/s.

Table 7.30: Input parameters of hole 12, first case.

Value: / *Parameter:*	*original*	*lower range*	*upper range*	*remarks*
b (m)	1.35	1.20	1.50	Well-defined
d_s (m)	0.34	0.19	0.49	At the left side
h_0 Melville & C. (m)	0.31	0.21	0.43	Calculated from water levels
h_0 HEC-18 (m)	0.31	0.21	0.43	between Q=230 m^3/s and Q=316
h_0 Hoffmans &Verheij (m)	0.32	0.22	0.43	m^3/s.
d_{50} (mm) general	8.40	6.95	9.85	
d_{50} (mm) armour	14.81	13.72	15.90	In front of tree
t (hour)	192			equals 8 days
K_s	1.0	0.9	1.1	
Discharge end of scour	230	m^3/s		h= 0.18 m
aground when:	316	m^3/s		

Table 7.31: Results of calculations at hole 12, first case.

Flow velocity (m/s)	*Melville and Coleman*	*HEC-18* *with general sediment characteritics*	*HEC-18* *using characteristics of the armour layer*	*Hoffmans and Verheij*
Critical velocity	**1.16**	**1.04**	**1.25**	**1.11**
Original	**0.62**	**0.63**	**0.76**	**0.85**
b+	0.62	0.62	0.74	0.85
b-	0.64	0.64	0.78	0.85
d_s+	0.76	0.79	0.94 1.26*)	0.98 0.97-3.00*^{2})
d_s-	0.49	0.52	0.39	0.72
h_0+	0.61	0.62	0.76	0.84
h_0-	0.68	0.63	0.76	0.89 1.00-3.00*^{2})
d_{50}+	0.53	0.66	0.77	0.88
d_{50}-	0.73	0.59	0.75	0.82
K_s+	0.61	0.61	0.73	0.82
K_s-	0.66	0.67	0.80	0.89

The results are presented with an accuracy of centimetres/second. This accuracy has only been used to show a better distinction between the influence of the various parameters.
*): Also live bed conditions can occur.
*^{2}): Also live bed conditions can occur, which entails that the approach flow velocity is indifferent to the measured scour depth.

Case 2: tree stayed at the same place during the flood of 2001

Table 7.32: Input parameters of hole 12, second case.

Value: / *Parameter:*	*original*	*lower range*	*upper range*	*remarks*
b (m)	1.35	1.20	1.50	Well-defined
d_s (m)	0.34	0.19	0.49	At the left side
h_0 Melville & C. (m)	0.50	0.39	0.63*)	Calculated from water levels for higher discharges than Q=230 m^3/s
h_0 HEC-18 (m)	0.49	0.37	0.63	
h_0 Hoffmans &Verheij (m)	0.51	0.41	0.63	
d_{50} (mm) general	8.40	6.95	9.85	
d_{50} (mm) armour	14.81	13.72	15.90	In front of tree
t (hour)	1872			Equilibrium depth attained
K_s	1.0	0.9	1.1	
Discharge start of scour	230	m^3/s		h= 0.18 m
aground when:	X	m^3/s		

*): This water depth exceeds the ratio h_0/H=1.2, So h_0=0.57 m has been used in the calculations
The scour period equals 78 days.

Table 7.33: Results of the calculation at hole 12, second case.

Flow velocity (m/s)	*Melville and Coleman*	*HEC-18* *with general sediment characteritics*	*HEC-18* *using characteristics of the armour layer*	*Hoffmans and Verheij*
Critical velocity	**1.27**	**1.12**	**1.35**	**1.25**
Original	**0.61**	**0.63**	**0.77**	**0.84**
b+	0.60	0.62	0.76	0.83
b-	0.62	0.64	0.78	0.84
d_s+	0.72	0.77	0.92	0.93
d_s-	0.49	0.35	0.35	0.74
h_0+*)	0.61	0.63	0.77	0.84
h_0-	0.62	0.63	0.76	0.84
d_{50}+	0.51	0.68	0.78	0.87
d_{50}-	0.73	0.58	0.75	0.80
K_s+	0.58	0.61	0.74	0.82
K_s-	0.64	0.67	0.80	0.86

The results are presented with an accuracy of centimetres/second. This accuracy has only been used to show a better distinction between the influence of the various parameters.
*): h_0+= 0.57

Figure 7.10: Scour hole number 12. In the background the tree at hole number 11 is visible.

Hole 13: old obstacle close to the main channel

This obstacle lies close to the main channel. The bore of this tree is covered with sediment, so it can be reasoned that this hole must be formed several years ago and that the process of sediment transport covered the downstream part of the tree. The estimated maximum water depth exceeds the height of the root wad by a ratio larger than 1.2, so the question arises if the scour formulae are applicable to this obstacle. When the calculated water depths are used, which are presented in Table 7.34, the ratio between water depth and height of the tree is about 1.9. In further calculations the representative water depth (h_0) is reduced until this ratio h_0/H=1.2, which was the case at h_0= 0.94 metres. So scour formulae are not suitable to describe the scour process at this obstacle, also because the maximum water depth at the flood is much larger than the height of the tree. The shape of the tree's root wad with the adjoining debris is similar to a circular pier. Left side and front of the scour hole has been filled with fine sediments. Small wooden debris can be found at the right side of the obstacle. Blackberry, poplars and grasses grow at the lee sides of the object.

Table 7.34: Input parameters used at hole 13.

Value: / *Parameter:*	*original*	*lower range*	*upper range*	*remarks*
b (m)	2.70	2.50	2.90	Irregular shape due to debris
d_s (m)	0.79	0.64	0.94	measured at the right side obstacle
h_0 Melville & C. (m)	1.46*)	1.35	1.58	Calculated using water depths from a discharge of 230 m^3/s. h_0= 0.94 m
h_0 HEC-18 (m)	1.45*)	1.35	1.58	
h_0 Hoffmans &Verheij (m)	1.45*)	1.35	1.57	
d_{50} (mm) general	8.40	6.95	9.85	Averaged particle size diameter of the upstream and downstream sample.
d_{50} (mm) armour	14.63	13.56	15.70	
t (hour)	1872			Equilibrium depth attained
K_s	1.0	0.9	1.1	uncertainty due to debris
Discharge start of scour aground when:	230 X	m3/s m3/s		h= 1.05 m, arbitrary chosen

*): The ratio between water depth and height of the root wad appeared to be larger than 1.2. So the water depth has been reduced until h_0/H=1.2. The used water depth equals 0.94 metres.

Table 7.35: Results of the calculation at hole 13.

Flow velocity (m/s)	*Melville and Coleman*	*HEC-18* *with general sediment characteritics*	*HEC-18* *using characteristics of the armour layer*	*Hoffmans and Verheij*
Critical velocity	**1.41**	**1.25**	**1.47**	**1.42**
Original	**0.73**	**0.90**	**1.06**	**1.04**
b+	0.72	0.89	1.05	1.04
b-	0.75	0.91	1.08	1.05
d_s+	0.80	1.02	1.20*^{2}) 1.55	1.10
d_s-	0.67	0.79	0.94	0.98
h_0+*)	x	x	x	x
h_0-	x	x	x	x
d_{50}+	0.63	0.94	1.07	1.08
d_{50}-	0.86	0.84	1.05	1.00
K_s+	0.70	0.85	1.00	1.01
K_s-	0.77	0.97	1.14	1.08

The results are presented with an accuracy of centimetres/second. This accuracy has only been used to show a better distinction between the influence of the various parameters.
*): h_0= 0.94 is the only water depth used in this calculation.
*^{2}): The measured scour depth equals to the calculated flow velocity at both clear-water as live bed conditions.

Hole 14: composition of small debris covered with vegetation

This obstacle is composed of small wooden debris. Due to this debris, flow velocities decelerate and fine sediments accumulate between the debris. It can be reasoned that this scour hole originates from several years ago. Vegetation started to grow, which speeded up the deposition of sandy sediment, until the form has been reached as it is now. It might be possible that there is a tree under all the debris and sand, which initiated the formation of a scour hole at this position. Deep scour holes can be found at each side of the obstacle, but there is no scour at the front of the debris. It is difficult to extract a pier-like shape from this object. The debris only affects local morphology of the riverbed. It is most likely that the scour formulae cannot be applied to this obstacle. The flow pattern at this obstacle does not presumably contain a downflow, which is characteristic for the flow pattern around a bridge pier. Also the maximum water level h_{max} equals 2.7 metres while the height of the obstacle H is 0.7 m. But for the completeness, calculations are shown below.

Table 7.36: Input parameters of hole 14.

Value: / *Parameter:*	*original*	*lower range*	*upper range*	*remarks*
b (m)	2.08	(1.78)	(2.38)	difficult to determine
d_s (m)	0.79	(0.64)	(0.94)	at both sides of the object
h_0 Melville & C. (m) h_0 HEC-18 (m) h_0 Hoffmans &Verheij (m)	1.20*) 1.19*) 1.19*)	(1.10) (1.10) (1.10)	(1.31) (1.31) (1.30)	Calculated from water level occurring at discharges higher than 120 m^3/s The discharge at h_0=0.88 m is 180 m^3/s
d_{50} (mm) general d_{50} (mm) armour	8.40 13.82	(6.95) (12.75)	(9.85) (14.89)	Averaged particle size from the upstream and downstream sample.
t (hour)	3480			equals to 145 days
K_s	1.0	(0.9)	(1.1)	pier shape not visible
Discharge start of scour aground when:	180 X	m^3/s m^3/s		

*): The ratio between the water depth and the height of the tree h_0/H= 1.62 m. The used water depth has been reduced until the value of h_0= 0.88 m.
The figures between brackets () are not used in the computation.

The calculated water depths presented in the table above are close to the averaged water depths that occur at a discharge larger than 180 m^3/s. So this scour hole does not supply information about the peak of the flood of 2001, because the scour process is assumed to be active during the whole winter period of 2001. Results of the calculation are presented below:

Table 7.37: Result of the calculation at hole 14.

Flow velocity (m/s)	*Melville and Coleman*	*HEC-18* *with general sediment characteritics*	*HEC-18* *using characteristics of the armour layer*	*Hoffmans and Verheij*
Critical velocity	1.39	1.23	1.45	1.45
Original	0.79	0.95	1.13*[2]) 1.50	1.07

The results are presented with an accuracy of centimetres/second. This accuracy has only been used to show a better distinction between the influence of the various parameters.
*[2]): Measured scour depth occurs both under clear-water as under live bed scour.

The local critical velocity at a water depth of 0.88 metres is about 1.45 m/s. It could well be that the average local flow velocity during the winter period was about in a range of 0.7 to 1.0 m/s at the position of this scour hole.
Figure 7.11 shows two photographs of the same obstacle. The left one has been taken in May 2002 whereas the right one shows the situation in July 2002. In May there was no vegetation growth, while

the obstacle was almost covered with vegetation in July. The figure shows that the existence of debris makes it easier for plants to root on a point-bar.

Figure 7.11: Two photographs of the hole 14. The left photograph was taken in May 2002. The right picture shows the situation in July 2002.

Hole 15: most downstream obstacle composed of small debris

Hole 15 is situated at a somewhat higher position at the point-bar downstream of hole 14. It is also a composition of several small trees and debris just as hole 14. Again, it is an old object, on which fine sediments and debris accumulated over time. The deepest scour depths can be found at both sides of the object. The scour in front of the original obstacle has been filled with fine sediments during the last years. This is good soil for grasses, which roots hampers the erosion process in front of the tree. Therefore the flow pattern changes in such way that the application of scour formulae can be questioned. Furthermore, the maximum water level is twice as large as the height of the obstacle. The shape of the obstacle is more or less similar to a circular pier, but has a very small height. Downstream of the obstacle, large deposits of sands can be found. Also the composition of the local armoured bed consists of a large percentage of fine sediment compared to the more upstream part of the point-bar. It is assumed that these fine sediments have been deposited during the last part of the flood.

Table 7.38: Input parameters used at hole 15.

Value: / *Parameter:*	*original*	*lower range*	*upper range*	*remarks*
b (m)	6.30	6.10	6.50	edges are ill-defined
d_s (m)	0.89	0.74	1.04	measured at left scour hole
h_0 Melville & C. (m)	0.86	0.75	0.98	Calculated using water depths from
h_0 HEC-18 (m)	0.85	0.74	0.98	a discharge of 230 m^3/s.
h_0 Hoffmans &Verheij (m)	0.89	0.78	1.01	
d_{50} (mm) general	8.40	6.95	9.85	
d_{50} (mm) armour	13.45	12.36	14.54	in front of scour hole
t (hour)	1872			equilibrium depth attained
K_s	1.0	0.9	1.1	
Discharge start of scour	230	m3/s		h= 0.5 m, arbitrary chosen
aground when:	X	m3/s		

Table 7.39: Results of the calculations at hole 15.

Flow velocity (m/s)	*Melville and Coleman*	*HEC-18* *with general sediment characteritics*	*HEC-18* *using characteristics of the armour layer*	*Hoffmans and Verheij*
Critical velocity	**1.39**	**1.22**	**1.43**	**1.35**
Original	**0.69**	**0.84**	**0.95**	**1.01**
b+	0.69	0.83	0.94	1.01
b-	0.69	0.84	0.96	1.01
d_s+	0.75	0.93	1.05	1.07
d_s-	0.64	0.74	0.85	0.95
h_0+*)	0.67	0.83	0.95	1.00
h_0-	0.73	0.84	0.96	1.03
d_{50}+	0.59	0.87	0.96	1.05
d_{50}-	0.82	0.79	0.94	0.97
K_s+	0.67	0.79	0.90	0.98
K_s-	0.73	0.90	1.02	1.05

The results are presented with an accuracy of centimetres/second. This accuracy has only been used to show a better distinction between the influence of the various parameters.

7.5 Analysis of the results

The results of the calculation at each scour hole are presented above. Now these results, which are summarised in Table 7.40, will be compared to each other. Table 7.40 shows some main input parameters such as the width, scour depth, and the representative water depth. The values at the right side of the table present the used critical depth averaged velocity and the results of the calculated flow velocities.

Table 7.40: Summarised results at each obstacle.

	width b (m)	*measured d_s (m)*	*scour time t (hrs)*	*water depth h_0 (m)*	*Melville & Coleman*		*HEC-18 general*		*HEC-18 armour*		*Hoffmans & Verheij*	
					U_c (m/s)	U (m/s)	U_c (m/s)	U (m/s)	U_c (m/s)	U (m/s)	U_c (m/s)	U (m/s)
Hole 1	2.36	1.26	1872	1.4	1.50	0.88	1.34	1.17/1.57	1.70	1.36/1.91	1.53	1.11
Hole 2, c.1	2.50	0.82	744	0.93	(1.40)	(0.73)	(1.24)	(0.88)	(1.53)	(1.04)	(1.44)	(1.01)
case 2			192	0.85	(1.38)	(0.77)	(1.22)	(0.91)	(1.51)	(1.04)	(1.41)	(1.02)
Hole 3	2.23	0.79	744	0.69*)	(1.34)	(0.79)	(1.18)	(0.95)	(1.54)	(1.14)	(1.44)	(1.14)
Hole 4	2.41	0.98	1560	0.90	1.40	0.80	1.23	1.01/1.24	1.34	1.15/1.50	1.28	0.97
Hole 5	2.49	1.35	1560	1.32	1.48	0.91	1.32	1.22/1.65	1.60	1.41/2.01	1.51	1.11
Hole 6, c.1	8.55	0.94	1560	0.51	1.27	0.82	1.12	0.79	1.35	0.90	1.26	1.12 *2)
case 2			984	0.70	1.34	0.75	1.18	0.79	1.42	0.89	1.34	1.06
Hole 7	1.3	0.93	624	0.83	1.38	0.99	1.22	1.17/1.80	1.65	1.43/2.35	1.53	1.25
Hole 8, c.1	2.27	0.42	48	0.63	1.32	0.66	1.16	0.73	1.43	0.84	1.29	0.89
case 2			72	0.78	1.37	0.65	1.21	0.71	1.49	0.83	1.35	0.87
Hole 9	2.89	0.70	1392	0.93	(1.36)	(0.69)	(1.20)	(0.83)	(1.49)	(0.98)	(1.39)	(1.02)
Hole 10	1.76	0.52	288	0.72	1.35	0.68	1.19	0.76	1.46	0.91	1.34	0.92
Hole 11	2.14	0.55	1392	0.89	(1.39)	(0.66)	(1.23)	(0.75)	(1.45)	(0.88)	(1.39)	(0.92)
Hole 12, c.1	1.35	0.34	192	0.31	1.16	0.62	1.04	0.63	1.25	0.76	1.11	0.85
case 2			1872	0.50	(1.27)	(0.61)	(1.12)	(0.63)	(1.35)	(0.77)	(1.25)	(0.84)
Hole 13	2.7	0.79	1872	1.45	(1.41)	(0.73)	(1.25)	(0.90)	(1.47)	(1.06)	(1.42)	(1.04)
Hole 14	2.08	0.79	3480	1.20	(1.39)	(0.79)	(1.23)	(0.95)	(1.45)	(1.13/1.50)	(1.45)	(1.07)
Hole 15	6.3	0.89	1872	0.86	(1.39)	(0.69)	(1.22)	(0.84)	(1.43)	(0.95)	(1.35)	(1.01)

1. Results of the flow velocities (*U*) separated by "/" exist both under clear-water as under live bed conditions.
2. The results presented between brackets () can be disputed because the shape of the obstacle might not be represented as a shape of a bridge pier or because the maximum water level was much larger than the height of the obstacle.

*): calculated water depth was higher than height obstacle. Representative water depth set to h_0=1.2*H*, *H*= height of obstacle from ground level.

*2): Measured scour depth equals also to the computed scour depth under live bed conditions. This formula is independent of the approach flow velocity under live bed conditions.

Regarding the results presented in above, the following can be concluded:

- The largest flow velocities can be found at hole 5. Regarding the order of magnitude of the flow velocities at each point-bar, the conclusion is that the largest measured scour depths can be found at the upstream side of the point-bar implying that here the largest flow velocities occurred. The particle size distribution of the armoured riverbed is also the coarsest at the upstream side of the point-bar, which supports the assumption that here the highest flow velocities occurred during the flood.
- The measured scour depth d_s is in the same order of magnitude as the representative water depth (h_0). Because of the long time period at which the scour is assumed to be active, the water levels at the peak of the flood have small influence on the representative water depth h_0.
- A lower representative water depth leads to larger results in the flow velocities, which is illustrated by the two cases at hole 8. The effect on the resulting flow velocities are small though.
- The results of both cases at hole 6 show the importance of the rightness of the chosen water level at which the scour process starts. The point at which scour starts, is subjected to uncertainty and can only be estimated because there is no unifying definition for the start of scour. The definition of the start of scour depends on the flow velocity, which is unknown.
- The calculations at hole 2 are examples to show the effect of time to the occurred flow velocities. The time effect appeared to be marginal at most cases. The difference in flow velocity presented at hole 2 are presumably the result of a difference in representative water depth h_0.

- The results presented between brackets can be questioned because of the applicability of the scour formulae. These formulae may not be applied at these large wooden debris because of the following reasons. First, the maximum water depth h_{max} may be much larger than the height H of the wooden obstacle. As a consequence, the flow pattern changes and scour formulae are not valid. When the water level exceeds the height of an obstacle, this will lead to a smaller scour depth compared to the situation that the height of an obstacle is equal to the water depth. So, the water depth used in the calculations should be reduced if the water depth exceeds the height H of the obstacle, but it is unknown to what extend this reduction should be. Second reason is the existence of small wooden debris at the scour hole or adjacent the main obstacle. The amount of debris that filled the scour hole has large influence to the flow pattern around the main obstacle. Therefore the small debris mainly determines whether an obstacle can be schematised as a bridge pier. Hence, the applicability of scour formulae mainly depends on the amount of debris at the obstacle and scour hole itself.

Knowledge of local water levels is important to be able to calculate with scour formulae and to possibly predict an occurred flow velocity. The water levels should be known because:

- The magnitude of the critical velocity is dependent of the chosen water depth. So the value of the critical velocity varies in time.
- The estimation of the time period is dependent on the time series of the water levels. The time effect is also affected by the water levels via the critical velocity, which depends on the water depth.
- The ratio between the representative water depth h_0 and the width b of the obstacle is an important parameter predicting the depth of scour and thus the approach velocity under clear-water conditions. An increase in the representative water depth leads to lower calculated flow velocities. Therefore, a right definition of the representative water depth h_0, which depends on local water levels, is necessary to be able to predict the occurred flow velocities. So, laboratory studies should be executed to study the definition of a representative water depth more extensively. The definition in this study is based on the averaged influence of all h_0/b ratios during the time period that scour was assumed to be active.

In general, the results of the calculations apply to the time period at which the scour process was active. In most cases this period was rather long or the scour process was assumed to occur after the peak of the flood. Therefore these calculations are not able to predict the flow velocities that occurred at the peak of the flood. The high water levels at the peak of the flood do not have significant effect on the representative water depth. Nevertheless, the results may present the averaged flow conditions that are necessary to create the measured scour depth.

Figure 7.12 shows a graph of the different scour formulae at hole 1 for the scour depth and the necessary flow velocity to attain this scour depth. Because other parameters affect the scour depth as well, the graphs are different for each wooden obstacle. The graph of the other obstacles can be found in appendix E. The approach velocity strongly influences the scour depth under clear-water conditions. So, a small variation of the approach velocity leads to a large variation in the scour depth. Under live bed conditions, the scour depth generally is indifferent of the flow velocity, which means that the occurred flow elocity cannot be predicted. Only the HEC-18 formula differentiates the flow velocity under live bed conditions.

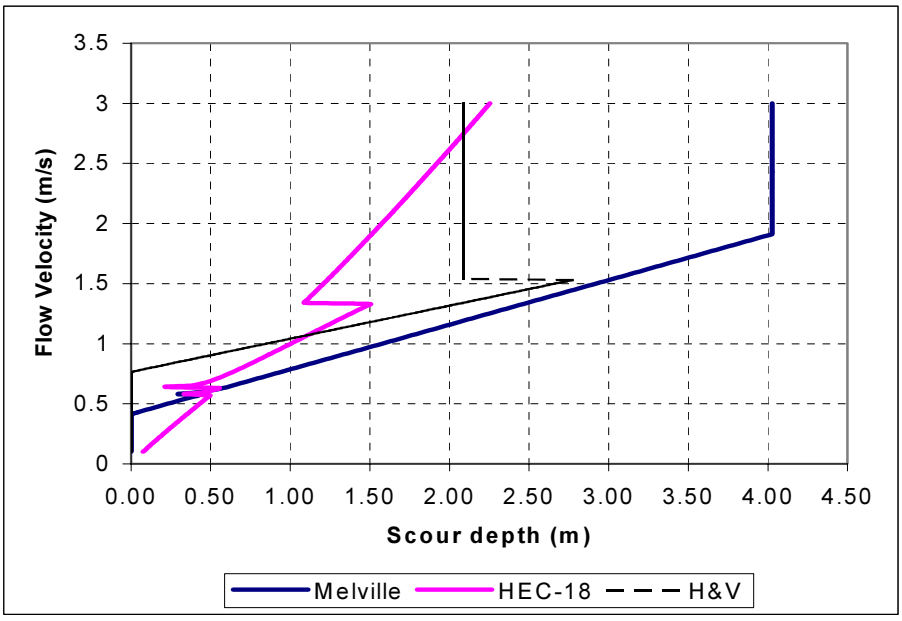

Figure 7.12: Graph of the the flow velocity against scour depth at hole 1.

The results for the used scour formulae are not similar to each other. An independent check of the calculation results is impossible, due to the lack of measured flow velocities. Is was assumed beforehand that the use of different scour formulae could provide more confidence in the results if they were in a close range. Figure 7.13 shows all the results: they are in a relatively close range but vary likewise: the formula presented by Hoffmans & Verheij (1997) yields always larger results than the formula of Melville & Coleman (2000). The results of the flow velocities of the HEC-18 formula are the most dependent on the scour depth.

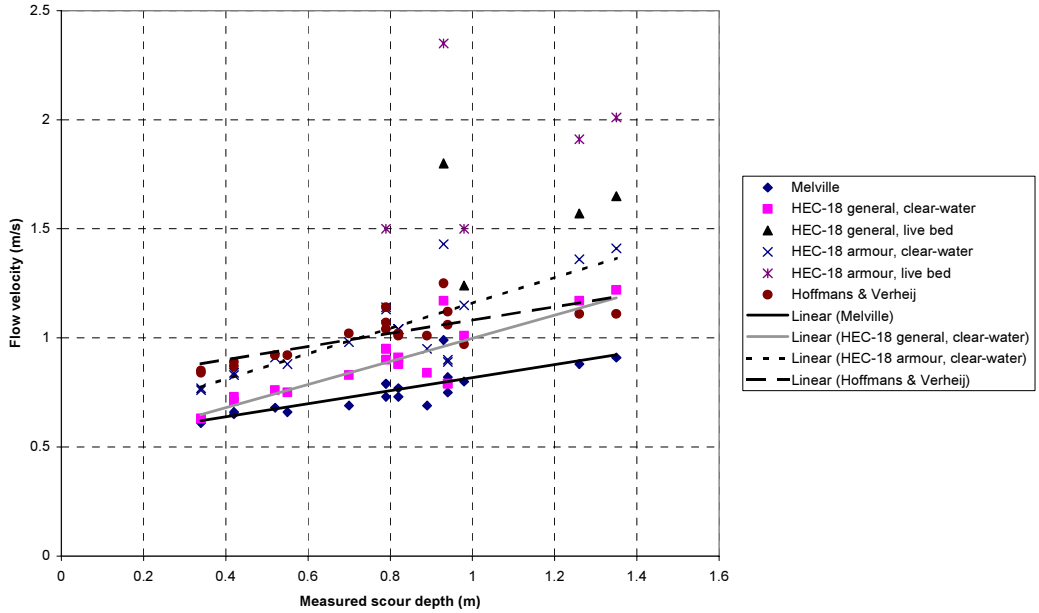

Figure 7.13: All the calculated flow velocities are plotted against the measured scour depth. Also the results of the scour holes at which the scour formulae are assumed to be inapplicable are used.

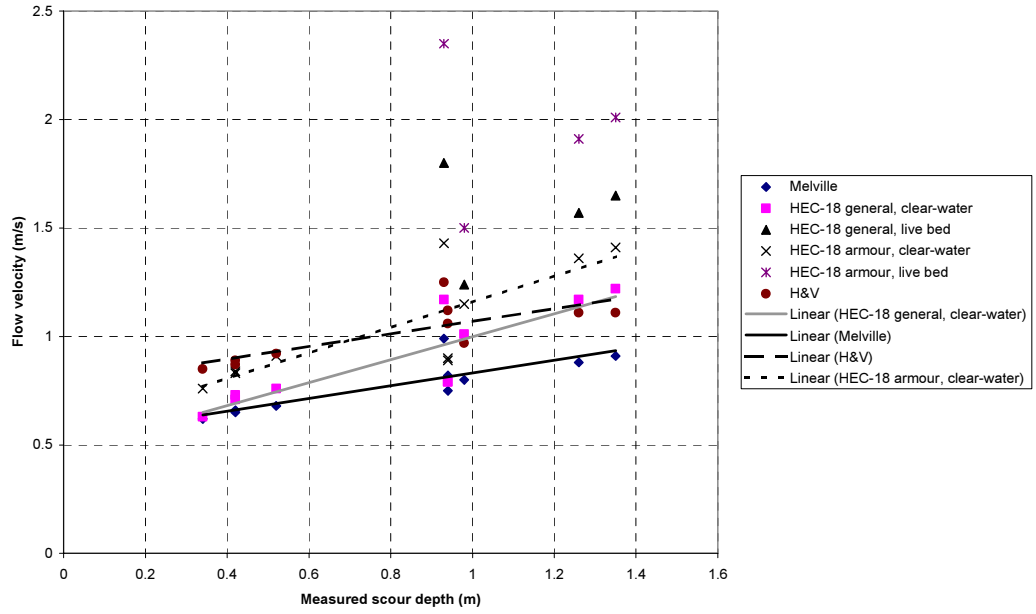

Figure 7.14: The results of the flow velocities are plotted against the measured scour depth. Only the results of the obstacles at which scour formulae are assumed applicable, are presented. The trendlines of Figure 7.13 and this figure show neglectable differences.

The figure above shows only the results of the obstacles at which the scour formulae are assumed to be valid. In comparison with Figure 7.13, the obstacles that have a scour depth of around 0.8 metres appeared to be useless. The presented flow velocities at those obstacles are close to the trendline because the same scour formulae are used with similar values for the input parameters. It cannot be concluded that the results of the omitted obstacles might be useful. A variation in the scour depth results in a smaller variation of the flow velocity. The formula of HEC-18 shows the largest differentiation of the flow velocity dependent on the scour depth.

Large wooden debris that are positioned closely to each other, can be compared to each other because local flow conditions are assumed to change gradually. So, a correlation can be assumed for obstacles positioned close to each other. Hole 2 and 3 at the southern point-bar can be compared, as well as number 9 and 10, and hole 11 and 12, both at the northern point-bar. Unfortunately, the results of hole 2, 3, 9, 11, and 12 are assumed to be meaningless because the scour formulae cannot be applied to these wooden obstacles. So a comparison between the results is not possible to achieve more confidence in the results of the computations.

At the end of this chapter the question arises what should be improved in order to increase the accuracy of the calculations. Eminent is a good knowledge of local water levels during a flood. The water depth influences the results directly by the ratio h_0/b and indirectly through the critical velocity and through the determination of the scouring period. So more accurate time series of the water levels are necessary. From these data the representative water depth h_0 can be obtained. The definition of this water depth should be examined more carefully, preferably through laboratory experiments.
These experiments could also lead to a scour formula especially designed for scour around large wooden debris. Futhermore the effects of small debris drifting to the main tree during the flood can be investigated at these experiments. Last, a better definition of the point at which scour starts is necessary to predict the the time effects, which can also be investigated during experiments.

8 Conclusions

The main question this thesis tries to answer is what the local flow velocities were during the flood of 2001 at a designated study area in the river Allier. These velocities can possibly be derived by studying the characteristics of local scour holes around large wooden debris on the riverbed that act as obstacles to the flow. The depth of the scour hole appeared to be the best indication for the occurred flow velocity. The scour process is similar to that around bridge piers because the shape of the scour hole around the large wooden debris resembles the shape of the hole around a bridge pier. This similarity is an indication that both flow patterns are equal.
Empirical scour formulae predict the scour depth dependent of the local flow conditions. These formulae are used inverted to calculate a flow velocity from a measured scour depth. The local flow velocities during a flood could not be extracted from the depth of the scour hole because of the following reasons:

- The development in time of the wooden obstacle is unknown at the occurrence of the flood. Only the final shape of the object is visible after a flood. The depth of scour is among others dependent of the bridge pier like shape of the large wooden debris. The shape of the obstacle must represent a bridge pier like shape and even so it may have changed during the flood due to small debris that drifts to the main obstacle. Also the position of the debris relative to the main tree trunk might have changed during the flood. So, the conditions of the shape of the obstacle under which the scour took place can only be estimated.
- The shape of the obstacle can sometimes not be presented as a bridge pier shape. As a result, the flow pattern around the large wooden debris is dissimilar to that around a bridge pier. The different flow pattern may affect the depth of scour, which leads to the conclusion that scour formulae cannot be applied.
- Small wooden debris filled the scour hole in front of the main obstacle, which most possibly affects the flow pattern around the obstacle. The flow directed downwards by the obstacle and the so-called horseshoe vortex are assumed to be the main scour force. The small debris could change or diminish these flow characteristics in such way that the scour process is being hampered and a smaller scour depth is attained.
- The scour hole can be filled by fine sediments during the last stage of the flood. As a result, it is more difficult to measure the maximum scour depth that occurred during the flood. The uncertainty of the depth of a scour hole leads to the conclusion that the scour depth may not be a good predictor for the occurred flow velocity.
- The period at which scour is assumed to be active, is mostly large compared to the period of the flood's peak or is assumed to start after the peak of the flood. As a consequence, the results of the calculations apply to the time period at which the scour process was active. Hence, these calculations are not able to predict the flow velocities that occurred at the peak of the flood, because the flow conditions before and after the peak also influenced the scour depth. Nevertheless, the results may possibly present the averaged flow conditions that are necessary to create the measured scour depth, but do not provide information about the morphological processes during the highest stage of the flood.
- There is a lack of local water level measurements at the study area. The water levels are derived from limited data, which leads to a large uncertainty in the prediction of the occurred water levels during the flood. Knowledge of local water levels is important because the local water depth influences many parameters used in the scour formulae. Furthermore, the assumed maximum water depth h_{max} is in most cases much larger than the height H of the wooden obstacle during the flood. As a consequence, the flow pattern changes and the scour formulae cannot be applied.

As can be concluded from above the local flow velocities during a flood cannot be derived from the characteristics of local scour holes. Main reasons are the lack of knowledge about the development of the scour hole and the uncertainty of the input parameters over time. The shape of the large wooden debris could sometimes not be schematised as a bridge pier. Also it is uncertain what the local

conditions were during the flood. Thus, a quantitative estimation of the occurred flow velocities appears to be impossible, also because the results from computations cannot being checked independently. However, in a qualitative way, the following can be considered about the local flow velocities during a flood.

- Regarding the variation of the flow velocities at the floodplain, the highest local flow velocities of the point-bar are likely to occur at the upstream part of the point-bar. At this point the water flows from the main channel onto the floodplain. The coarsest sediment can be found here, and the deepest scour holes are also positioned at the upstream part of the point-bar. According to the results of the calculations, the highest flow velocities are assumed to occur at the upstream part of the point-bar and at locations close to the main channel.
- The initiation of scour marks the lower boundary for the occurred flow velocities during a flood. Scour around a wooden obstacle starts when the local flow velocity is approximately larger than half the critical velocity, which stands for the depth averaged velocity for incipient motion of the riverbed sediment. The critical velocity varies with the local water depth.
- The critical velocity marks the transition between clear-water and live bed scour. Live bed scour occurs when sediment from upstream is continuously supplied to the scour hole. Due to the graded sediment, an armour layer occurs, which hampers the sediment supply from upstream. The particle size distribution of the armour layer in the study area shows spatial variation, which is an indication of the existence of a dynamic armour bed in the river Allier. This assumption leads to the conclusion that the local flow velocities could be higher than the critical velocity, at least during a part of the flood of 2001.

Recommendations

The conclusion of this study is that local flow velocities cannot be derived from the depth of the scour hole. Now the question arises what should be improved or should be known in order to be able to derive an occurred flow velocity from a scour depth. Of eminent importance is the knowledge of local water levels during a flood. The water depth influences the results directly by the ratio h_0/b and indirectly through the critical velocity and through the determination of the scouring period. So more accurate time series of the water levels are necessary.

The representative water depth h_0 can be obtained from these water level data. The definition of the representative water depth should be examined more carefully, preferably through laboratory experiments. These experiments could also lead to a scour formula especially designed for scour around large wooden debris. Furthermore, the effects of small debris drifting to the main tree during the flood can be investigated at these experiments. A better definition of the point at which scour starts is necessary to predict the time effects, which can also be investigated during experiments. The experiments could lead to a decrease in the uncertainty of the occurred conditions at the obstacle during a flood. Observations of the movement of large wooden debris during a flood also clarify the conditions under which the scour process occurs.

The effort and time put into these experiments should be compared to the possibilities to do on-site measurements when a flood occurs. Knowledge of water levels during the flood is necessary and the step towards flow velocity measurements might then be relatively small. However, the movement of large wooden debris could hinder velocity measurements.

The conclusion of this study does not imply that research at wooden obstacles at floodplains can be regarded as useless. The interaction between the large wooden debris and the morphology of the point-bar can be investigated. Also the effects of the obstacles to the rooting of pioneer vegetation can be examined. So the tree trunks at the point-bars of the river Allier are still suitable study objects for further research.

9 Discussion

The goal of this study is to determine the local flow velocities that occurred during the flood of 2001. Flow velocities can be derived from different approaches. The depth of the scour hole appeared to be the best (and only) indication to derive these flow velocities from, but further study resulted in the conclusion that the scour holes do not provide sufficient information about local flow velocities at the highest stage of the flood of 2001.

Scour holes at point-bars in the River Allier originate from large wooden debris, which fell into the river due to bank erosion. The large wooden debris ran aground during a flood and formed an obstacle to the local flow. As a result, a scour hole developed around the debris. The scour process is assumed to be similar to that around bridge piers. The shape of the scour hole around the large wooden debris is mostly similar to the shape of the hole around a bridge pier, which is an indication that both flow patterns are equal. This study uses scour formulae reversibly to calculate flow velocities. The use of scour formulae to calculate flow velocities could be justified in a steady state situation. But the occurrence of a flood is far from a steady state situation. Water levels change in time as well as flow velocities and sediment properties of the riverbed due to armouring. So the possibility to use scour formulae to derive flow velocities can be questioned. To answer this question, the different factors influencing scour depth will be discussed hereafter.

The shape of a bridge pier influences the depth of scour. The shape of an obstacle, which consists of several trees and large wooden debris, should be compared to the shape of a bridge pier. Due to the irregularities in the shape of root wad and adjoining debris, it turned out to be difficult to find an indisputable representative pier diameter and pier shape factor. Now the question arises if a large root wad of a tree with adjoining debris could be represented as a bridge pier. The flow pattern around a bridge pier has a three-dimensional character with a downward pressure gradient that generates a down flow. This down flow acts as a vertical jet and is together with the so-called horseshoe vortex the main erosive force of the scour process. When the flow pattern around the obstacle is similar to the flow pattern at a bridge pier or abutment, the debris can be schematised as a pier. Small wooden debris in front of the main obstacle decreases the similarity with bridge piers. Small wooden debris does not cause scour on itself but mostly deepens the scour at large tree trunks due to an enlargement of the original obstacle.

According to literature the maximum depth of the scour hole is attained in front of the obstacle. This is contradictory to most cases in the study area, where the maximum depth can be found at the sides of the tree. Generally, the scour holes are partly filled with fine sediments, which is assumed to occur in the last phase of the flood when water levels are decreasing. The general form of a scour hole with scour close to the obstacle and deposition of sediment downstream of the obstacle is in accordance to the theory.

Many tree trunks show asymmetrical scour holes. An oblique orientation of the tree compared to the flow direction can be one of the causes for an asymmetrical scour hole. Also the position compared to the (main) gully can be a reason. Last, the shape of the obstacle may be able to cause an asymmetrical scour hole. The presence of debris in the hole could also result in an asymmetrical scour hole.

Scour holes around obstacles provide useful information about the local flow direction during various stages of a flood. The flow direction mostly agrees with the orientation of the obstacle. So this direction was measured during the fieldwork. A study of the precise shape of the scour hole proved a slight difference in flow direction, which means that obstacles mostly show some small oblique orientation to the flow direction. The flow direction appeared to change during the flood, which follows from the different orientation of sediment close to the tree. At decreasing flood levels, the local flow orientation is more directed to the main channel.

Large obstacles show extended scour holes and bank formation downstream of the tree. A large obstacle causes significant morphological effects to the point-bar if the length scale of local morphological effects due to scouring is large compared to the width of the point-bar.

The wooden obstacles at the point-bars have a positive effect to the development of pioneer vegetation at point-bars. Vegetation that are positioned on the higher bank downstream a scour hole, has better chances to survive because of the higher level of the bank. Also sandy deposits near the obstacle

provide good soil for vegetation growth. The obstacle also protects small plants from dehydration by wind.

As a characteristic of a sediment mixture consisting of sand and gravel, armouring of the bed occurs. The finer particles are eroded from the bed and as a result the riverbed consists of a coarser upper part protecting the lower layer. The armouring leads to an increase in the critical bed shear stresses that the riverbed can resist. The coarsest sediment can be found at the upstream part of the point-bar, gradually decreasing to finer particles in downstream direction. So the particle size distribution of the sediment at the point-bars shows spatial variations, which is characteristic for the occurrence of a dynamic armour layer. This assumption leads to the conclusion that local flow velocities could exceed the critical flow velocity of the armoured bed during the peak of the flood.
Downstream of some measured holes a sharp separation in sediment size of the riverbed was visible. The line of separation has more or less the same orientation as the flow direction. The process that caused this phenomenon is unknown, but it was likely to occur during the last phase of the flood. Armouring also occurs at the scour holes near the obstacles. This implies that mainly the coarser part of the particle size distribution affects the depth of scour because fine sediments are assumed to be already in motion before the coarse sediment starts to move. So armouring reduces the scour depth at an obstacle.

Flow velocities could not be derived from the assumed difference in mean particle size diameter upstream and downstream the obstacle compared to the difference in turbulence. Firstly, the assumption that upstream sediment characteristics are coarser than the downstream distribution appeared to be invalid at some obstacles. Secondly, the difference in turbulence could not be predicted because of the irregular shape of the tree trunk and of the time dependency of the occurring turbulence. An averaged turbulence could not be determined and has no meaning here.

The existence of scour holes around wooden debris showed that certain minimum flow velocities are required during the occurrence of a flood. The scour formula of HEC-18 gives a relation for the approach velocity required to initiate scour. Input parameters in this formula are the width of the obstacle and the critical velocity (U_c). The latter is the most important parameter predicting the minimum flow velocities. Other formulae from Melville and Coleman (2000) and Hoffmans and Verheij (1997) state that the scour process starts at $0.5*U_c$. In practice, the differences between both formulae are small. The use of the critical velocity implies that local water depths and sediment distribution are essential in predicting the minimum flow velocities.

The results of the calculations cannot be independently checked by site measurements. Thus, the suitability of the use of scour formulae can only be determined by considering the sensitivity of the results on the variation of the different input parameters and by the mutual equivalence of the results. It appeared that the results of the scour formulae show mutual consistent differences, the flow velocities according to Melville & Coleman are mostly lower than the results of the formula of Hoffman & Verheij. The HEC-18 formula generally yields the highest flow velocities.
Concerning the computations of the occurred flow velocities at the different scour holes, the following considerations must be regarded:

- The scour process is assumed to start at a certain combination of water level and flow velocity. The point at which scour starts, is subjected to uncertainty and can only be estimated. Because the definition of the start of scour depends on the flow velocity, which is unknown. So, the start of scour is estimated from local water levels. A certain discharge is chosen to point out the start of scour. This discharge is fairly arbitrary chosen based on engineering judgement. The results of both cases at hole 6 show the importance of a rightly chosen water level at which the scour process start.
- This study defines a representative water depth h_0 in order to take the effect of changing water levels into account. The definition in this study is based on the averaged influence of all h_0/b ratios during the time period that scour was assumed to be active. The ratio between the representative water depth h_0 and the width b of the obstacle is an important parameter predicting

the depth of scour and thus predicting the approach velocity under clear-water conditions. An increase in the representative water depth leads to lower calculated flow velocities. Therefore, a right definition of the representative water depth h_0, which depends on local water levels, is necessary to be able to predict the occurred flow velocities. So, laboratory studies should be executed to study the definition of a representative water depth more extensively.

- As stated before, the maximum water depth h_{max} is in most cases much larger than the height H of the wooden obstacle. As a consequence, the flow pattern changes and scour formulae are not valid. When the water level exceeds the height of an obstacle, this will lead to a smaller scour depth compared to the situation that the height of an obstacle is equal to the same water depth. If the water depth is kept constant, the depth of scour will be larger at the obstacle that rises above water level, as compared to an obstacle that lies entirely flooded. So, the water depth used in the calculations (h_0) should be reduced if the water depth exceeds the height H of the obstacle. However, it is unknown to what extend this reduction should be. This study uses the arbitrary assumption that if the ratio between the representative water depth h_0 and the height of the tree H is smaller than 1.2, the excess of water level does not affect the scour depth. This assumption leaves out of consideration that the maximum water level h_{max} at the flood of 2001 is much larger than the height of the obstacle H. As a consequence, the flow pattern changes and the scour formulae cannot be applied.
- The measured scour depth d_s is in the same order of magnitude as the representative water depth (h_0). Because of the long time period at which the scour was assumed to be active, the highest water levels at the peak of the flood have small influence on the representative water depth h_0. This could imply that the definition of the representative water depth might be wrong.
- A lower representative water depth leads to larger resulting flow velocities, which is illustrated by the two cases at hole 8. The effects to the results of the flow velocities are small though.
- The effect of time to the computation of the occurred flow velocities is small. In most cases the equilibrium depth is attained. Very wide obstacles show a significant time effect as a consequence of the used formula. In the calculations, only the resulting flow velocities of those obstacles that are probably deposited during the last flood, are influenced by time effects.
- Most calculated velocities are smaller than the critical flow velocity for the threshold of movement of the bed material. This means that clear-water conditions would apply to the occurrence of a flood. This is contradictory to the general assumption that the sediment of the riverbed is in motion during a flood and that a dynamic armour layer with some dune formation may be present.
- Under clear-water conditions, the depth of scour is to a large extend affected by the approach velocity; a small increase in the flow velocity leads to a large increase in the scour depth. Inversely, the scour depth is not able to make a good differentiation between the occurred flow velocities. So a large variation in the scour depth yields a small variation in the occurred flow velocity. Furthermore, the scour depth is generally assumed to be indifferent of the flow velocity under live bed conditions, which means that a measured scour depth cannot predict an occurred flow velocity.

Knowledge of local water levels is important to be able to calculate with the scour formulae and to possibly predict an occurred flow velocity. The water levels should also be known because the magnitude of the critical velocity also depends on the chosen water depth. As a consequence, the value of the critical velocity varies in time. Secondly, the estimation of the time period is dependent of the time series of the water levels. The time effect is also affected by the water levels via the critical velocity, which depends of the water depth.

As described above, the maximum flow velocities could not be derived from the characteristics of the scour holes. The main reason is the lack of essential information about the development of the scour hole and input parameters over time. Due to the small wooden debris that drifted against the main obstacle during the flood, the history of a scour hole is uncertain and can only be predicted using different cases in which different assumptions were made regarding the development in time of the scour hole. It also means that scour holes provide little information about the chronology of a flood.

Before this study started, it was assumed that the scour process only occurred at the highest peak of the flood. Therefore the research to the scour holes seemed to provide useful information about the flow velocities during the short peak of the flood. But the scour process was active during a longer time than the peak of the flood and therefore the results might be representative for an averaged flow velocity during the time that scour was active. So the scour holes might only provide information about the average flow conditions. Concluded, scour holes are valuable sources of information about morphological processes in the river Allier, but they cannot predict the flow velocities during the peak of the flood. Unfortunately, the peak of these floods has great impact to the morphology of the river.

References

Adams, J., *Gravel size analysis from photographs*. Journal of hydraulics division, ASCE, No. 105, p. 1247-1285, 1979.

Bart, P.J., *Overbank flow in the river Allier, A flow model.* Section Hydraulic Engineering, Delft University of Technology, 2000.

Baudrick, C.A. & Grant, G.E., *When do logs move in rivers?* Water resources research, Vol. 36, No. 2, p. 571-583, 2000.

Berg, J., van den & Kramer, J. de & Keinhans, M. & Wilbers, A., *De Allier als morfologisch voorbeeld voor de Grensmaas, deel 1: vergelijkbaarheid en rivierpatroon*. Natuurhistorisch maanblad, juli 2000, p. 188-122, 2000.

Blom, A., *Planform changes and overbank flow in meandering rivers, the river Allier, part 1-Report.* Section Hydraulic Engineering, Delft University of Technology, 1997.

Breusers, H.N.C. & Nicollet, G. & Shen, H.W., *Local scour around cylindrical piers*, Journal of Hydraulic Research, I.A.H.R., Vol 15, No. 3, p. 211-252, 1977.

Bunte, K. & Abt, S.R., *Sampling Surface and Subsurface Particle-Size Distributions in Wadable Gravel- and Cobble-Bed Stream for Analysis in Sediment, Transport, Hydraulics, and Streambed Monitoring.* United States Department of Agriculture, Forest Service, General Technical Report RMRS-GTR-74, 2001.

Breusers, H.N.C. & Raudkivi, A.J., *Scouring*. Hydraulic structures design manual, No. 2, Balkema, Rotterdam, 1991.

Chiew, Y. & Melville, B.W., *Temporal development of local scour depth at bridge piers*. North American Water and Environment Congress, ASCE, Anaheim California, USA, 1996.

Cohen, K., *Spatial variability of gravel beds pavements in the Allier*. Vakgroep Fysische Geografie, Faculteit Ruimelijke Wetenschappen, Universiteit Utrecht, 1998.

Driesprong, A., *Boundary Shear Stress and Hydraulic Roughness in the Allier River.* Department of Environmental Sciences, Faculty of Physical Geography, Utrecht Univerity, 2001.

Escarmeia, M. & May, R.W.P., *Scour around structures in tidal flows.* Report SR 521, HR Wallingford, April 1999.

Ettema, R., *Scour at bridge piers*. Report No. 216, School of Engineering, The university of Auckland, Auckland, New Zealand, 527pp.

Harris, J.D., *Hydraulic design of bridges*. Chapter I, MTC Drainage Manual, Drainage and Hydrology section, Ontario Ministry of Transportation, Downsview, Ontario, Canada, 1988.

Hoffmans, G.J.C.M., *Stability of loose material (current)*. PAO course, Delft, 4-12 April 2002.

Hoffmans, G.J.C.M. & Verheij, H.J., *Scour Manual*. Balkmena, Rotterdam, 1997.

Kamil, H.M. & Othman, K., *Simulation of flow around piers*. Journal of Hydraulic Research, ASCE, Vol 40, No. 2, p. 161-174, 2002

Keinhans, M. & Berg, J., van den & Wilbers, A. & Kramer, J. de, *De Allier als morfologisch voorbeeld voor de Grensmaas, deel 3: sedimenttransport en afpleistering*. Natuurhistorisch maanblad, september 2000, p. 202-207, 2000.

Kramer, J. de, *Oevererosie en meandermigratie in de Allier*. Vakgroep Fysische Geografie, Faculteit Ruimelijke Wetenschappen, Universiteit Utrecht, 1998.

Kramer, J. de & Wilbers, A. & Berg, J., van den & Keinhans, M., *De Allier als morfologisch voorbeeld voor de Grensmaas, deel 2: oevererosie en meandermigratie*. Natuurhistorisch maanblad, augustus 2000, p. 189-198, 2000.

Melville, B.W. & Chiew, Y., *Time Scale for Local Scour at Bridge Piers*. Journal of Hydraulic Engineering, ASCE, Vol 125, No. 1, p. 59-65, 1999.

Melville, B.W. & Coleman, S.E., *Bridge Scour*. Water Resources Publications, Highlands Ranch, Colorado, USA, 2000

Melville, B.W. & Raudkivi, A.J., *Effects of foundation geometry on bridge pier scour*. Journal of Hydraulic Engineering, ASCE, Vol. 122, No 4, p. 203-209, 1996.

Melvile, B.W. & Sutherland, A.J., *Design method for local scour at bridge piers*. Journal of Hydraulic Engineering, ASCE, Vol. 114, No 10, p. 1210-1226, 1988.

Neill, C.R., *Note on initial movement of coarse uniform bed material*. Journal of Hydraulic Research, ASCE, Vol 17, No. 2, p. 247-249, 1968.

Neessen, C.A.J., Three dimensional flow patterns in the river Allier, graduation thesis, Vakgroep Fysische Geografie, Faculteit Ruimelijke Wetenschappen, Universiteit Utrecht, 2000.

Raudkivi, A.J., *Functional Trends of Scour at Bridge Piers*. Journal of Hydraulic Engineering, ASCE, Vol 112, No. 1, p. 1-12, 1986.

Richardson, E.V. & Davis, S.R., *Evaluating scour at bridges, fourth edition*. U.S. Department of Transportation, Federal Highway Administration, Publication No. FHWA NHI 01-001, Hydraulic Engineering Circular 18, 2001.

Rijn, L.C. van, *Principles of sediment transport in rivers estuaries and coastal seas*. Aqua Publications, Amsterdam, 1993.

Schiereck, G.J., *Introduction to Bed, bank and shore protection*. Delft University Press, Delft, 2001

Thorne, C.R. & Bathurst, J.C. & Hey, R.D., *Sediment Transport in Gravel-Bed Rivers*. John Wiley & Sons Ltd., Great Britain.

Wilbers, A., *De Allier, een Rivier met Twee Patronen*. Vakgroep Fysische Geografie, Faculteit Ruimelijke Wetenschappen, Universiteit Utrecht, 1997.

Appendix A: Scour formulae

There are different scour formulae to predict the scour depth around bridge piers. This appendix describes the method of the formulae used in this study. These formulae are from Melville & Coleman (2000), from Richardson & Davis (2001), and from Hoffmans & Verheij (1997). The formula from Richardson & Davis (2001) is referred as HEC-18.
General parameters are:

b = width of pier (m)
U = mean flow velocity (m/s)
U_c = critical flow velocity (m/s)
h_o = flow depth (m)
K = correction factors
d_s = scour depth (m)
d_{se} = equilibrium scour depth (m)

Melville and Coleman (2000)

This formula originates from the Auckland university in New Zealand. It is based on the measurement data from different laboratory studies over the years. General form of the formula is:

$$d_s = K_{h_o b} * K_I * K_d * K_s * K_\theta * K_G * K_t \qquad \text{(A.1)}$$

Where:

K_{h0b} = flow depth - foundation size (depth-size) factor
K_I = flow intensity factor
K_d = sediment size factor
K_s = pier shape factor
K_θ = foundation alignment factor
K_G = approach channel geometry (=1)
K_t = time factor

Flow depth - foundation size (depth-size) factor is represented by:

$$\begin{aligned} K_{h_o b} &= 2.4b && \frac{b}{h_o} < 0.7 \\ K_{h_o b} &= 2\sqrt{h_o b} && 0.7 < \frac{b}{h_o} < 5 \\ K_{h_o b} &= 4.5h_o && \frac{b}{h_o} > 5 \end{aligned} \qquad \text{(A.2)}$$

In deep flows, the strength of the horseshoevotex and associated downflow is related to the transverse size of the pier. Thus the scour depth is dependent on the pier size. The horseshoe vortex, the principal cause of scour, is affected by the formation of the surface roller that forms at the leading edge of the pier. These two vortexes have opposite directions of rotation. In principle, as long as they do not interfere with each other, the local scour depth is independent of flow depth (narrow piers). With decreasing flow depth, the surface roller becomes more dominant. This renders the base vortex less capable of entraining sediment and thus reducing the local scour depth. The local scour is said to occur at wide piers in such cases (Melville & Chiew, 1999). If the flow shallowness decreases more, the scour depth becomes again independent of the width of the pier, which is illustrated in Figure A.1.

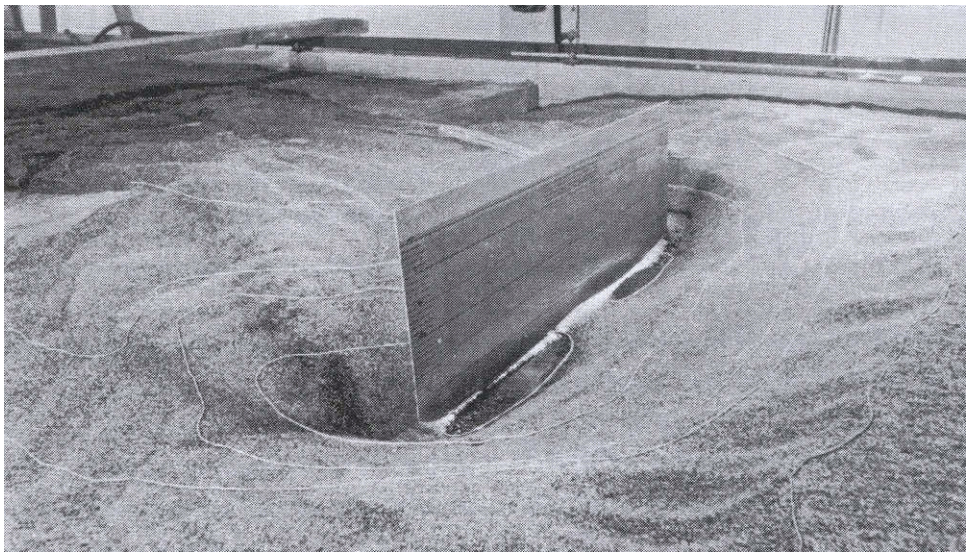

Figure A.1: Scour at a wide pier. The maximum depth is at the end of the pier and not at the middle of the pier (from Melville & Coleman, 2000).

Flow intensity factor K_I

This factor represents the flow intensity defined by $\frac{U}{U_c}$. U_c stands for the critical flow velocity that indicates the threshold of motion. When $U \approx U_c$ the maximum scour depth has a peak value. To take the effect of armouring into account an another velocity parameter has been introduced: U_a, which stands for the armour peak velocity. The ratio $\frac{U}{U_a}$ is a measure for the flow intensity for scour with non-uniform sediments. If $\frac{U}{U_a} < 1$ armouring of the bed occurs as scour proceeds and clear water conditions are considered to exist. The flow intensity factor K_I is represented by:

$$\begin{aligned} K_I &= \frac{U-(U_a-U_c)}{U_c} && \frac{U-(U_a-U_c)}{U_c} < 1 \\ K_I &= 1 && \frac{U-(U_a-U_c)}{U_c} \geq 1 \end{aligned} \qquad \text{(A.3)}$$

The flow intensity factor K_I is dependent on the approach velocity when clear-water conditions apply. Under live bed conditions, the scour depth becomes independent of the flow velocity.
The threshold velocity U_c is calculated with the following method:
Find u_{*c} for d_{50} from shields diagram with (ψ=0.055):

$$u_{*c} = 0.0305 d_{50}{}^{0.5} - 0.0065 d_{50}{}^{-1} \qquad \text{(A.4)}$$

The critical velocity U_c follows from the logarithmic velocity distribution for fully turbulent flow:

$$\frac{U_c}{u_{*c}} = 5.75 \log\left(5.53 \frac{h_0}{d_{50}}\right) \qquad \text{(A.5)}$$

The armour peak velocity U_a is calculated using the following equations:

$$
\begin{aligned}
d_{50a} &= \frac{d_{\max}}{1.8} \\
u_{*ca} &= 0.0305 d_{50a}{}^{0.5} - 0.0065 d_{50a}{}^{-1} \\
\frac{U_{ca}}{u_{*ca}} &= 5.75 \log\left(5.53 \frac{h_0}{d_{50a}} \right) \\
U_a &= 0.8 U_{ca}
\end{aligned}
\qquad \text{(A.6)}
$$

The effect of armouring on the scour depth is presented in figure A.2.

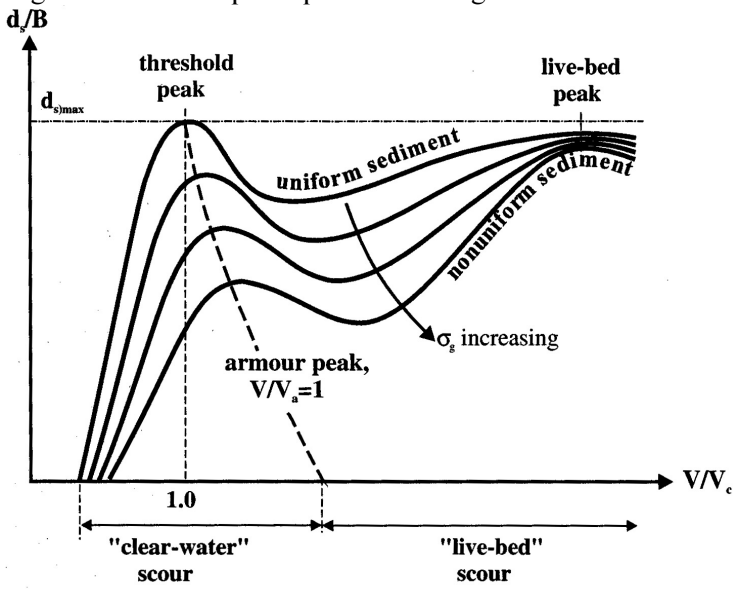

Figure A.2: Local scour depth variation with flow intensity (from Melville and Coleman, 2000). V *is equal to* U. *The parameter* σ_g *stands for the uniformity of the sediment of the bed.*

Sediment size factor K_d

When the sediment is very coarse compared to the pier diameter a reduction in scour depth may be expected. The local scour depth is influenced by sediment size when $\frac{b}{d_{50}} < 50$. For local scour at pier, Ettema (1980) explained that for smaller values of the sediment coarseness ratio, individual grains are large relative to the groove excavated by the downflow. The erosion process is hampered because the porous bed dissipates some energy of the downflow (Melville & Coleman, 2000). If $\frac{b}{d_{50}} > 25$ then K_d=1.0, which is the case at all scour holes.

Pier shape factor K_s

The standard foundation shape is a ciculair pier (K_s=1.0). Shape effects of other pier shapes are given as multiplying factors that account for the difference in local scour due to the deviating shape. Pier shape factors have a range from 0.65 to 1.2. Rectangular piers have K_s=1.1 and cirular piers have K_s=1.0, which are the most commonly used values in this research.

Foundation alignment factor K_θ

When piers are aligned with the flow (direction θ=0°) then K_θ=1.0.

Time factor K_t

The time factor is defined as the ratio of local scour depth d_s at a particular time t to the equilibrium scour depth d_{se}, which occurs at time t_e. The factor K_t is dependent of clear water and live bed scour conditions. Under live bed conditions, the equilibrium scour depth is attained rapidly so K_t=1.0.
For local scour at circular bridge piers under clear water conditions, K_t is described below:

$$K_t = \exp\left\{-0.03\left|\frac{U_c}{U}\ln\left(\frac{t}{t_e}\right)\right|^{1.6}\right\} \tag{A.7}$$

With t_e (in days), which combines the effect of flow shallowness and flow intensity as:

$$\begin{aligned} t_e(days) &= 48.26\frac{b}{U}\left(\frac{U}{U_c}-0.4\right) && \frac{h_0}{b}>6, \frac{U}{U_c}>0.4 \\ t_e(days) &= 30.89\frac{b}{U}\left(\frac{U}{U_c}-0.4\right)\left(\frac{h_0}{b}\right)^{0.25} && \frac{h_0}{b}\le 6, \frac{U}{U_c}>0.4 \end{aligned} \tag{A.8}$$

This time factor remained unregarded in this research.

Hydraulic Engineering Circular no 18 (HEC-18) (2001)

This formula originates from Richardson and Davis (2001). This formula is based on an equation from the Colorado State University (CSU) and is recommended for both clear-water as live bed scour.
General form of the formula is:

$$d_s = 2.0 * K_s * K_\theta * K_3 * K_4 * K_w * \left(\frac{h_0}{b}\right)^{0.35} * Fr^{0.43} * b \tag{A.9}$$

Where:

K_s = Pier nose shape factor
K_θ = Correction factor for angle of attack of flow
K_3 = bed condition factor
K_4 = Correction factor for armouring by bed material size
K_w = Correction factor for very wide piers

$$Fr = \frac{V}{\sqrt{gh_0}}$$

Pier nose shape factor K_s

The standard foundation shape is a ciculair pier (K_s=1.0). Shape effects of other pier shapes are given as multiplying factors that account for the difference in local scour due to the deviating shape. Pier nose shape factors have a range from 0.9 to 1.1. Rectangular pier noses have K_s=1.1.

Pier alignment factor K_θ

This is the same factor as the foundation alignment factor in the formula of Melville. When piers are aligned with the flow direction then $\theta = 0^o$ and K_θ=1.0. When $\theta \neq 0^o$ and the full length of the pier (L) is subjected to the flow, the factor is:

$K_\theta = \left(\cos\theta + \frac{L}{b}\sin\theta\right)^{0.65}$. If L/b is larger than 12, use L/b=12.

Bed correction factor K_3

The bed correction factor results from the fact that for plane bed conditions the maximum scour may be 10 percent greater than computed by the main equation (A.9). If there is a dune bed configuration

of with large dunes during floods, the maximum scour depth may be 30 percent greater than calculated by equation (A.9). This may occur at very large rivers. For smaller stream that have dune configuration at flood flow, the dunes will be smaller and the maximum scour may be only 10 to 20 percent larger than. In the writers opinion this factor K_3 acts as a safety factor and therefore it is set to 1.0 for clear-water conditions. For live bed conditions K_3=1.1.

Correction factor for armouring by bed material size

This factor K_4 decreases scour depth for armouring of the scour hole. It is applicable for bed materials that have a d_{50} equal to or larger than 2.0 mm and d_{95} equal to or larger than 20 mm.
The correction factor K_4 can be written as:

$$K_4 = 0.4\left(V_R\right)^{0.15} \tag{A.10}$$

Where:

$$V_R = \frac{U - U_{icd_{50}}}{U_{cd_{50}} - U_{icd_{95}}} > 0 \tag{A.11}$$

U_{icdx} = the approach velocity required to initiate scour at the pier for the grain size d_x.

$$U_{icd_x} = 0.645\left(\frac{d_x}{b}\right)^{0.053} U_{cd_x} \tag{A.12}$$

U_{cdx} = the critical velocity for incipient motion for the grain size d_x.

$$U_{cd_x} = 6.19 h_0^{\frac{1}{6}} d_x^{\frac{1}{3}} \tag{A.13}$$

d_x = grain size for which x percent of the bed material is finer.
Equation (A.13) yields the same results as the Shields concept using a ψ_c=0.043 and the assumption of a hydraulically smooth bed.
The minimum value for K_4 is 0.4 and should only used when $U<U_{icd50}$.

Correction factor for very wide piers (K_w)

Flume studies on scour depths at wide piers in shallow flows and field observations of scour depth at bascule piers in shallow flow indicate that the CSU equation overestimate scour depths. Therefore a correction factor K_w has been applied. This correction factor should only be used when:
$\frac{h_0}{b} < 0.8$ and $\frac{b}{d_{50}} > 50$ and the flow is subcritical.
The factor is represented by:

$$\begin{aligned} K_w &= 2.58\left(\frac{h_0}{b}\right)^{0.34} Fr^{0.65} && \frac{V}{V_c} < 1 \\ K_w &= 1.0\left(\frac{h_0}{b}\right)^{0.13} Fr^{0.25} && \frac{V}{V_c} \geq 1 \end{aligned} \tag{A.14}$$

This factor is based on limited data from flume experiments. Nevertheless, it will be applied to this research because the results of the scour formulas should not include a safety factor, which applies to the design of scour depths at bridge piers. An overestimation of the local scour depth results in lower occurring flow velocities.

Hoffmans and Verheij (1997)

On the basis of experimental data, Breusers et al. (1977) developed two formulas for clear-water scour and live bed scour. The general form of the formula is:

$$d_{se} = 1.5 K_i b \tanh\left(\frac{h_0}{b}\right) \qquad U > U_c$$

$$d_{se} = 2.0 K_i b \left(\frac{2U}{U_c} - 1\right) \tanh\left(\frac{h_0}{b}\right) \qquad 0.5 < \frac{U}{U_c} < 1 \qquad \text{(A.15)}$$

$$K_i = K_s * K_\theta * K_g$$

Where:

U_c = critical mean velocity (m/s)
U = mean velocity (m/s), $U=Q/A$, Q is discharge (m^3/s), A is cross section (m^2)
K_s = pier shape factor
K_θ = pier alignment factor
K_g =factor for the influence of gradation of the bed material

If the approach velocity is smaller than half the critical velocity, no scouring will predicted. As can be seen in equation (A.15), the scour depth becomes independent of the local flow velocity under live bed conditions. So this equation is only able to compute a flow velocity when clear-water conditions apply.

Pier shape factor K_s

The standard foundation shape is a ciculair pier (K_s=1.0). Shape effects of other pier shapes are given as multiplying factors that account for the difference in local scour due to the deviating shape. Pier shape factors have a range from 0.65 to 1.2. Rectangular piers have K_s=1.1, circular piers have K_s=1.0.

Pier alignment factor K_θ

This is the same factor as the foundation alignment factor in the formula of Melville. When piers are aligned with the flow direction then $\theta = 0^o$ and K_θ=1.0. When $\theta \neq 0^o$ and the full length of the pier (L) is subjected to the flow, the factor is:

$K_\theta = \left(\cos\theta + \frac{L}{b}\sin\theta\right)^{0.62}$. There is a small difference in the value of the power compared to the equation of HEC-18.

Factor for the influence of gradation of the bed material K_g

The influences of the particle size diameter and the density of the sediment are usually taken into account in the critical flow velocity. The gradation of the bed material also influences the scour depth and can be characterised by: $\sigma_g = \frac{d_{84}}{d_{50}}$. The coefficient K_g has a range from 1 for uniform sediments to K_g=0.2 for non-uniform sediments with a σ_g=>4. The relation between Kg and σ_g is based on little field data and should therefore be used with care.

Appendix B: Information about the scour holes

This appendix contains the datasheets of all scour holes, as explained in chapter 4. Secondly, the shape of each scour hole can be found together with a picture. The positions of the scour holes in the study area are illustrated in the figure below:

Figure B.1: Position of all scour holes at the study site. Aerial photograph is from 2000.

Appendix C: Cross-section defined at the study area

This appendix will describe the cross-sections as used in chapter 5. The positions of the cross-sections can be found in figure C.1. Four cross-section are defined with in the study area. The northern cross-section located at the point-bar of "Chateau the Lys", the middle profile located at the point-bar near the farm "Le Verdelet", and two cross-sections located at the southern point-bar. First the cross-section will be showed, followed by a table presenting the data used to divide the discharge over cell as described in section 5.3.1.

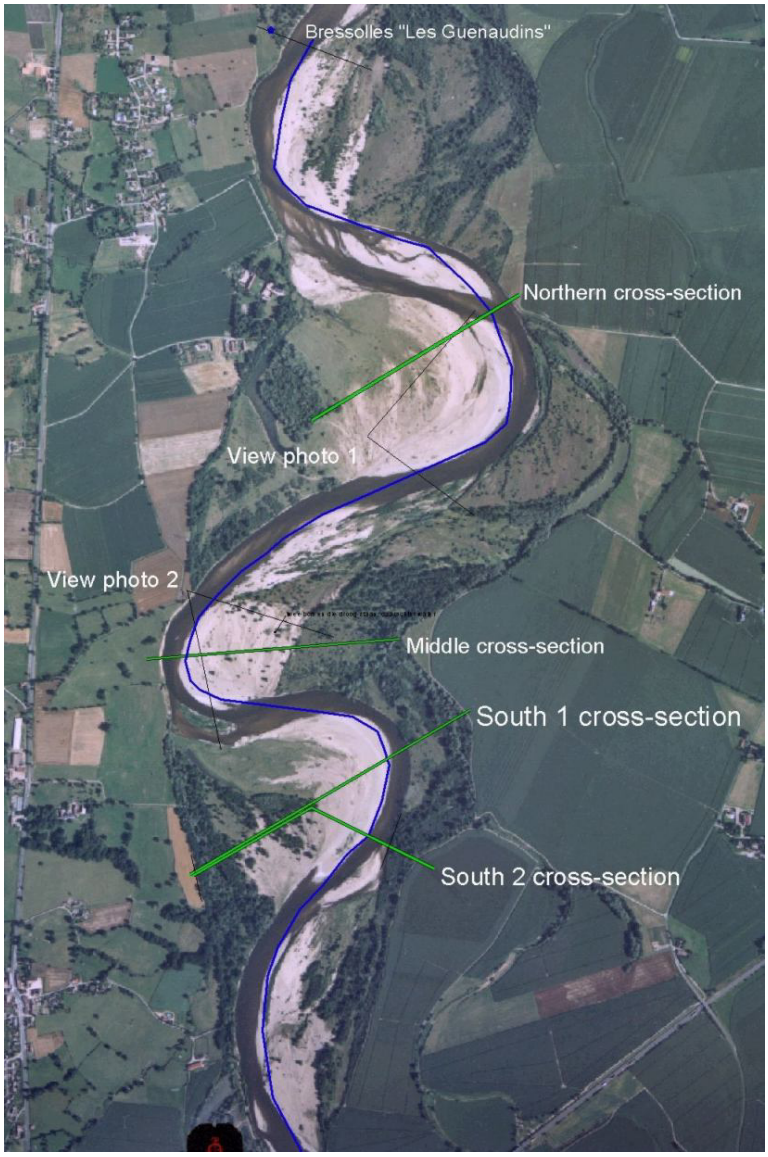

Figure C.1: Aerial picture of the study site with the locations of the cross-sections and viewpoints of the used photographs.

Cross-section at the northern point-bar near "Chateau de Lys"

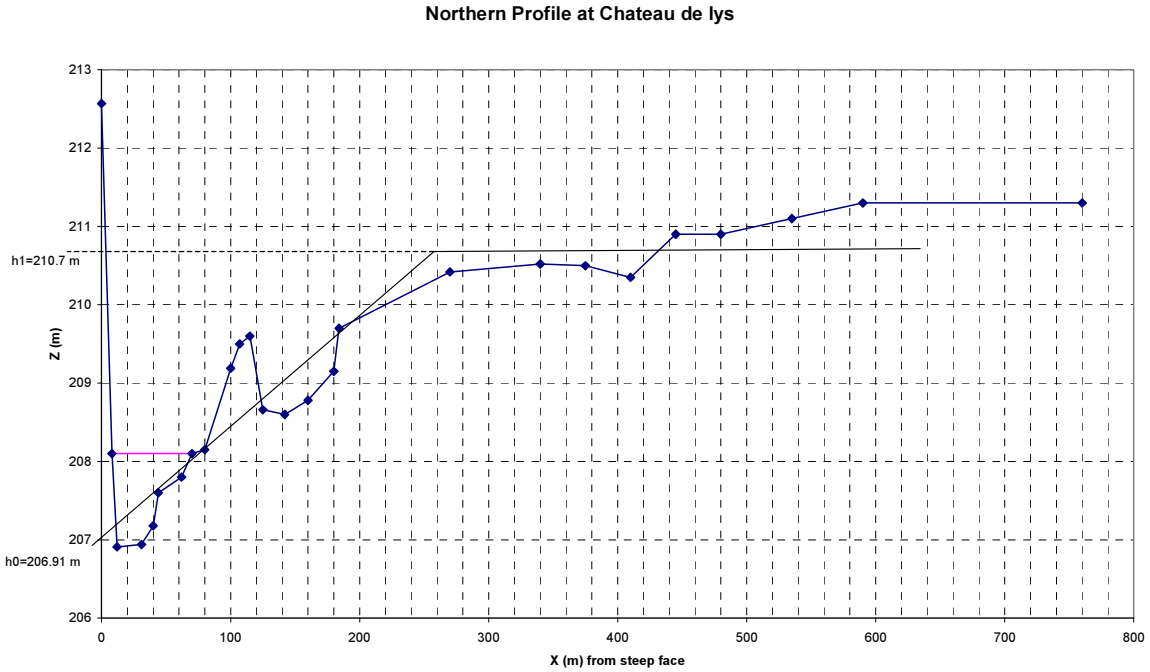

Parameters used to distribute discharge over the cross-section:

Water line	208.1	Z (m)			
Cell	*B (m)*	*cum B (m)=X*	*Zb (m)*	*d (m)*	*C (m1/2/s)*
1	10	10	209.5	-1.4	50
2	10	20	206.5	1.6	50
3	10	30	206.7	1.4	50
4	10	40	207.05	1.05	50
5	10	50	207.5	0.6	50
6	10	60	207.7	0.4	50
7	10	70	207.95	0.15	50
8	10	80	208.13	-0.03	50
9	10	90	208.5	-0.4	50
10	10	100	208.85	-0.75	50
11	10	110	209.3	-1.2	50
12	10	120	209.5	-1.4	50
13	10	130	208.7	-0.6	50
14	10	140	208.65	-0.55	50
15	10	150	208.6	-0.5	50
16	10	160	208.65	-0.55	50
17	10	170	208.85	-0.75	50
18	10	180	209.05	-0.95	50
19	10	190	209.6	-1.5	50
20	20	210	209.8	-1.7	40
21	20	230	210	-1.9	40
22	20	250	210.2	-2.1	40
23	20	270	210.35	-2.25	40
24	40	310	210.45	-2.35	30
25	40	350	210.52	-2.42	30
26	40	390	210.5	-2.4	30
27	40	430	210.5	-2.4	30
28	20	450	210.8	-2.7	30
29	40	490	210.9	-2.8	30
30	100	590	211.15	-3.05	20
31	170	760	211.3	-3.2	20

Cross-section at the middle point-bar near farm "le Verdelet"

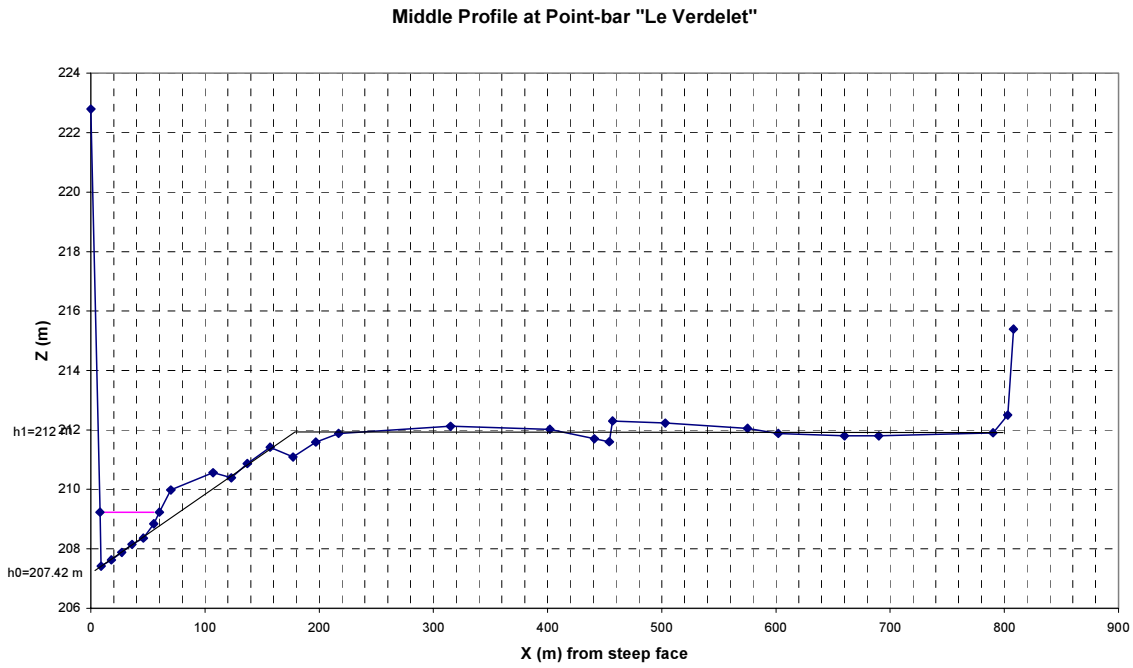

Parameters used to distribute discharge over the cross-section:

Water level	209.23	Z (m)			
Cell	*B (m)*	*cum B (m)=X*	*Zb (m)*	*d (m)*	*C (m1/2/s)*
1	10	10	212	-2.77	50
2	10	20	207.4	1.83	50
3	10	30	207.7	1.53	50
4	10	40	208.15	1.08	50
5	10	50	208.36	0.87	50
6	10	60	208.84	0.39	50
7	10	70	209.6	-0.37	50
8	10	80	210	-0.77	50
9	20	100	210.27	-1.04	50
10	20	120	210.5	-1.27	50
11	20	140	210.55	-1.32	50
12	20	160	211.2	-1.97	50
13	20	180	211.3	-2.07	50
14	20	200	211.35	-2.12	50
15	200	400	212	-2.77	45
16	20	420	211.9	-2.67	45
17	20	440	211.8	-2.57	45
18	20	460	211.7	-2.47	45
19	120	580	212.2	-2.97	30
20	200	780	211.9	-2.67	30
21	20	800	212.1	-2.87	30
22	8	808	213	-3.77	30

Cross-section at the southern point-bar: South 1, straight profile

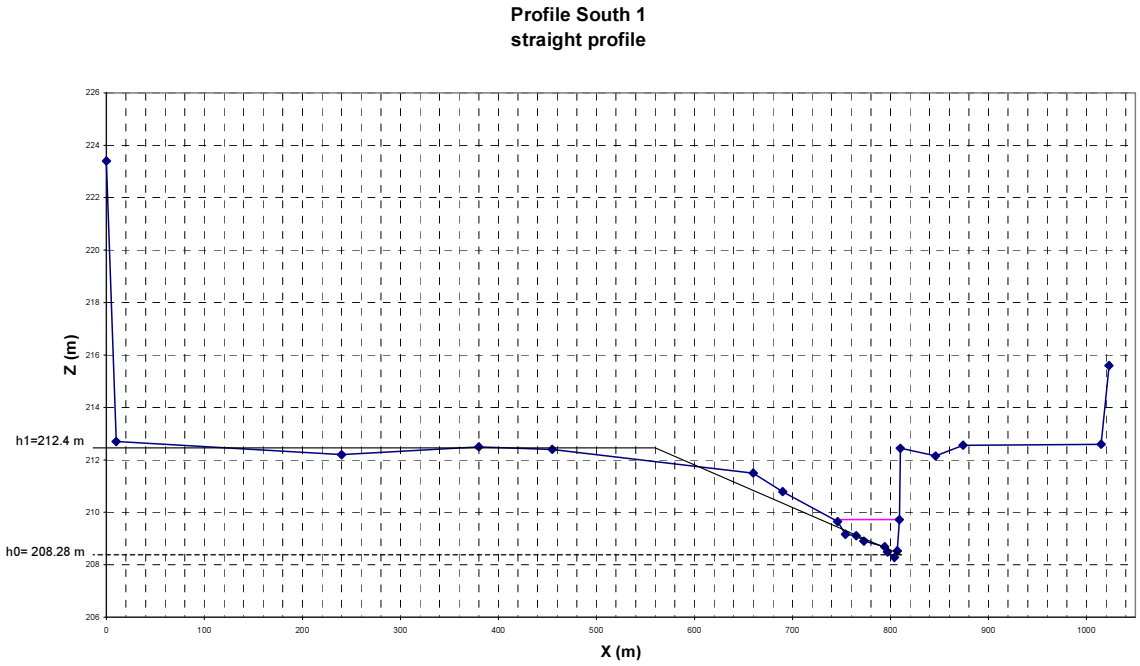

Parameters used to distribute discharge over the cross-section:

Water level	209.72	Z (m)			
Cell	*B (m)*	*cum B (m)=X*	*Zb (m)*	*d (m)*	*C (m1/2/s)*
1	370	370	212.5	-2.8	30
2	80	450	212.45	-2.75	30
3	40	490	212.2	-2.5	50
4	40	530	212	-2.3	50
5	40	570	211.8	-2.1	50
6	40	610	211.6	-1.9	50
7	40	650	211.55	-1.85	50
8	10	660	211.3	-1.6	50
9	10	670	211	-1.3	50
10	10	680	210.8	-1.1	50
11	10	690	210.6	-0.9	50
12	10	700	210.4	-0.7	50
13	10	710	210.2	-0.5	50
14	10	720	210	-0.3	50
15	10	730	209.85	-0.15	50
16	10	740	209.75	-0.05	50
17	10	750	209.16	0.54	50
18	10	760	209.11	0.59	50
19	10	770	208.9	0.8	50
20	10	780	208.8	0.9	50
21	10	790	208.4	1.3	50
22	10	800	208.8	0.9	50
23	20	820	212.4	-2.7	30
24	20	840	212.2	-2.5	30
25	20	860	212.4	-2.7	30
26	140	1000	212.6	-2.9	20
27	10	1010	214	-4.3	20

Cross-section at the southern point-bar: South 2, bended profile

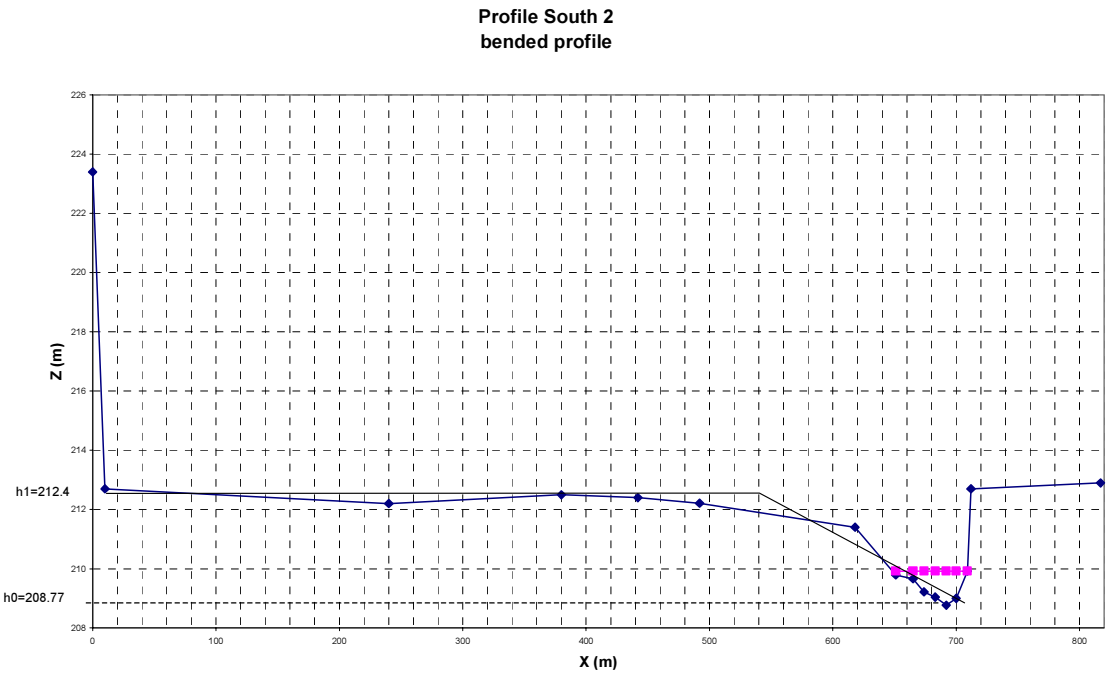

Parameters used to distribute discharge over the cross-section:

Water level	209.92	Z (m)			
Cell	*B (m)*	*cum B (m)=X*	*Zb (m)*	*d (m)*	*C (m1/2/s)*
1	370	370	212.5	-2.58	30
2	70	440	212.45	-2.53	30
3	40	480	212.3	-2.38	50
4	20	500	212.2	-2.28	50
5	20	520	212.1	-2.18	50
6	20	540	211.9	-1.98	50
7	20	560	211.8	-1.88	50
8	20	580	211.6	-1.68	50
9	20	600	211.5	-1.58	50
10	20	620	211.4	-1.48	50
11	10	630	210.9	-0.98	50
12	10	640	210.5	-0.58	50
13	10	650	210	-0.08	50
14	10	660	209.75	0.17	50
15	10	670	209.66	0.26	50
16	10	680	209.3	0.62	50
17	10	690	209.04	0.88	50
18	10	700	208.7	1.22	50
19	10	710	209.4	0.52	50
20	107	817	212.8	-2.88	20

Appendix D: schematisation of the cross-sections

Because all defined river profiles at the study site are positioned at bends of the river, the cross-profile may be schematized as a triangular profile. shows this schematisation.

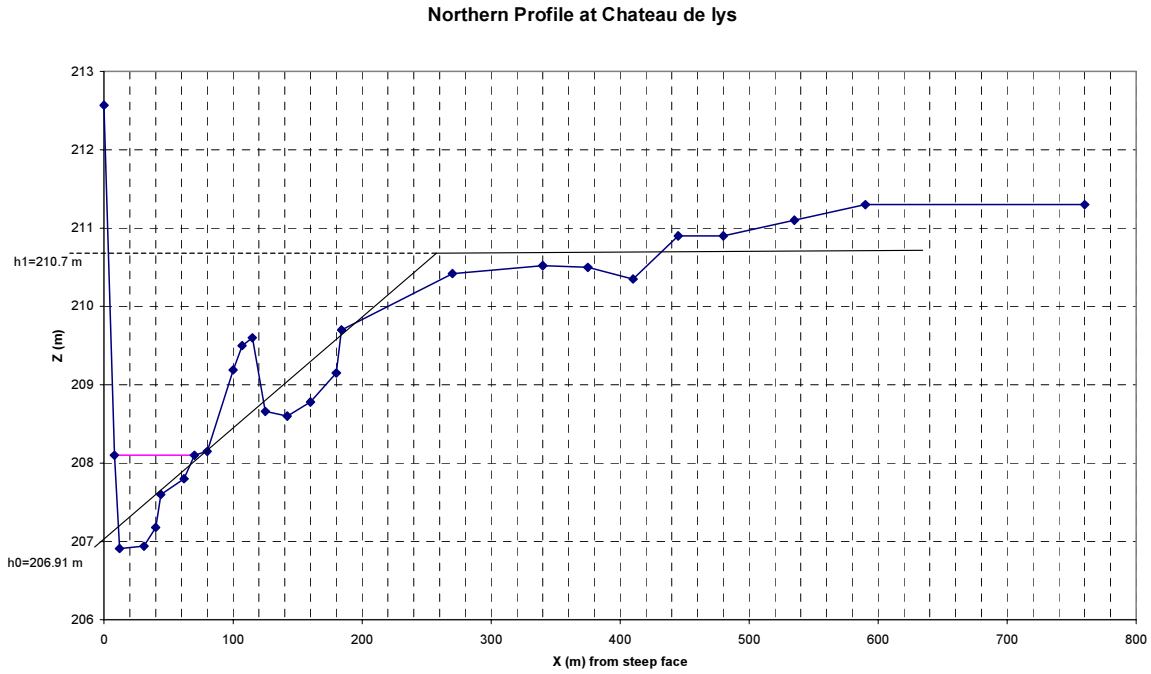

Profile at the pointbar of Chateau de Lys with schematisation of the bed profile.

The form of a Q-h relation is in general: $Q = a(h)^b$. Coefficient *b* describes the kind of bed profile and coefficient *a* is used to fit the relation to the data sets.

Consider a triangular bed profile:

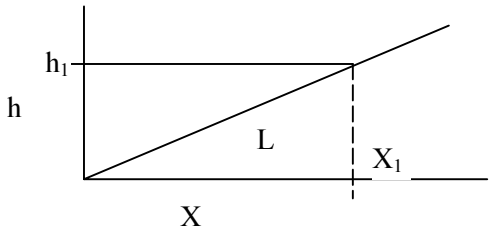

The width of the channel can be described as:

$$X = ah + b \tag{D.1}$$

with:

$$a = \frac{X_1}{h_1} \tag{D.2}$$

$$b = 0$$

The surface *A* as function of *h* is then: $A = \frac{1}{2}ah^2$. the coefficient b comes from a relation between the discharge *Q* and the water depth *h*. The formula of Chézy gives:

$$Q = AC\sqrt{Ri}$$
$$R = \frac{A}{P} \qquad \text{(D.3)}$$

where *P* is the wetted perimeter: $P = h + L$. *L* is the length of the hypotenuse of the triangle with height *h* and width *X*. If $\tan\alpha = \frac{X_1}{h_1}$ then $L = \frac{h}{\cos\alpha}$.

Because $X_1 \quad h$, cos α can be written as $\cos\alpha \approx \frac{h_1}{X_1} \approx \frac{1}{a}$.

$$P = L + h = (1+a)h$$

So
$$R = \frac{A}{P} = \frac{\frac{1}{2}ah^2}{(1+a)h} \qquad \text{(D.4)}$$

The formula of Chézy becomes then:

$$Q = \frac{1}{2}ah^2C\sqrt{\left(\frac{\frac{1}{2}ah^2}{(1+a)h}\right)i} \qquad \text{(D.5)}$$

The formula can be rewritten to:

$$Q = \frac{1}{2}ah^2C\sqrt{\left(\frac{\frac{1}{2}ah}{(1+a)}\right)i} \qquad \text{(D.6)}$$

From this formula the coefficient *b* in Q-h relation can be derived. The coefficient *b* equals to 2.5.This means that for a triangular cross-section the Q-h relation has the form:

$$Q = a(h)^{2.5} \qquad \text{(D.7)}$$

Appendix E: Flow velocity as function of scour depth at the obstacles

Hole 1: large tree to main channel

Input parameters:

Parameter	*Value*
Width *b* (m)	2.36
Height *H* (m)	1.47
Scour depth d_s (m)	1.26
h_0 Melville & C. (m)	1.42
h_0 HEC-18 (m)	1.44
h_0 Hoffmans &Verheij (m)	1.41
d_{50} (mm) general	8.40
d_{50} (mm) armour	17.23
t (hour)	1872
Shape factor K_s (-)	1.1

The general sediment properties are used in the formula of HEC-18

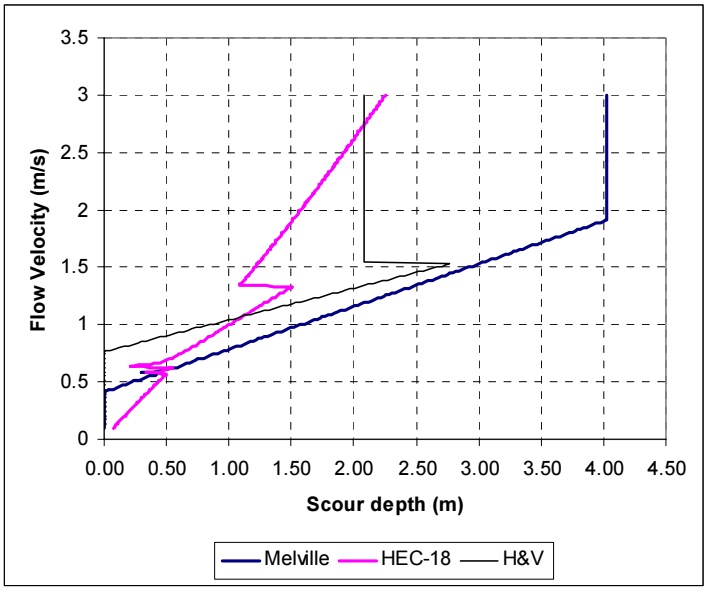

Hole 2: large bare bore with large root wad. Much debris in front of root wad

Input parameters of case 1:

Parameter	*Value*
Width *b* (m)	2.50
Height *H* (m)	2.25
Scour depth d_s (m)	0.82
h_0 Melville & C. (m)	0.93
h_0 HEC-18 (m)	0.92
h_0 Hoffmans &Verheij (m)	0.94
d_{50} (mm) general	8.40
d_{50} (mm) armour	15.62
t (hour)	744
Shape factor K_s (-)	1.1

The general sediment properties are used in the formula of HEC-18

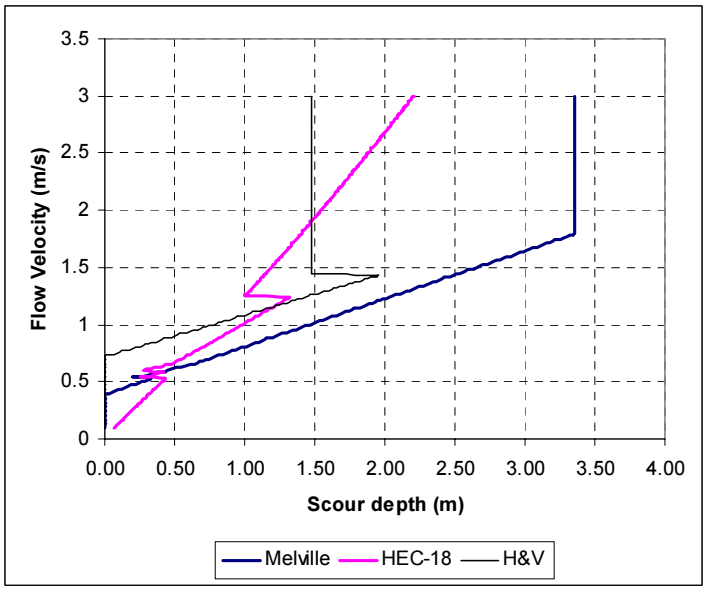

Input parameters of case 2, hole 2:

Parameter	*Value*
Width b (m)	2.50
Height H (m)	2.25
Scour depth d_s (m)	0.82
h_0 Melville & C. (m)	0.85
h_0 HEC-18 (m)	0.85
h_0 Hoffmans &Verheij (m)	0.85
d_{50} (mm) general	8.40
d_{50} (mm) armour	15.62
t (hour)	192
Shape factor K_s (-)	1.1

The general sediment properties are used in the formula of HEC-18

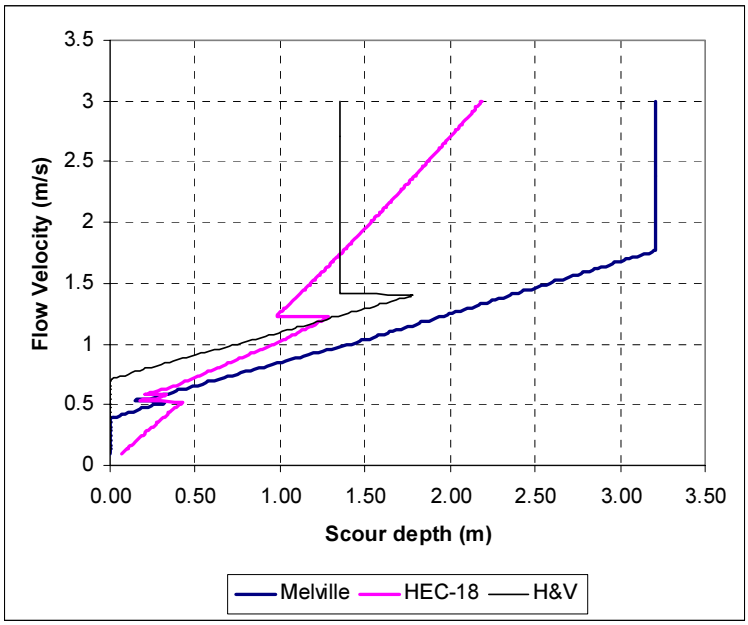

Hole 3: three bores with adjoining debris

Input parameters:

Parameter	*Value*
Width b (m)	2.23
Height H (m)	0.58
Scour depth d_s (m)	0.79
h_0 Melville & C. (m)	0.72*)
h_0 HEC-18 (m)	0.71
h_0 Hoffmans &Verheij (m)	0.73
d_{50} (mm) general	8.40
d_{50} (mm) armour	18.42
t (hour)	774
Shape factor K_s (-)	1.0

*): Representative water depth set to h_0=1.2H: h_0 = 0.69 m

The general sediment properties are used in the formula of HEC-18

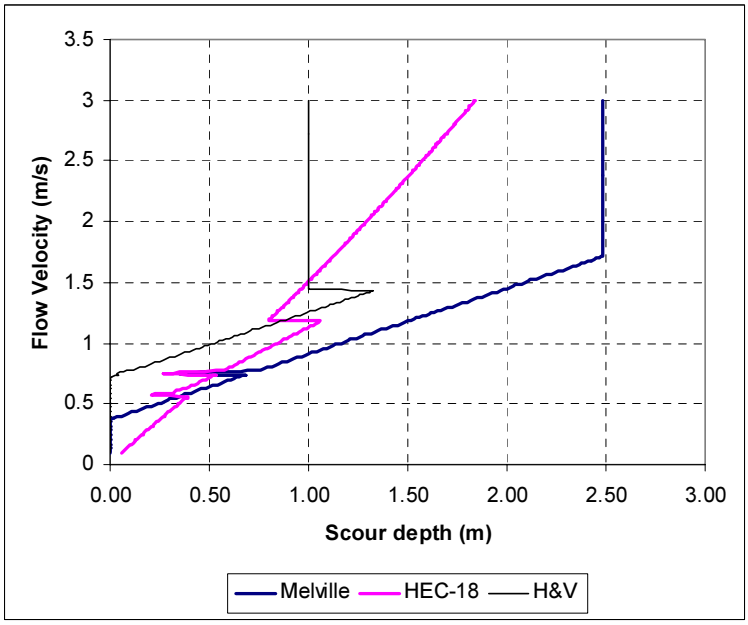

Hole 4: large object at the end of the southern point-bar

Input parameters:

Parameter	*Value*
Width b (m)	2.41
Height H (m)	1.32
Scour depth d_s (m)	0.98
h_0 Melville & C. (m)	0.90
h_0 HEC-18 (m)	0.89
h_0 Hoffmans &Verheij (m)	0.90
d_{50} (mm) general	8.40
d_{50} (mm) armour	10.79
t (hour)	1560
Shape factor K_s (-)	1.1

The general sediment properties are used in the formula of HEC-18

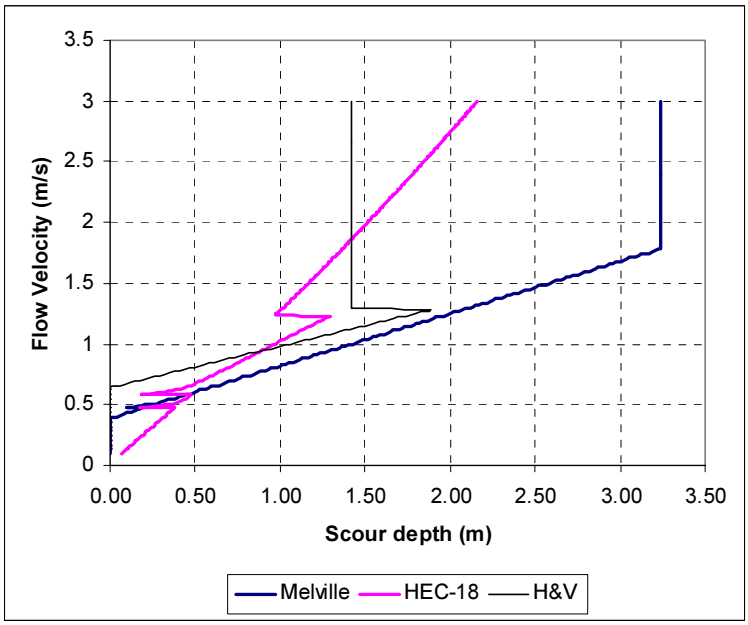

Hole 5: old tree close to main channel, middle point-bar

Input parameters:

Parameter	*Value*
Width b (m)	2.49
Height H (m)	2.18
Scour depth d_s (m)	1.35
h_0 Melville & C. (m)	1.33
h_0 HEC-18 (m)	1.32
h_0 Hoffmans &Verheij (m)	1.32
d_{50} (mm) general	8.40
d_{50} (mm) armour	15.05
t (hour)	1560
Shape factor K_s (-)	1.1

The general sediment properties are used in the formula of HEC-18

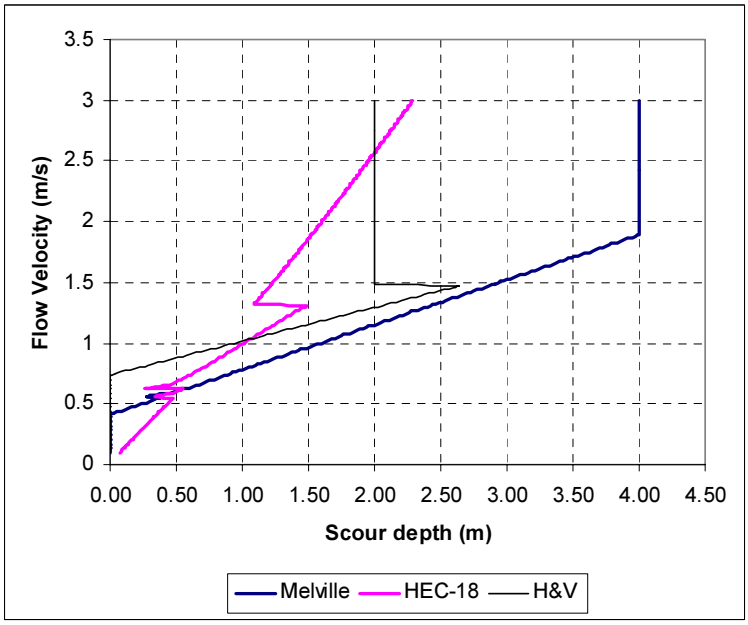

Hole 6: two living trees with wooden debris

Input parameters of case 1:

Parameter	*Value*
Width b (m)	8.55
Height H (m)	1.46
Scour depth d_s (m)	0.94
h_0 Melville & C. (m)	0.51
h_0 HEC-18 (m)	0.50
h_0 Hoffmans &Verheij (m)	0.55
d_{50} (mm) general	8.40
d_{50} (mm) armour	14.59
t (hour)	1560
Shape factor K_s (-)	1.1

The general sediment properties are used in the formula of HEC-18

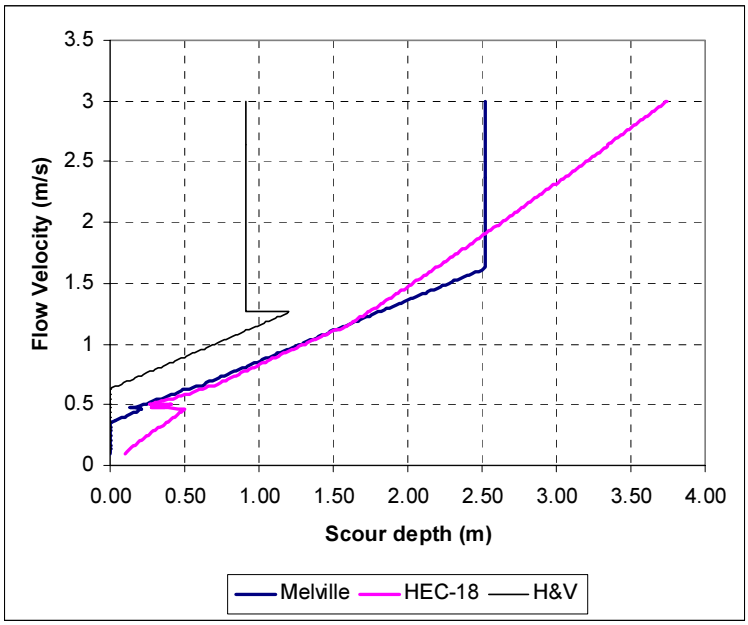

Input parameters of case 2, hole 6:

Parameter	*Value*
Width b (m)	8.55
Height H (m)	1.46
Scour depth d_s (m)	0.94
h_0 Melville & C. (m)	0.70
h_0 HEC-18 (m)	0.69
h_0 Hoffmans &Verheij (m)	0.73
d_{50} (mm) general	8.40
d_{50} (mm) armour	14.59
t (hour)	984
Shape factor K_s (-)	1.1

The general sediment properties are used in the formula of HEC-18

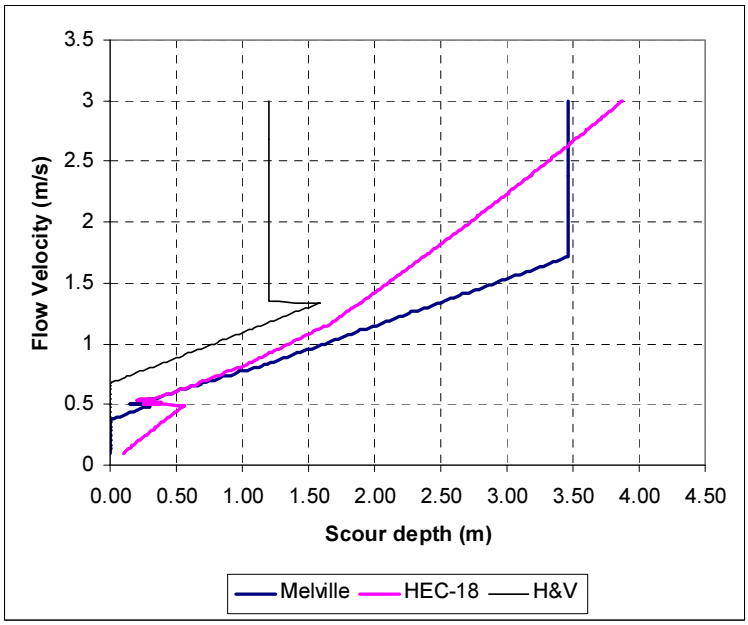

Hole 7: large tree at the upstream side of the northern point-bar

Input parameters:

Parameter	*Value*
Width *b* (m)	1.30
Height *H* (m)	1.67
Scour depth d_s (m)	0.93
h_0 Melville & C. (m)	0.83
h_0 HEC-18 (m)	0.83
h_0 Hoffmans &Verheij (m)	0.82
d_{50} (mm) general	8.40
d_{50} (mm) armour	20.83
t (hour)	624
Shape factor K_s (-)	1.0

The general sediment properties are used in the formula of HEC-18

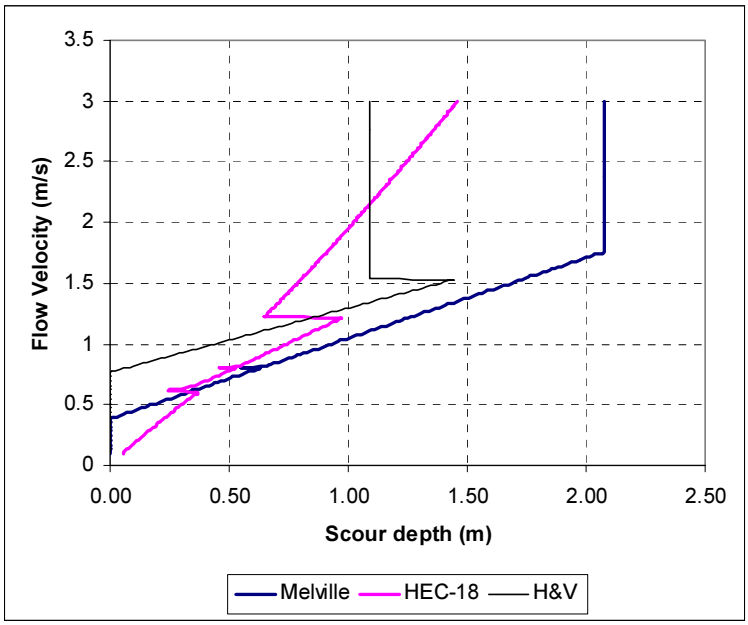

Hole 8: large tree far on point-bar

Input parameters of case 1:

Parameter	*Value*
Width *b* (m)	2.27
Height *H* (m)	2.20
Scour depth d_s (m)	0.42
h_0 Melville & C. (m)	0.63
h_0 HEC-18 (m)	0.62
h_0 Hoffmans &Verheij (m)	0.64
d_{50} (mm) general	8.40
d_{50} (mm) armour	15.80
t (hour)	48
Shape factor K_s (-)	1.1

The general sediment properties are used in the formula of HEC-18

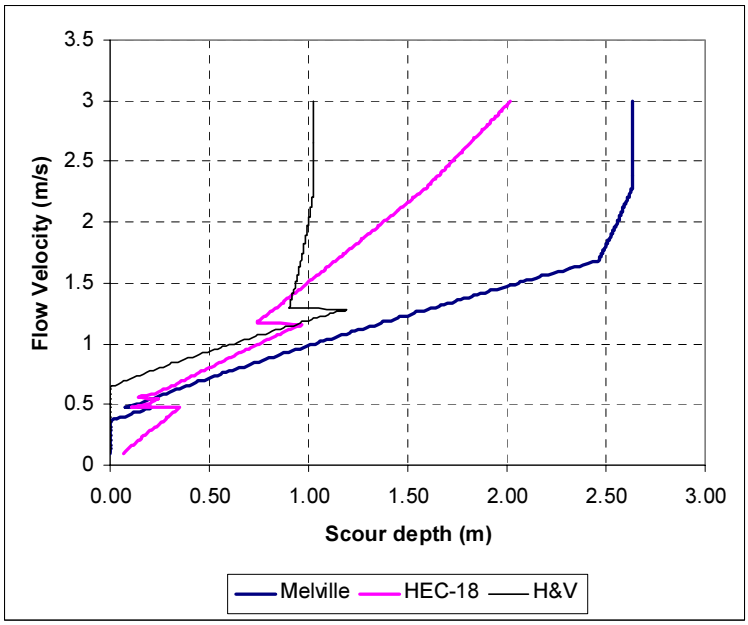

Input parameters of case 2, hole 8:

Parameter	*Value*
Width b (m)	2.50
Height H (m)	2.25
Scour depth d_s (m)	0.82
h_0 Melville & C. (m)	0.78
h_0 HEC-18 (m)	0.78
h_0 Hoffmans &Verheij (m)	0.80
d_{50} (mm) general	8.40
d_{50} (mm) armour	15.62
t (hour)	72
Shape factor K_s (-)	1.1

The general sediment properties are used in the formula of HEC-18

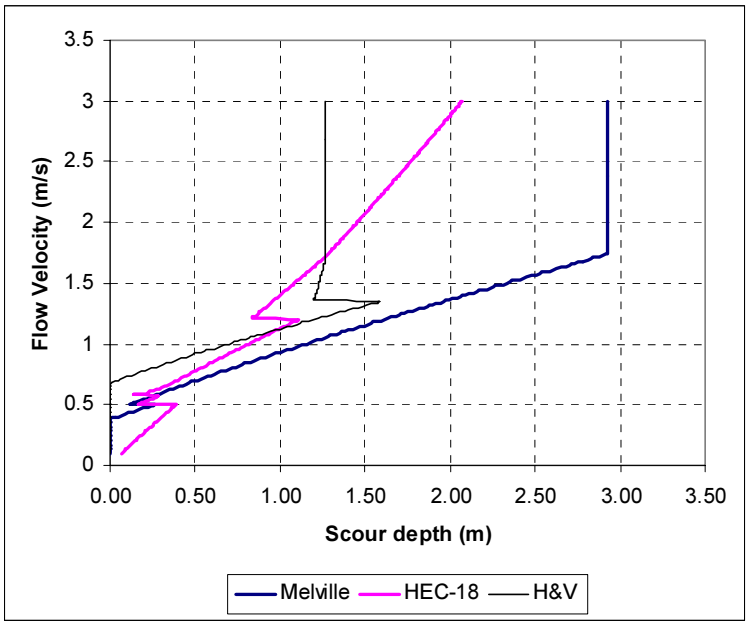

Hole 9: large obstacle composed of several trees and debris

Input parameters:

Parameter	*Value*
Width b (m)	2.89
Height H (m)	0.64
Scour depth d_s (m)	0.70
h_0 Melville & C. (m)	0.93*)
h_0 HEC-18 (m)	0.92
h_0 Hoffmans &Verheij (m)	0.94
d_{50} (mm) general	8.40
d_{50} (mm) armour	15.81
t (hour)	1392
Shape factor K_s (-)	1.0

*): Representative water depth set to h_0=1.2H: h_0 = 0.77 m

The general sediment properties are used in the formula of HEC-18

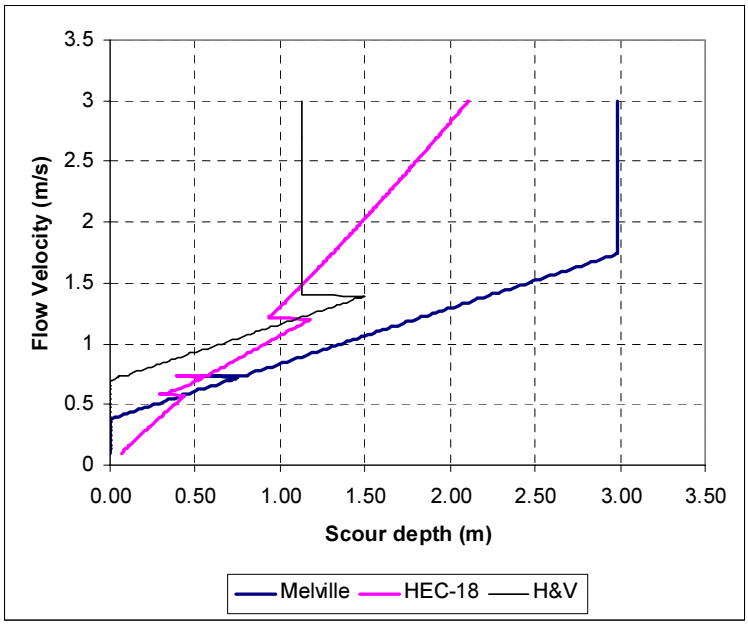

Hole 10: small tree next to hole 9

Input parameters:

Parameter	*Value*
Width *b* (m)	1.76
Height *H* (m)	0.59
Scour depth d_s (m)	0.52
h_0 Melville & C. (m)	0.72
h_0 HEC-18 (m)	0.72
h_0 Hoffmans &Verheij (m)	0.73
d_{50} (mm) general	8.40
d_{50} (mm) armour	15.58
t (hour)	288
Shape factor K_s (-)	1.0

The general sediment properties are used in the formula of HEC-18

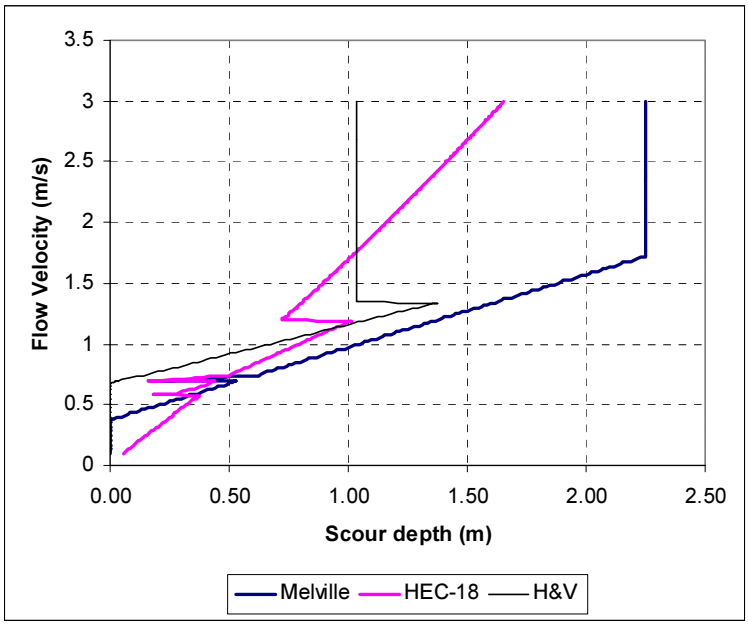

Hole 11: obstacle composed of several trees with wooden debris

Input parameters:

Parameter	*Value*
Width *b* (m)	2.14
Height *H* (m)	1.60
Scour depth d_s (m)	0.55
h_0 Melville & C. (m)	0.89
h_0 HEC-18 (m)	0.88
h_0 Hoffmans &Verheij (m)	0.89
d_{50} (mm) general	8.40
d_{50} (mm) armour	13.77
t (hour)	1392
Shape factor K_s (-)	1.0

The general sediment properties are used in the formula of HEC-18

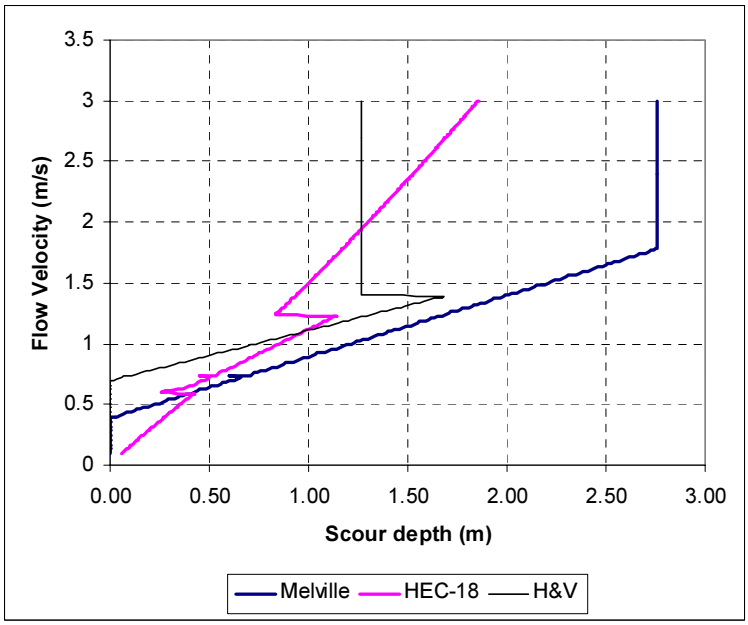

Hole 12: small tree close to hole 11

Input parameters of case 1:

Parameter	*Value*
Width *b* (m)	1.35
Height *H* (m)	0.47
Scour depth d_s (m)	0.34
h_0 Melville & C. (m)	0.31
h_0 HEC-18 (m)	0.31
h_0 Hoffmans &Verheij (m)	0.32
d_{50} (mm) general	8.40
d_{50} (mm) armour	14.81
t (hour)	192
Shape factor K_s (-)	1.0

The general sediment properties are used in the formula of HEC-18

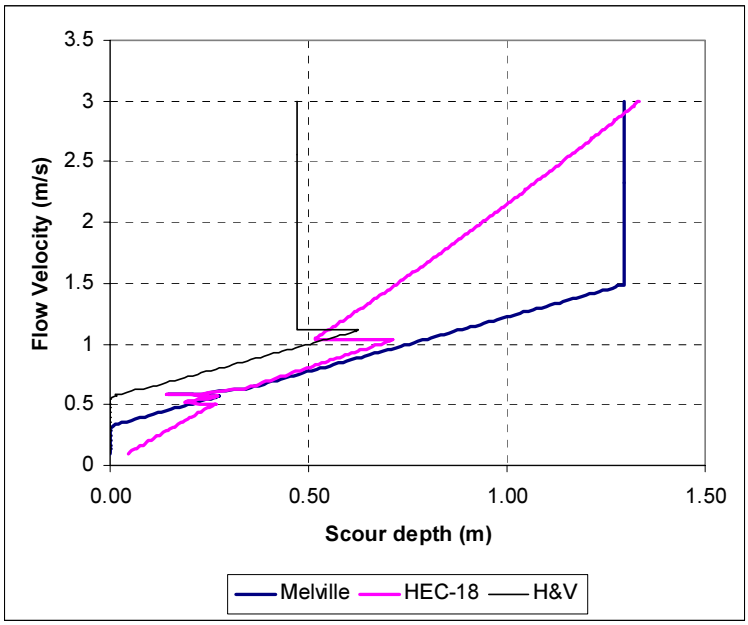

Input parameters of case 2:

Parameter	*Value*
Width *b* (m)	2.50
Height *H* (m)	2.25
Scour depth d_s (m)	0.82
h_0 Melville & C. (m)	0.50
h_0 HEC-18 (m)	0.49
h_0 Hoffmans &Verheij (m)	0.51
d_{50} (mm) general	8.40
d_{50} (mm) armour	15.62
t (hour)	1872
Shape factor K_s (-)	1.1

The general sediment properties are used in the formula of HEC-18

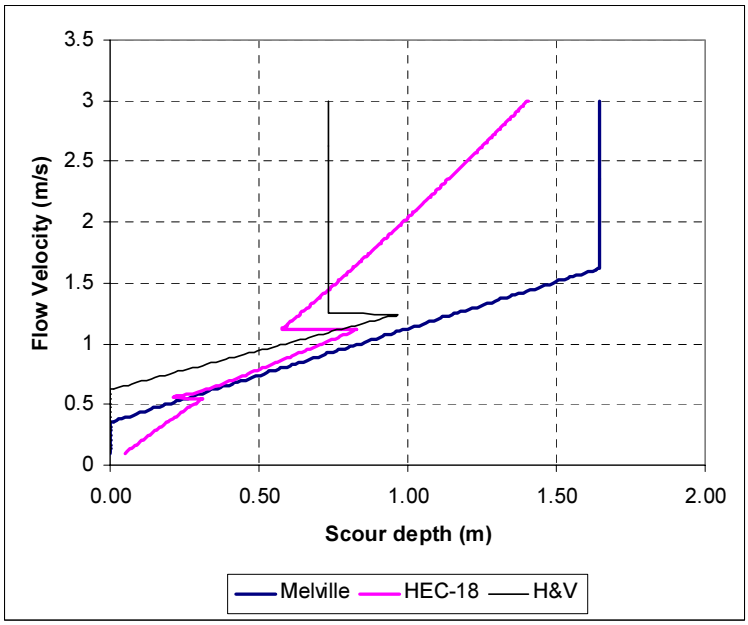

Hole 13: old obstacle close to main channel

Input parameters:

Parameter	*Value*
Width b (m)	2.70
Height H (m)	0.78
Scour depth d_s (m)	0.79
h_0 Melville & C. (m)	1.46*)
h_0 HEC-18 (m)	1.45
h_0 Hoffmans &Verheij (m)	1.45
d_{50} (mm) general	8.40
d_{50} (mm) armour	14.63
t (hour)	1872
Shape factor K_s (-)	1.0

*): Representative water depth set to h_0=1.2H: h_0 = 0.94 m

The general sediment properties are used in the formula of HEC-18

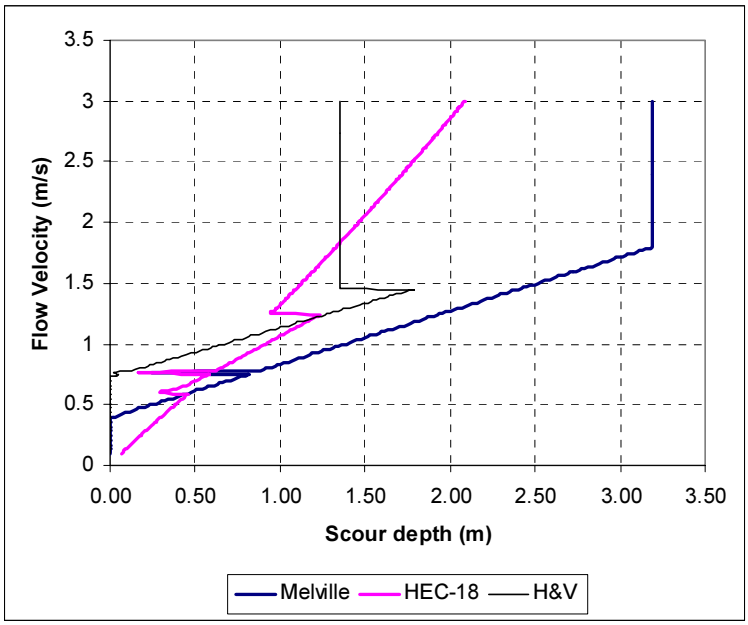

Hole 14: composition of small debris covered with vegetation

Input parameters:

Parameter	*Value*
Width b (m)	2.08
Height H (m)	0.73
Scour depth d_s (m)	0.79
h_0 Melville & C. (m)	1.20*)
h_0 HEC-18 (m)	1.19
h_0 Hoffmans &Verheij (m)	1.19
d_{50} (mm) general	8.40
d_{50} (mm) armour	13.82
t (hour)	3480
Shape factor K_s (-)	1.0

*): Representative water depth set to h_0=1.2H: h_0 = 0.88 m

The general sediment properties are used in the formula of HEC-18

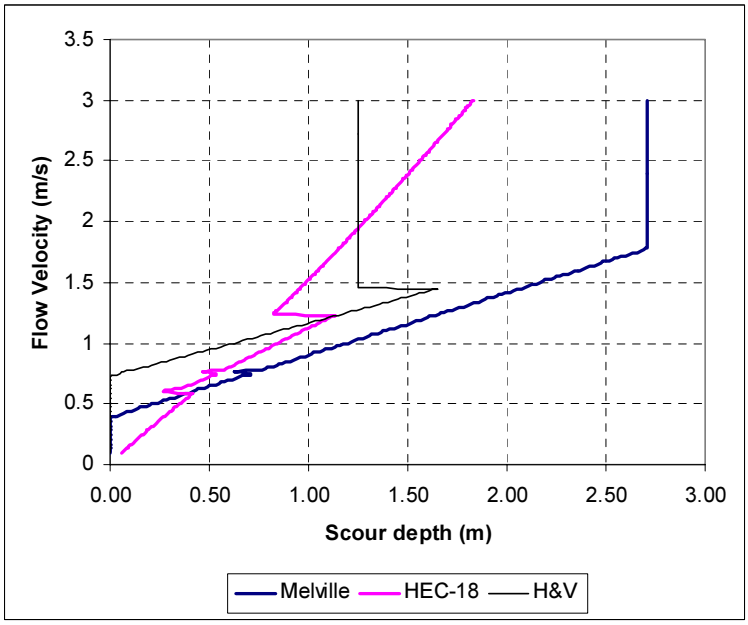

Hole 15: most downstream obstacle composed of small debris

Input parameters:

Parameter	*Value*
Width *b* (m)	6.3
Height *H* (m)	1.03
Scour depth d_s (m)	0.89
h_0 Melville & C. (m)	0.86
h_0 HEC-18 (m)	0.85
h_0 Hoffmans &Verheij (m)	0.89
d_{50} (mm) general	8.40
d_{50} (mm) armour	13.45
t (hour)	1872
Shape factor K_s (-)	1.0

The general sediment properties are used in the formula of HEC-18